Geophysical Fluid Dynamics and the Calculus of Moving Space

By

Joel Simon Feske

B.A., Bowdoin College, 2012

M.S., Carnegie Mellon University, 2015

Thesis

Submitted in partial fulfillment of the requirements for the Degree of Doctor of Philosophy in the Department of Earth, Environmental and Planetary Sciences at Brown University

PROVIDENCE, RHODE ISLAND

May 2026

This dissertation by Joel Feske is accepted in its present form by the Department of Earth, Environmental, and Planetary Science as satisfying the dissertation requirement for the degree of Doctor of Philosophy.

Date 28 APR 2026

Baylor Fox-Kemper, Advisor

Recommended to the Graduate Council

Date 4/28/2026

Mara Freilich

Mara Freilich, Reader

Date 4/28/2026

Jonathan Lilly, Reader

Date 4/28/2026

Christian Huber, Reader

Date 4/28/2026

Victor Tsai, Reader

Approved by the Graduate Council

Date

David P. Lindstrom, Dean of the Graduate School

Curriculum Vitae

Education

Ph.D., Earth, Environmental, and Planetary Science
Brown University (Providence, RI), 2026

M.S., Mechanical Engineering
Carnegie Mellon University (Pittsburgh, PA), 2015

B.A., Physics
Bowdoin College (Brunswick, ME), 2012

Publications

Papers

Lilly, J. M., Feske, J. S., Fox-Kemper, B., and Early, J. J. (2024). Integral theorems for the gradient of a vector field, with a fluid dynamical application. *Proceedings of the Royal Society A: Mathematical, Physical and Engineering Sciences*, 480 (2293).

Lippman-Bell, J. J., Zhou, C., Sun, H., Feske, J. S., and Jensen, F. E. (2016). Early-life seizures alter synaptic calcium-permeable AMPA receptor function and plasticity. *Molecular and Cellular Neuroscience*, 76, 11-20.

In Preparation

Feske, J. S., Lilly, J. M., and Fox-Kemper, B. (2026). Fantastical Forces and Where to Find Them or: A Tensor Time Derivative for Geophysical Fluids in Deforming Coordinate Systems. In prep.

Feske, J. S., Fox-Kemper, B., and Lilly, J. M. (2026) Beyond Vertical Coordinates: A Generalized Framework for Ocean Model Equations with Anisotropic Diffusivity. In prep.

Teaching

2022
Teaching Assistant, *Earth, Environmental and Planetary Science*, (Brown University, Providence, RI)
Course: Mathematical Methods in Geosciences

2021
Teaching Assistant, *Earth, Environmental and Planetary Science*, (Brown University, Providence, RI)
Course: Introduction to Oceanography

2014
Course Assistant, *Mechanical Engineering*, (Carnegie Mellon University, Pittsburgh, PA)
Course: Mathematical Methods of Engineering

2012
Course Grader, *Physics and Astronomy*, (Bowdoin College, Brunswick, ME)
Course: Physics of the Environment

2011
Physics Tutor, *Physics and Astronomy*, (Bowdoin College, Brunswick, ME)

Professional Development

Invited Lectures

March 2026, **STUOD Sandbox**
Fantastical Forces and Where to Find Them
Imperial College, Mathematics (London, UK)

October 2024, **Fluid Mechanics Seminar**
Integral theorems for the gradient of a vector field, with a fluid dynamical application
Royal Society Publishing

Conference Presentations

February 2026
A Tensor Time Derivative for Fluid Dynamics in General Deforming Coordinate Systems
AGU Ocean Sciences Meeting (Glasgow, UK)

February 2024
Exact expressions for turbulence parameterizations in general curvilinear coordinates
AGU Ocean Sciences Meeting (New Orleans, LA)

January 2024
A Covariant, Anisotropic Redi Diffusion Tensor
Workshop on Eddy Dynamics, Detection, and Impacts (Leavenworth, WA)

February 2022
Coordinate Agnostic Approach to Ocean Modeling, Or: How I Learned to Stop Worrying and Love Tensor Analysis
AGU Ocean Sciences Meeting (Online)

Awards and Fellowships

2026: Postdoctoral Scholar Program
Woods Hole Oceanographic Institution (Woods Hole, MA)

Acknowledgments

I would like to thank several people that I have relied upon throughout both this project and my life.

Baylor Fox-Kemper, who has been the best advisor and mentor I could have hoped for. Your humor, kindness, and enthusiasm are infectious, and I've always left your office feeling encouraged. Your knowledge of the field is inspiring both in its breadth and its depth, and might have been intimidating if not accompanied by your unwavering friendliness and support. Our research group, both past and present advisees and the SEAPhOD group more broadly, is full of such warm and thoughtful people; I feel fortunate to have been included. Thank you for providing me with the space to explore these ideas that I find so fascinating, and with the guidance that allowed me to succeed.

Jonathan Lilly, who has acted as an informal co-advisor and mentor. I'm so grateful for the hours and days and weeks that you've poured into this project. The care you take in your thinking has expanded both the rigor and conceptual depth of this work and immeasurably improved my understanding of it. Your calm and mindful way of inhabiting the world is a pleasure to witness, and you have introduced me to so many kind and thoughtful people.

To all those who have served on my preliminary examination and thesis committees over the years—Baylor, Jonathan, Victor Tsai, Manu Di Lorenzo, Mara Freilich, Brad Marston, and Christian Huber—thank you all for the time you have spent reading my proposal and my thesis and for your thoughtful commentary; you have encouraged me to specify the motivation and

broaden the scientific context of this project, and both the work and my education are all the better for it. To Victor in particular—I have enjoyed and will miss our conversations on the train over the last six years.

Stephen Griffies, who has been so generous with his time and attention over the years. Thank you for answering my email when I first contacted you in the summer of 2019 regarding your book *Fundamentals of Ocean Climate Models*, and for speaking to me on the phone for over an hour before I even applied to graduate school; it is only because of that conversation that I ended up in the field of ocean physics. It is also from you that I first heard the name Baylor Fox-Kemper.

Though I don't know them personally, I must thank two wonderful teachers whose work helped bring this project to life. Leonard Susskind, whose *Theoretical Minimum* books and lectures are simply the most brilliant works of pedagogy I have ever encountered, and have been invaluable to my understanding of the structure and practice of modern physics. And Pavel Grinfeld, whose book *Introduction to Tensor Analysis and the Calculus of Moving Surfaces* has fundamentally altered the course of my life. I ordered this book on a lark in September of 2018, and I often wonder what I would be doing now if I hadn't. Certainly not this.

Anna Lo Piccolo, my friend and a fellow student of Baylor's who defended only a day after I did—your warmth, kindness, and frankness are so refreshing. After a year of knowing you as a mere floating head on Zoom, it was a relief to meet you in person and to immediately have a friend. I was so fortunate to go through this process with you, and I wish you all the best in what comes next.

Nihal Shrinath, a friend of two decades and through many transitions. Some years ago, while in line for refreshments at the AMC Boston Common movie theater, you remarked off-hand that you "could see" me "doing a Ph.D. at some point." Back then I could not see it myself. The moment I realized I would at least try was when you told me you'd been accepted for a J.D./M.S. in Environmental Science at Stanford and were going to be "pretty overeducated, but whatever."

It was only then that I realized I wanted to be pretty overeducated too. I can always count on your enthusiasm for cooking, demography, and hip-hop samples, or your willingness to walk eleven miles for pizza.

Benjamin Driver, only incidentally my fellow student at Brown. I'm quite glad your parents made you come to Fessenden halfway through eighth grade, and even more glad that we both ended up living in Pittsburgh in 2014 so we could reconnect. Our near ceaseless correspondence since then has covered everything from Kepler's *Somnium* and tidally-locked coordinates to the satirical prowess of Mike Judge, and now fatherhood. I'm certain that without your example and your encouragement I wouldn't be here polishing this dissertation. Thank you for your confidence in me, and may the Great Exchange begin.

To my parents Carlee Blamphin and Steven Feske, thank you for all of the unconditional love and support, and now for being such loving grandparents. Mom, thank you for giving me rhythm and humor and the ability (or at least the compulsion) to imitate ambient noises. It has been a gift to live so close and to spend working days at home with you as you help care for the boys. Dad, thank you for reading to me about spherical cows and rosy-fingered dawn and for the napkin lectures on Latin grammar, calculus, music theory, the optic chiasm and everything else. You've taught me that things are what they are, to speak about them clearly and, of course, that "what we cannot speak about, we must pass over in silence."

To some other new-ish grandparents of note: Marie Lefton and Arthur Young. Thank you for welcoming me into your family so openly nearly twenty years ago and for all the love and care that you give to us and the boys. We are so lucky to have you nearby.

Thank you to my boys; you have put this process into perspective and given me such joyful time away from work. Silas, your endless curiosity is wonderful. From owls and dragonflies, to rockets and trains, and building and fixing things—it is such a pleasure to learn with you, to build with you, and to watch you try to explain everything you encounter. Shane, you are so intrepid, mischievous, and silly. I love to "Run! Run! Run!" with you, and admire your constant insistence on “Book! Book! Book!” I cannot wait to see what you both have to teach me.

To Amarilice, thank you for making me laugh. I love you, and I love hanging out with you. Thank you for your unconditional support in all aspects of our life; I certainly could not have accomplished any of this without you by my side. I’ve been buoyed by your unwavering confidence in me and your good-natured eye-rolling through my paroxysms of self-doubt. You are such a wonderful wife and the most caring mother to our boys. As I often point out to them: they’re lucky I have such great taste. I cannot believe my good fortune to have found you so early on.

Contents

Acknowledgments **vii**

1 INTRODUCTION **1**

1.1 Seawater dynamics motivate coordinate choice . . . 2

1.2 Tensor analysis sets us up for success . . . 5

1.3 Our extrinsic stance . . . 6

2 Fantastical Forces and Where to Find Them **14**

2.1 Introduction . . . 17

2.2 Preliminaries: definitions, notation, and conventions . . . 22

2.2.1 Space, coordinate systems, and basis vectors . . . 22

2.2.2 Index notation . . . 27

2.2.3 Index juggling . . . 28

2.2.4 Tensor operations . . . 29

2.3 Spatial derivatives in curvilinear coordinates . . . 33

2.3.1 Changing representations involve the identity tensor . . . 35

2.3.2 Spatial differentiation . . . 36

2.3.3 Index swapping rules . . . 39

2.4 Time derivatives in curvilinear coordinates . . . 40

2.4.1 Frames and settings . . . 40

2.4.2 The intrinsic derivative in static frames . . . 44

2.4.3 The material derivative in static frames 46
2.4.4 Velocities and settings 47
2.4.5 Transforming rates of change 49
2.4.6 The intrinsic derivative in moving settings 50
2.4.7 The material derivative in moving settings 52
2.5 The momentum equation in moving coordinates 53
2.5.1 Transformation to a rotating and translating frame 53
2.5.2 The momentum equation in a moving setting 56
2.5.3 Recovery of the rigid frame equation 60
2.6 Discussion 62
2.6.1 The apparent acceleration 62
2.6.2 The generalized Coriolis force 63
2.6.3 The generalized centrifugal force 65
2.6.4 Euler and translational force 67
2.6.5 The fantastical force 68
2.6.6 Contravariant versus covariant representations 69
2.6.7 Generalized intrinsic derivatives in terms of Lie derivatives 71
2.7 Conclusions 73
2.8 Appendix 1A: The metrinilic property for Jacobians 76
2.8.1 The covariant derivative 77
2.8.2 The Lie derivative 77
2.9 Appendix 1B: The intrinsic derivative for covariant components 81
2.10 Appendix 1C: Intrinsic Derivative of Scalar Field τ 83
2.11 Appendix 1D: Intrinsic Derivative of Reynolds Stress $u^i u^j$ 84
2.12 Appendix 1E: Oldroyd and the Intrinsic Time Derivative 85

3 Beyond Vertical Coordinates **96**

3.1 Introduction 97

3.2 Definitions, Notation, and Conventions 100

3.2.1 Inertial and Moving Settings 100

3.2.2 Time Dependence of Metric Components 102

3.2.3 Matrix Representations of 2nd Order Tensors 103

3.2.4 Surfaces 105

3.3 Fluid Equations 108

3.3.1 The Rotating Frame 109

3.3.2 The Rotating Buoyancy Setting 111

3.4 Common Approximations 115

3.4.1 Perfect Fluids in an Accelerating or Rotating Frame 115

3.4.2 Ocean Primitive Equations 115

3.5 Useful Bases and Their Metric Coefficients 121

3.5.1 Tracer Coordinates 121

3.5.2 The Geoid Basis $\mathcal{G}$ 127

3.5.3 The Terrain-following Basis $\mathcal{T}$ 130

3.6 Turbulence Parameterizations 131

3.6.1 The Redi Tensor 131

3.6.2 Transverse Anisotropic Form 132

3.6.3 Small Slope Approximation 134

3.7 Summary & Discussion 136

3.8 Appendix 2A: Useful Objects in Spherical Coordinates 137

3.9 Appendix 2B: The Transformation to Rotating Buoyancy Coordinates 138

4 The Gradient Tensor Theorem: Proof, Utility, and Limitations 148

5 Conclusion 154

List of Tables

2.1 Common vector operations, written both in symbolic notation and in index notation, with the basis vectors associated with the index notation expressions shown in the final column. Here $\boldsymbol{\nabla} \equiv \boldsymbol{e}^i \partial_i$ denotes the familiar nabla or del operator as expressed in curvilinear coordinates, $\otimes$ denotes the tensor product, ∇_i is the covariant derivative acting on tensor components, and ε^{ijk} is the Levi-Civita or alternating tensor, all of which are defined subsequently. In later tables we will omit the final column because the basis is implied by index placement. 30

2.2 Common vector identities involving the tensor product, written in both symbolic and index notation. 30

2.3 Operations for isolating the portions of a second-order tensor $\boldsymbol{A}$ exhibiting various types of symmetries in symbols and index notation. 32

2.4 A table of different time derivatives appearing in this work. χ is a general path along which differentiation occurs. We understand the material derivative of a tensor to be taken following a fixed parcel label ξ. The intrinsic derivatives are constructed to produce components of the corresponding total derivatives acting on tensors. One further sort of time derivative, the convected derivative of Oldroyd (1950), is discussed in Appendix E and omitted here. 41

2.5 Conservation of momentum in the absence of external forces. The first row shows the symbolic form in a rigid frame rotating with potentially variable angular velocity $\boldsymbol{\Omega}$ and translating with velocity $d\boldsymbol{S}/dt$. The second and third rows show the index form for a general moving, deforming setting; u^i is the relative velocity in that setting. The indexed equations are far more general because the moving coordinate system is not constrained to be rigid, but rather moves *and* deforms according to the setting velocity field $\boldsymbol{\mathcal{V}} = \mathcal{V}^i \boldsymbol{e}_i$. The indexed terms generalize those encountered in the rigid case. When we choose the rigid setting velocity $\boldsymbol{\mathcal{V}} = \boldsymbol{\mathcal{K}} = \boldsymbol{\Omega} \times \boldsymbol{r} + d\boldsymbol{S}/dt$, the lower rows reduce to the first. Additional forces $\boldsymbol{F}$ can be applied to the right-hand side. 60
2.6 A table of derivatives of the various components of the identity $\boldsymbol{I}$. Each can be derived by representing components of $\boldsymbol{I}$ as dot products of basis vectors, themselves vector-valued tensor components, and applying the product rule. . . 79
2.7 A table of derivative commutators. The commutator is understood to be applied to the relevant components of the tensor in each column. 80

3.1 Rotating fluid equations in symbolic and index notations. We have the absolute fluid velocity $\boldsymbol{v} = \boldsymbol{u} + \boldsymbol{\mathcal{V}}$, where $\boldsymbol{u}$ is the fluid velocity as measured locally in the moving setting, and $\boldsymbol{\mathcal{V}}$ is the absolute velocity of the moving setting. Setting velocity $\boldsymbol{\mathcal{V}}$ is $\Omega\bar{\varphi} = \Omega r c_\theta \hat{\varphi}$ in the case of pure rotation. This choice for $\boldsymbol{\mathcal{V}}$, or indeed any choice for which $\nabla_{(j}\mathcal{V}_{i)} = 0$, results in a conservative Coriolis-like term $\mathcal{V}^j \nabla_j \mathcal{V}^i$ which could be absorbed into the gravitational potential g, however this is not the case for general $\boldsymbol{\mathcal{V}}$—see section 2.6.3. The tracer transport equation can be used either for salinity S or potential temperature Θ. κ_τ is the isotropic background diffusivity of the relevant tracer τ, and $\$$ is the anisotropic Redi tensor—see section 3.6.2. To close this equation set we must also include an equation of state $b = b(S, \Theta, p)$. 116

3.2 The hydrostatic approximation represented in various coordinate systems. The reader may confirm that in each case we have $e_i k^i = \hat{\boldsymbol{k}}$, $k_i k^i = 1$, and $e_i k^i k_j \nabla^j p = \hat{\boldsymbol{k}} \partial_z p$. When the basis has a true vertical basis vector, its component representation of the gravitational force is nonzero only in that direction. Otherwise it is a linear combination of all basis directions. Normally we would write covariant components as row vectors, but we write them here as column vectors simply to save space. The final expression of $k^i k_j \nabla^j p$ for the rotated orthogonal basis $\mathcal{RO}$ is left to the reader to derive, for it would not fit in this table. 119

3.3 Metric tensors for simple geometries. ν is geocentric co-latitude, θ is geocentric latitude, and Θ is geodetic latitude. α and μ are parameters defined so that for the oblate spheroid that best approximates the Earth (say, the GRS80 reference ellipsoid), $\alpha \cosh \mu$ is the equatorial radius of Earth, and $\alpha \sinh \mu$ is the polar radius of Earth. As elsewhere, s_θ, c_θ, and ch_μ denote $\sin\theta$, $\cos\theta$, and $\cosh\theta$, respectively. a is the radius of the toroidal coordinates' reference circle. 122

3.4 The Redi tensor projected into various density coordinate systems, increasingly aligned with its eigenbasis (its principal axes). The individual components of $\boldsymbol{R}$ are more physically meaningful the greater this alignment, seen best in the $\mathcal{RO}$ basis. Hydrostatic models might still prefer Young's Dual basis $\tilde{\mathcal{Y}}$ because it permits a vertically separable momentum equation, as shown in Table 3.2. The reader may confirm that in each case we have $e_i \nabla^i \tau = \boldsymbol{\nabla} \tau$. We define $n^i \equiv \nabla^i \tau / |\boldsymbol{\nabla} \tau|$ and $L^2 \equiv |\boldsymbol{L}|^2 = L_x^2 + L_y^2$ is the squared magnitude of the slope vector. κ is quasi-horizontal diffusivity. Components are presented in terms of the geometric objects σ, L, and $\boldsymbol{\nabla} \tau$ for brevity and to encourage physical intuition, but these can be readily expressed in terms of the components of $\boldsymbol{L}$ according to equations (3.55) - (3.58). See Figure 3.3 for geometric depictions of these coordinate systems. 133

3.5 The names given to the various setting velocities. Velocities that are derivatives of y^a *or* that hold y fixed are absolute, while the others are relative. Notice that the table is antisymmetric, so we only need three unique labels for the interaction of three settings. Indices are omitted here. 140

List of Figures

1.1 Adapted from Griffies et al. (2000a), Figure 1. Different regions of the ocean are most easily modeled in different coordinates depending on the dominant symmetry breaking: height (z) where the geopotential gradient dominates, neutral buoyancy where the density (ρ) gradient dominates, or terrain-following (σ) where the topography gradient dominates. Misalignment between iso-surfaces of different coordinates can cause numerical errors. For example when isopycnal diffusion is approximated as constant-height, a component of the diffusion occurs erroneously in the diapycnal direction (Veronis, 1975). 4

2.1 A schematic showing quantities in an inertial frame (black), chosen without loss of generality to be stationary, and a general moving, deforming coordinate system as often used in GFD (teal). 88

2.2 The setting velocity $\boldsymbol{\mathcal{V}}$, shown in white, is a vector field that generates a diffeomorphism of space. **Left**: $\boldsymbol{\mathcal{V}} = \boldsymbol{\Omega} \times \boldsymbol{r}$ generates rotation of the sphere. In this case, $\boldsymbol{\mathcal{V}}$ is a Killing vector field because rotation is a rigid transformation for which $\nabla_{(i}\mathcal{V}_{j)} = 0$. **Right**: A swirling and shearing diffeomorphism of the plane. Here $\nabla_{(i}\mathcal{V}_{j)} \neq 0$, and we see a straining deformation. There is no divergent deformation because this $\boldsymbol{\mathcal{V}}$ was generated from a stream function, so $\nabla_i \mathcal{V}^i = 0$. Note: these figures were generated programmatically using Matlab (left) and Python's Manim package (right) with the assistance of ChatGPT. 89

3.1 Visualization of the normal and transverse projection operators acting on the components of a vector $\boldsymbol{w}$. 106
3.2 Definition of the x-component of the slope vector $\boldsymbol{L} = L_x\hat{\boldsymbol{\imath}} + L_y\hat{\boldsymbol{\jmath}}$. The y-component is defined analogously as $L_y = -\partial_y\tau/\partial_z\tau$. The ith basis vector in the iso-surface of τ is the projection of the ith Cartesian basis vector onto that surface along $\hat{\boldsymbol{k}}$. 121
3.3 Visualization of the four definitions of tracer coordinates discussed in section 3.5.1, showing Young's basis $\mathcal{Y}$, Young's dual basis $\tilde{\mathcal{Y}}$, scaled orthogonal coordinates $\mathcal{SO}$, and rotated orthogonal coordinates $\mathcal{RO}$. 123
3.4 Definition of the λ-component of the slope vector $\boldsymbol{L}$. The θ-component is defined analogously as $L_\theta = -\partial_\theta\Phi/\partial_r\Phi$. The ith basis vector in the iso-surface of Φ is the projection of the ith spherical basis vector onto that surface along $\hat{\boldsymbol{r}}$. 129
3.5 The geometric operations performed by the transverse isotropic Redi diffusion tensor $\boldsymbol{R}$ and the transverse-anisotropic diffusion tensor \$. Whereas $\boldsymbol{R}$ performs a simple orthogonal projection onto the neutral surface scaled by the local diffusivity, \$ allows us the freedom to rotate the projection within the neutral plane, biasing diffusion towards the direction of the largest eigenvector. 134

4.1 This figure was created by Jonathan Lilly, and appears as figure 1 of Lilly et al. (2024). That caption is quoted here: An illustration of the use of the gradient tensor theorem in observational oceanography. The (a) vorticity ζ, (b) normal strain ν, and (c) shear strain σ in a snapshot of a numerical simulation of a quasigeostrophic eddy termed BetaEddyOne (Early and Lilly, 2023) are shown, each normalized by the Coriolis frequency $f \equiv 2\Omega \sin\phi$ where Ω is the angular rotation rate of the Earth and ϕ is the model's central latitude. The eddy is sampled along the triangular tracks, as described in the text, and the colours of the circular disks show the average values of the three quantities within each triangular cell as inferred from the information along its boundary using the 2D gradient tensor theorem. Note that the divergence vanishes for this quasigeostrophic model. 152

CHAPTER 1

INTRODUCTION

Geophysical fluid dynamics is a peculiar field. Every text on fluids quickly introduces the notions of Eulerian and Lagrangian representations of flow—perspectives that, respectively, remain fixed as the fluid moves through them, or that move along with the fluid (Aris, 1962, e.g.). That is, we have two natural choices in observing and modeling a fluid: sit still in the inertial lab frame and watch the fluid move by, or follow a fluid parcel and measure the changes it experiences. GFD, almost uniquely, lives between these two choices.

GFD is the classical, non-relativistic study of rotating, stratified flow over rough topography and within a thin, nearly spherical shell surrounding the solid earth. Rotation is crucial: we have access to an Eulerian frame, but that frame is not inertial. Although an inertial frame exists—in which the earth rotates freely while we stand by and watch—such a thing is only conceptual, and we cannot take measurements there directly. Furthermore the ocean and the atmosphere are roughly confined to the surface of a sphere, and so curved, non-Euclidean space are fundamental. Of course there are standard conventions for handling these facts—spherical coordinates, the Coriolis force, etc.—see any introductory GFD text such as Chapter 2 of Vallis (2017). This becomes more complex when we introduce coordinates based on geophysically broken symmetries.

The peculiarly hybrid nature of time-dependent geophysical coordinates appears, for example, when we consider the governing dynamics of seawater. Density or "neutral buoyancy" coordinates and terrain-following σ-coordinates move as the fluid moves, but are not advected perfectly with the fluid as Lagrangian coordinates would be. We choose coordinates depending on the dominant broken symmetry in each region of the ocean. In the mixed layer there is only weak stratification, and the geopotential gradient dominates. In the interior ocean flow is adiabatic along surfaces of neutral buoyancy, and the potential density gradient dominates. Near the bottom, flow is governed by topography and the σ gradient dominates. We now motivate these different choices and discuss the difficulties they introduce.

1.1 Seawater dynamics motivate coordinate choice

Coherent water masses, defined by their density class, deform and flow around and underneath one another, but maintain their identity even over the course of millennia (Veronis, 1975). At large scales, transport within the ocean is nearly adiabatic (Griffies et al., 2000a), and so water masses intermix only very slowly in a process named *diapycnal* (across-density) or *dianeutral* (across neutral buoyancy) diffusion. Density coordinates are useful here because their isosurfaces are naturally oriented along the directions of large-scale flow.

Maintaining water mass integrity is crucial, for example, in climate models that must accurately predict the effect of excess heat uptake by the ocean. Heat sequestration in the deep ocean occurs mostly inside of density surfaces that outcrop at the sea surface and slope down into the interior (Newsom et al., 2023). Heat is transported down along these surfaces by isopycnal mixing, and it is estimated that through this process the ocean has absorbed 90% of the excess radiative heat trapped since the industrial revolution began (Griffies et al., 2015).

Early models using height (z) coordinates approximated isopycnal diffusion by mixing along surfaces of constant height, see Figure 1.1. This was numerically simpler and, after all, the slopes of density surfaces are small; as mentioned earlier, the ocean is a thin shell covering the earth, and is therefore far wider than it is deep. This approximation caused what is known as the "Veronis effect" – tracers were mixed horizontally across neutral-buoyancy potential density surfaces far more in models than in the actual ocean (Veronis, 1975). Diapycnal mixing in the real ocean happens at scales of $10^{-5} m^2 s^{-1}$ (Griffies et al., 2000a) compared to scales of $10^3 m^2 s^{-1}$ for isopycnal mixing (Griffies et al., 2000b). This difference of eight orders of magnitude means that small errors in the representation of isopycnal surfaces introduce significant spurious diapycnal mixing—one one-millionth of the isopycnal mixing rotated erroneously into the diapycnal direction will overwhelm the true diapycnal mixing by one hundred times. Spurious diapycnal mixing limits the ability of models to realistically maintain the integrity of distinct water masses (Griffies et al., 2000a; Hirschi et al., 2020), and though the Veronis effect was first pointed out in 1975, its minimization is still actively pursued (Griffies et al., 2000b; Ilıcak et al., 2012; Griffies et al., 2015). Models with spuriously high dianeutral mixing produce an unrealistically diffuse ocean state and prevent accurate prediction on long timescales.

Density coordinates are not useful over the entire ocean, particularly in the mixed layer where they have insufficient resolution (Petersen et al., 2015), and near the bottom boundary where flow is governed by sea floor topography (Griffies et al., 2000a) and is not adiabatic. Mixed layer and bottom boundary layer flow are better represented by geopotential and terrain-following σ-coordinates, respectively, but the misalignment of the isosurfaces of these coordinates with neutral buoyancy potential density surfaces leads again to spurious dianeutral mixing (Griffies et al., 2000a,b). Terrain-following coordinates also introduce significant horizontal pressure gradient errors near steeply sloping topography (Griffies et al., 2000a).

Below the length scale of the model grid, turbulent mixing must be parameterized, and physically realistic parameterizations are most naturally represented in density coordinates. Models that use terrain-following coordinates (Griffies, 2018) or a generalized vertical coordinate (Gibson et al., 2017) struggle to faithfully represent neutral physics, particularly when flowing over topography such as sills (Hirschi et al., 2020). Lemarié et al. (2012) show that it is difficult to implement common turbulence closures in σ-coordinates.

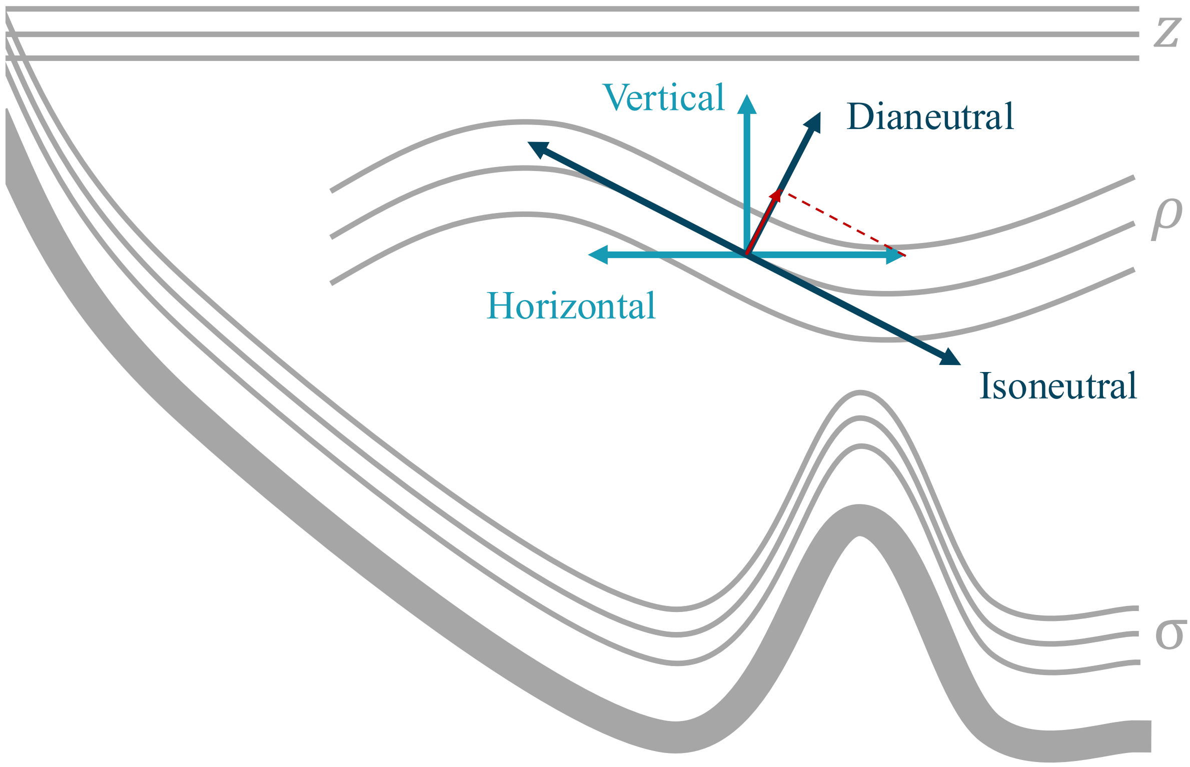

Figure 1.1: Adapted from Griffies et al. (2000a), Figure 1. Different regions of the ocean are most easily modeled in different coordinates depending on the dominant symmetry breaking: height (z) where the geopotential gradient dominates, neutral buoyancy where the density (ρ) gradient dominates, or terrain-following (σ) where the topography gradient dominates. Misalignment between iso-surfaces of different coordinates can cause numerical errors. For example when isopycnal diffusion is approximated as constant-height, a component of the diffusion occurs erroneously in the diapycnal direction (Veronis, 1975).

Isopycnal coordinate models effectively eliminate dianeutral mixing in the adiabatic flow of the interior ocean, even to the point where background mixing must be added back in (Griffies et al., 2000a). Paired with a linear equation of state, such models exhibit identically zero dianeutral mixing (Ilıcak et al., 2012), but more realistic, nonlinear equations of state are not integrable, meaning that there is no single scalar field defined throughout space whose gradient is everywhere normal to the local neutral plane. Though the neutral plane is defined at each point, these planes cannot be stitched together into a neutral surface, and we cannot choose a coordinate for which the isosurfaces are everywhere aligned with the directions of adiabatic transport (McDougall, 1987; Jackett and McDougall, 1997; Nycander, 2011).

Newer models introduce further complication. Hybrid coordinates (Bleck, 2002; Mellor et al., 2002; Metzger et al., 2006; Chassignet et al., 2009) and generalized vertical coordinates (Chassignet et al., 2006; Griffies, 2018) use a different vertical coordinate in different regions of the ocean. Arbitrary Lagrangian-Eulerian coordinates (Petersen et al., 2015; Gibson et al., 2017; Megann et al., 2022) flow with the fluid for time before a re-gridding step keeps them from becoming too deformed. What seems like a mundane choice—the coordinates we use to carve up space—has an outsize effect on our ability to accurately model the climate and understand its evolution over long time scales.

1.2 Tensor analysis sets us up for success

Tensor analysis seems tailor-made to address this varied and growing family of geophysical coordinates. By definition, tensors are geometric objects that exist apart from any representation with respect to a particular basis. The vector $\boldsymbol{v}$ with polar components $(r, \theta) = (1, \frac{\pi}{4})$ does not change when it is instead represented by Cartesian components $(x, y) = (\frac{1}{\sqrt{2}}, \frac{1}{\sqrt{2}})$. The same can be said of any vector field we encounter in GFD—velocity, momentum, vorticity, concentration gradients, etc—and of higher-order quantities such as stress and strain or the Redi/ Gent-McWilliams turbulence parameterization tensor (Redi, 1982; Gent and McWilliams, 1990). Although computer models must store these objects in memory as arrays of numbers, the particular numbers are meaningless without reference to a choice of basis—a choice of coordinates.

Tensor analysis and index notation provide a way to, on the one hand, write equations that manipulate tensor components and, on the other hand, maintain a strong connection to the geometric meaning of those component manipulations. We need not choose any particular coordinate system until it becomes convenient, but once we do, the equations spell out precisely the component-wise computation the computer must perform. We can write down equations that apply in all coordinates and maintain a clean separation between phenomena that are real, physical, and geometrical, and phenomena that are merely artifacts of one coordinate choice or another. For example, the velocity components of a fluid parcel in isopycnal coordinates might change because the particle accelerates or because density surfaces move vertically across it; the former is a physical change in the parcel's velocity, but the latter is not.

Furthermore, the index algebra of tensor components is relatively simple to learn, and has very few rules compared to the algebra of symbolic vectors. In fact, many of the second derivative and triple product identities compiled into lengthy tables for use in vector calculus derive from a single relation in tensor algebra: $\varepsilon^{ijk}\varepsilon_{k\ell m} = \delta^i_\ell \delta^j_m - \delta^j_\ell \delta^i_m$, for the purely antisymmetric Levi-Civita tensor ε and the Kronecker delta. These have straight-forward geometric interpretations as the components of the volume element and the identity tensor, respectively.

1.3 Our extrinsic stance

We are far from the first to recognize the utility of tensor analysis in fluid mechanics. Cartesian tensors often appear in introductory fluids texts precisely because they ease certain calculations. Kundu et al. (2016) is a standard example. As soon as we introduce curvilinear, time-varying coordinates, however, Cartesian tensors are not powerful enough. As discussed above, curvilinear coordinates are ubiquitous in GFD, and non-Cartesian tensors do appear in the literature (Griffies et al., 1998; Griffies, 1998, 2018).

The fully intrinsic tensor analysis[1] taught mostly in texts on general relativity (Misner et al., 1973; Wald, 1984; Carroll, 2019) has the power to handle completely generalized coordinates in spacetime (not only in space) and is used to model astrophysical fluids. For an example, see Hawley et al. (1984) on black hole accretion disks. Maddison and Marshall (2013) have applied the full spacetime formalism in their work on the Eliassen-Palm flux tensor, however in GFD this approach has distinct disadvantages. The full machinery of relativistic physics is overpowered to describe a branch of physics so solidly rooted in its Newtonian limit. Introducing needless mathematical abstraction and non-Euclidean spacetime means we cannot rely on our natural

[1]That is, intrinsic to the Lorentzian spacetime manifold.

intuitions about Euclidean space. Our intuitions are powerful when correctly applied, and so we aim to import only as much abstraction as we need while keeping our physical intuitions intact. In order to walk this line between abstraction and intuition, we borrow the extrinsic framing of tensor analysis presented by Grinfeld (2009, 2013).

Standard differential geometry and general relativity are careful to maintain a sharp distinction between the manifold $\mathcal{M}$, its tangent space $T_p\mathcal{M}$ at the point $p \in \mathcal{M}$, and its cotangent space $T_p^*\mathcal{M}$, the dual vector space to $T_p\mathcal{M}$. The collection of all tangent spaces stitched together is the tangent bundle $T\mathcal{M}$, and the cotangent bundle $T^*\mathcal{M}$ is defined analogously. If $\mathcal{M}$ is the surface of a sphere, $T_p\mathcal{M}$ is a plane tangent to the sphere at point p and $T\mathcal{M}$ is all the tangent planes taken together. If $\mathcal{M}$ contains our system, the ocean, then $T\mathcal{M}$ contains tangent vectors, e.g. velocities, and $T^*\mathcal{M}$ contains differential 1-forms (that is, covectors, dual vectors, linear functionals), e.g. gradients of scalars. Higher-order tensor fields are then elements of tensor products of $T\mathcal{M}$ and $T^*\mathcal{M}$. This is all rather more abstract than we'd like.

Operating in the Newtonian limit of gravity, GFD takes place in flat, Euclidean space $\mathcal{E}$. Though we might drop highly complex, time-varying curvilinear coordinates onto this space, the space itself is not exotic. In this case $T_p\mathcal{M}$ and $T_p^*\mathcal{M}$ can both be identified with $\mathcal{E}$, and this is true for any point p. Then we can picture their respective basis vectors $\boldsymbol{e}_i$ and $\boldsymbol{e}^i$ simply as trios of arrows in $\mathcal{E}$ instead of more abstractly as differential operators in tangent and cotangent spaces to $\mathcal{M}$. It also means that we can freely add together vectors from different points in space without worrying about parallel transporting them to the same point $p \in \mathcal{M}$. This is particularly important for integration over extended domains.

The extrinsic approach lets us hide much of the abstraction of differential geometry behind objects we can picture, preserving and even leaning on our intuitions about space. Nevertheless, almost all of the expressions we derive would hold in an intrinsic theory as well, and so to some extent the extrinsic stance is merely a useful lens that we can pick up or put down at will. We are free, for example, to interpret the reciprocal basis $\boldsymbol{e}^i$ of vectors instead as a basis of differential 1-forms $\mathrm{d}x^i$ for the purpose of integration (Needham, 2021) or discretization (Crane et al., 2013;

Crane, 2018). The action of either on a vector produces its components: $\boldsymbol{e}^i \cdot \boldsymbol{v} = \mathrm{d}x^i(\boldsymbol{v}) = v^i$. Abstraction is still available to us, but GFD and our physical intuitions live happily in the extrinsic world.

The second chapter of this work spells out this extrinsic approach to differential geometry, and extends the interpretation slightly from that appearing in Grinfeld (2013). It also extends the notion of *intrinsic time differentiation* to coordinate systems that translate, rotate, and deform as a function of time. The defining feature of the intrinsic derivative $\delta/\delta t$ is its action on tensor components to produce components of the tensor's time derivative: $\delta T^i/\delta t = \boldsymbol{e}^i \cdot d\boldsymbol{T}/dt$. We apply this to the velocity field to arrive at a momentum equation that clearly delineates contributions to the momentum from the observed velocity and separates them from two classes of apparent forces: *fictitious forces* arising from rigid coordinate motion, and *fantastical forces* arising from deforming coordinate motion.

The third chapter presents the full equations of motion for GFD in this framework, including common approximations and a parameterization of sub-grid turbulent diffusion. It also provides explicit forms for the metric tensor in various common GFD coordinates so that equations can be projected into those particular coordinate systems, shows how to transform into a moving frame, and demonstrates the composition of simple moving-frame transformations into more complex ones.

The fourth chapter presents a generalized integral theorem of which the divergence and Kelvin-Stokes theorems are special cases. It relies on the flatness of the extrinsic space $\mathcal{E}$ to allow results that do not follow from the standard Generalized Stokes Theorem of differential geometry, and we show why those results break on curved surfaces.

We take an unusually pedagogical stance throughout for two reasons. First, the audience is meant to be physical oceanographers and ocean modelers with diverse backgrounds in oceanography, physics, applied mathematics, and computer science, and we hope that the introduction to the subject offered here can make the work more broadly accessible. Those readers who are already familiar with the details should freely skip these sections. Second, our extrinsic stance, though not unique or original to this work, is nonetheless uncommon. Readers more familiar with general relativity or differential geometry as presented in a mathematics department might balk at some of our assertions which, while not true in general, are true for our case where we allow a universal, inertial, Euclidean extrinsic space.

This coordinate-agnostic approach to geophysical fluid dynamics has clarified the definitions of commonly used coordinate systems; rigorously separated true dynamics from coordinate artifacts; mechanized the sharing of methods such as turbulence parameterizations between coordinate systems; and straightforwardly generalized many approximations. With this foundation laid there are many exciting next steps to pursue, and we discuss these in the conclusion.

References

Aris, R. (1962). *Vectors, tensors and the basic equations of fluid mechanics*. Courier Corporation.

Bleck, R. (2002). An oceanic general circulation model framed in hybrid isopycnic-cartesian coordinates. *Ocean modelling*, 4(1):55–88.

Carroll, S. M. (2019). *Spacetime and geometry*. Cambridge University Press.

Chassignet, E., Hurlburt, H., Metzger, E. J., Smedstad, O., Cummings, J., Halliwell, G., Bleck, R., Baraille, R., Wallcraft, A., Lozano, C., Tolman, H., Srinivasan, A., Hankin, S., Cornillon, P., Weisberg, R., Barth, A., He, R., Werner, F., and Wilkin, J. (2009). US GODAE: Global ocean prediction with the HYbrid Coordinate Ocean Model (HYCOM). *Oceanography*, 22(2):64–75.

Chassignet, E. P., Hurlburt, H. E., Smedstad, O. M., Halliwell, G. R., Wallcraft, A. J., Metzger, E. J., Blanton, B. O., Lozano, C., Rao, D. B., Hogan, P. J., et al. (2006). Generalized vertical coordinates. *Oceanography*, 19(1):20.

Crane, K. (2018). Discrete differential geometry: An applied introduction. *Notices of the AMS, Communication*, 1153.

Crane, K., de Goes, F., Desbrun, M., and Schröder, P. (2013). Digital geometry processing with discrete exterior calculus. In *ACM SIGGRAPH 2013 Courses*, SIGGRAPH '13, New York, NY, USA. Association for Computing Machinery.

Gent, P. R. and McWilliams, J. C. (1990). Isopycnal mixing in ocean circulation models. *Journal of Physical Oceanography*, 20(1):150–155.

Gibson, A. H., Hogg, A. M., Kiss, A. E., Shakespeare, C. J., and Adcroft, A. (2017). Attribution of horizontal and vertical contributions to spurious mixing in an arbitrary lagrangian–eulerian ocean model. *Ocean Modelling*, 119:45–56.

Griffies, S. (2018). *Fundamentals of ocean climate models*. Princeton university press.

Griffies, S. M. (1998). The gent–mcwilliams skew flux. *Journal of Physical Oceanography*, 28(5):831–841.

Griffies, S. M., Böning, C., Bryan, F. O., Chassignet, E. P., Gerdes, R., Hasumi, H., Hirst, A., Treguier, A.-M., and Webb, D. (2000a). Developments in ocean climate modelling. *Ocean Modell.*, 2(3):123–192.

Griffies, S. M., Gnanadesikan, A., Pacanowski, R. C., Larichev, V. D., Dukowicz, J. K., and Smith, R. D. (1998). Isoneutral diffusion in a z-coordinate ocean model. *Journal of Physical Oceanography*, 28(5):805–830.

Griffies, S. M., Pacanowski, R. C., and Hallberg, R. W. (2000b). Spurious diapycnal mixing associated with advection in a z-coordinate ocean model. *Monthly Weather Review*, 128(3):538–564.

Griffies, S. M., Winton, M., Anderson, W. G., Benson, R., Delworth, T. L., Dufour, C. O., Dunne, J. P., Goddard, P., Morrison, A. K., Rosati, A., et al. (2015). Impacts on ocean heat from transient mesoscale eddies in a hierarchy of climate models. *Journal of Climate*, 28(3):952–977.

Grinfeld, P. (2009). Exact nonlinear equations for fluid films and proper adaptations of conservation theorems from classical hydrodynamics. *Journal of Geometry and Symmetry in Physics*, 16:1–21.

Grinfeld, P. (2013). *Introduction to tensor analysis and the calculus of moving surfaces*. Springer.

Hawley, J. F., Smarr, L. L., and Wilson, J. R. (1984). A numerical study of nonspherical black hole accretion. i equations and test problems. *The Astrophysical Journal*, 277:296–311.

Hirschi, J. J.-M., Barnier, B., Böning, C., Biastoch, A., Blaker, A. T., Coward, A., Danilov, S., Drijfhout, S., Getzlaff, K., Griffies, S. M., et al. (2020). The atlantic meridional overturning circulation in high-resolution models. *Journal of Geophysical Research: Oceans*, 125(4):e2019JC015522.

Ilıcak, M., Adcroft, A. J., Griffies, S. M., and Hallberg, R. W. (2012). Spurious dianeutral mixing and the role of momentum closure. *Ocean Modelling*, 45:37–58.

Jackett, D. R. and McDougall, T. J. (1997). A neutral density variable for the world's oceans. *Journal of Physical Oceanography*, 27(2):237–263.

Kundu, P. K., Cohen, I. M., and Dowling, D. R. (2016). *Fluid mechanics*. Elsevier Inc., sixth edition.

Lemarié, F., Kurian, J., Shchepetkin, A. F., Molemaker, M. J., Colas, F., and McWilliams, J. C. (2012). Are there inescapable issues prohibiting the use of terrain-following coordinates in climate models? *Ocean Modelling*, 42:57–79.

Maddison, J. R. and Marshall, D. (2013). The Eliassen-Palm flux tensor. *J. Fluid Mech.*, 729:69–102.

McDougall, T. J. (1987). Neutral surfaces. *Journal of Physical Oceanography*, 17(11):1950–1964.

Megann, A., Chanut, J., and Storkey, D. (2022). Assessment of the z time-filtered arbitrary lagrangian-eulerian coordinate in a global eddy-permitting ocean model. *Journal of Advances in Modeling Earth Systems*, 14(11):e2022MS003056.

Mellor, G. L., Häkkinen, S. M., Ezer, T., and Patchen, R. C. (2002). *A Generalization of a Sigma Coordinate Ocean Model and an Intercomparison of Model Vertical Grids*, pages 55–72. Springer Berlin Heidelberg, Berlin, Heidelberg.

Metzger, E. J., Hurlburt, H. E., Wallcraft, A. J., Cummings, J. A., Chassignet, E. P., and Smedstad, O. M. (2006). Global ocean prediction using hycom. In *2006 HPCMP Users Group Conference (HPCMP-UGC'06)*, pages 271–274. IEEE.

Misner, C. W., Thorne, K. S., and Wheeler, J. A. (1973). *Gravitation*. Macmillan.

Needham, T. (2021). *Visual Differential Geometry and Forms: A Mathematical Drama in Five Acts*. Princeton University Press.

Newsom, E., Zanna, L., and Gregory, J. (2023). Background pycnocline depth constrains future ocean heat uptake efficiency. *arXiv preprint arXiv:2307.11902*.

Nycander, J. (2011). Energy conversion, mixing energy, and neutral surfaces with a nonlinear equation of state. *Journal of Physical Oceanography*, 41(1):28–41.

Petersen, M. R., Jacobsen, D. W., Ringler, T. D., Hecht, M. W., and Maltrud, M. E. (2015). Evaluation of the arbitrary lagrangian–eulerian vertical coordinate method in the mpas-ocean model. *Ocean Modelling*, 86:93–113.

Redi, M. H. (1982). Oceanic isopycnal mixing by coordinate rotation. *Journal of Physical Oceanography*, 12(10):1154–1158.

Vallis, G. K. (2017). *Atmospheric and oceanic fluid dynamics*. Cambridge University Press.

Veronis, G. (1975). The role of models in tracer studies. *Numerical models of ocean circulation*, pages 133–146.

Wald, R. M. (1984). *General relativity*. University of Chicago press.

CHAPTER 2

Fantastical Forces and Where to Find Them

This chapter has been submitted for publication in the Journal of Physical Oceanography. I am the primary author on this submission, along with Jonathan Lilly and Baylor Fox-Kemper. The following summary is partially adapted from a research proposal recently submitted for the postdoctoral fellowship at Woods Hole Oceanographic Institution.

Summary

This chapter begins building a unified framework describing geophysical fluid dynamics in coordinate-agnostic tensor form. Models of geophysical fluid dynamics use a variety of coordinate systems depending on their needs. The Earth's oceans are always modeled in a rotating frame, but on top of this modelers might choose other time-varying settings: terrain-following coordinates where topography drives dynamics (Griffies et al., 2000a); density coordinates for adiabatic flow in the interior ocean (McDougall, 1987; Young, 2012); or even Arbitrary Lagrangian-Eulerian coordinates that flow with the fluid (Bleck, 2002; Griffies et al., 2015a, 2020). This chapter tackles two problems that arise in moving coordinate systems: time derivatives

of tensor components must account for time dependence in the coordinates themselves, and such coordinates introduce apparent forces on top of the familiar Coriolis and centrifugal forces arising in rotating frames.

To solve these problems, we introduce the frame velocity field $\boldsymbol{\mathcal{V}}$—the vector field that captures the moving frame's motion at each point with respect to an inertial frame. We can then decompose the total fluid velocity field $\boldsymbol{v}$ as the sum $\boldsymbol{\mathcal{V}} + \boldsymbol{u}$, where $\boldsymbol{u}$ is the velocity measured in the moving setting. Our first goal is to define a derivative operator $\delta/\delta t$ with the property that

$$\frac{d\boldsymbol{w}}{dt} = \boldsymbol{e}_i \frac{\delta w^i}{\delta t} \quad \text{or} \quad \boldsymbol{e}^i \cdot \frac{d\boldsymbol{w}}{dt} = \frac{\delta w^i}{\delta t}.$$

Repeated indices are understood to denote a summation according to the Einstein convention. Such a derivative exists for static, curvilinear coordinates y^a and is defined in Aris (1962) and Grinfeld (2013) as

$$\frac{\delta}{\delta t} \equiv \left(\left.\frac{\partial}{\partial t}\right|_y + v^a \nabla_a \right), \tag{2.61}$$

where $|_y$ denotes a partial derivative taken with static coordinates y^a held fixed, and ∇_a denotes a covariant derivative with respect to the a-th coordinate. We modify this definition to account for time-varying coordinates x^i, arriving at

$$\frac{\delta}{\delta t} \equiv \left(\left.\frac{\partial}{\partial t}\right|_x + v^i \nabla_i - \mathcal{L}_{\mathcal{V}} \right). \tag{2.129}$$

We have essentially decomposed the observed velocity $\boldsymbol{u}$ into $\boldsymbol{v} - \boldsymbol{\mathcal{V}}$ because each piece is doing something different: $\boldsymbol{v}$ effects an *active* transformation by actually moving the fluid; $\boldsymbol{\mathcal{V}}$ effects a *passive* transformation by moving only the coordinates. The covariant derivative $v^i \nabla_i$ along $\boldsymbol{v}$ is a generalization of the standard advection operator $(\boldsymbol{v} \cdot \boldsymbol{\nabla})$, while the Lie derivative $\mathcal{L}_{\mathcal{V}}$ is defined precisely to capture changes due to the *diffeomorphism*[1] generated by $\boldsymbol{\mathcal{V}}$. By subtracting it, we eliminate changes in the tensor components that are artifacts of this transformation, and which do not represent real change in the tensor field being differentiated.

[1]That is, a continuous, differentiable transformation of space.

Applying the intrinsic derivative operator (2.129) to the components of the absolute velocity field $\boldsymbol{v}$, we arrive at a momentum equation that contains explicit expressions for all of the apparent forces arising in an arbitrarily time-varying coordinate system:

$$\left.\frac{\partial u^i}{\partial t}\right|_x + u^j \nabla_j u^i = \boxed{-2u^j \nabla_j \mathcal{V}^i - \mathcal{V}^j \nabla_j \mathcal{V}^i - \left.\frac{\partial \mathcal{V}^i}{\partial t}\right|_x} + F^i. \tag{2.93}$$

The boxed terms capture all apparent forces arising in the moving setting x. The difference $\boldsymbol{\mathcal{V}}$ between the absolute velocity $\boldsymbol{v}$ and the observed velocity $\boldsymbol{u}$ of a particle in a moving setting contains all of the information about the time rate of change of the basis vectors according to the equation

$$\left.\frac{\partial \boldsymbol{e}_j}{\partial t}\right|_x = \boldsymbol{e}_i \nabla_j \mathcal{V}^i = \partial_j \boldsymbol{\mathcal{V}}, \tag{2.70}$$

where $\nabla_j \mathcal{V}^i$ are the matrix components of $\boldsymbol{\nabla} \otimes \boldsymbol{\mathcal{V}}$. For rigid transformations of space such as translation or rotation this matrix is antisymmetric, but general, non-rigid transformations that include shearing or divergence of the coordinate frame have a contribution from the symmetric part as well. Components of the apparent force vectors in the moving setting are all related to the frame velocity $\boldsymbol{\mathcal{V}}$ by the expressions

$$2u^j \nabla_j \mathcal{V}^i, \qquad \mathcal{V}^j \nabla_j \mathcal{V}^i, \qquad \left.\frac{\partial \mathcal{V}^i}{\partial t}\right|_x.$$

For a position vector $\boldsymbol{r}$ and angular velocity $\boldsymbol{\Omega}$, we can make the choice $\boldsymbol{\mathcal{V}} = \boldsymbol{\Omega} \times \boldsymbol{r}$ to effect rigid rotation. Then $\boldsymbol{\nabla} \otimes \boldsymbol{\mathcal{V}}$ is purely antisymmetric, and these terms respectively represent the familiar, *fictitious* Coriolis, centrifugal, and Euler forces, the last of which is nonzero only if the rotation rate Ω changes in time. For more general choices of $\boldsymbol{\mathcal{V}}$, $\boldsymbol{\nabla} \otimes \boldsymbol{\mathcal{V}}$ has a non-zero symmetric part that introduces unfamiliar *fantastical* forces, discussed in section 2.6.5.

Fantastical forces have a different character than fictitious forces; namely, their form depends on whether we choose to measure covariant or contravariant components of velocity. They are generated by the motion of the fluid itself in Lagrangian coordinates where we choose $\boldsymbol{\mathcal{V}} = \boldsymbol{v}$, by the motion of the free surface of the ocean in terrain-following coordinates, or by the heaving and shearing of density surfaces in isopycnal coordinates. For the last case, we provide explicit expressions for all such apparent forces in section 3.3.2. Armed with general, explicit expressions for these apparent forces, we can analyze their effect on our models.

2.1 Introduction

Geophysical fluid dynamics (GFD) is a non-relativistic branch of fluid dynamics in the Newtonian limit of gravity, centered on the effects of stratification, rotation, and topography. These features break the isotropy of fluid motion, privileging flow, stirring, and mixing in certain directions and within particular curved surfaces, for example iso-surfaces of neutral buoyancy. Numerical models exploit the geometry of broken symmetries with dynamically motivated choices of coordinates, such as a vertical direction aligned with effective gravity and thus hydrostatic balance. Such coordinate choices simplify equations and increase computational efficiency.

Coordinate systems do not exist. This is what makes them so useful: they can be chosen for convenience in the problem at hand. Nature prescribes the quantities—density, momentum, strain—that determine the state of a system, along with the laws by which the state evolves, and these physical quantities themselves are coordinate-free. This freedom from coordinate dependence is what we mean when we say that such quantities are tensor fields: all choices of their representations—all sets of components—correspond to the same object in nature. Technical definitions of tensors as transforming in certain ways under a change of coordinates or as multilinear functions from vectors to scalars are all constructed to ensure that we maintain a sharp separation between the tensor itself and our representation of that tensor's components.

Working with tensors in generalized coordinates, we can on the one hand choose any representation of nature that suits our problem, and on the other hand ensure that we are dealing with real, physical quantities that are not simply artifacts of our coordinate choice. Tensor equations that apply under all coordinates are particularly useful in geophysical fluid dynamics where we use space and time-varying coordinates to capture planetary rotation, and often also choose time-varying coordinates to simplify the dynamics of stratification.

Tensor analysis has the power to express the equations of fluid motion without approximation in as general a coordinate system as possible. This includes familiar, rigidly rotating and translating coordinate systems as well as potentially deforming systems such as isopycnal or terrain-following coordinates. Our first goal is to define a component-wise time derivative $\delta/\delta t$ which, when applied to the components of a tensor $\boldsymbol{T}$ in some basis, provides the components of the time derivative of the tensor $d\boldsymbol{T}/dt$ in the same basis. Such an operation must permit both spatial and temporal dependence of the coordinate bases linked to those components. The *intrinsic time derivative*, discussed in Aris (1962) and Grinfeld (2013) accomplishes this goal for spatially varying basis vectors, however, its definition presumes that for a given location the basis is fixed in time; this is virtually never the case in geophysical fluid dynamics. The *generalized intrinsic time derivative* introduced here extends this idea to permit time-dependent basis vectors. It takes on its most general form in the doubly-boxed equations (2.125) and (2.129).

Changes observed in the tensor field $\boldsymbol{T}$ depend not only on physical processes, but also on the observer's path through it, and the generalized intrinsic time derivative captures both types of change. If the observer's location tracks a fluid parcel, as in the Lagrangian fluid equations, this intrinsic derivative reduces to an intrinsic *material* derivative. With this material derivative finally in hand, we proceed to give expressions for the components of inertial velocity and acceleration in all coordinate systems, including rigidly rotating and translating but also deforming systems. These expressions include the familiar advection terms and "fictitious forces"—the Coriolis and centrifugal forces—but also include other, unfamiliar apparent forces that arise only in deforming systems. With the choice of Lagrangian coordinates, we connect these new terms to the convected time derivative of Oldroyd (1950) and to the Lie derivative that is so useful in geometric mechanics (Holm, 2025).

In GFD, different temporally and spatially dependent coordinate systems, often quite complex, are chosen for convenience in different situations. Most fundamentally, rotating frames of reference are typically used to separate the large velocities of planetary motion from the relative velocities more easily measured by earthbound observers. Similarly, deforming coordinates are often used to capture the anisotropic flows along the most natural surfaces.

In physical oceanography, coordinate choices generally depend on the region of interest (Fox-Kemper et al., 2019): near the surface and in regions of weak stratification, height coordinates are used; near the sea floor, topography drives dynamics and terrain-following, or σ, coordinates are preferred; and away from the boundaries in regions of strong stratification, isopycnal coordinates (McDougall, 1987; Young, 2012) are typically chosen to capture the undulation of density surfaces. More generally, Lagrangian coordinates (e.g., Salmon, 2013) flow with a fluid while Eulerian systems stay fixed in coordinate space as the fluid moves through them. The Arbitrary Lagrangian-Eulerian method (e.g., Petersen et al., 2015; Gibson et al., 2017; Megann et al., 2022) and other complex coordinates as used in the HYCOM (Bleck, 2002; Halliwell, 2004) and MOM6 (Griffies et al., 2020) numerical models combine these approaches, allowing the grid to flow with the fluid for a time, and resetting before it becomes too deformed.

The choice of coordinate system bears upon the accuracy of numerical models. Finite machine precision can introduce error into simulations, and an improper choice of coordinates will exacerbate that error. For example, it has long been known that modeling tracer transport in height coordinates leads to the Veronis effect: if lateral transport is calculated perpendicular to the geopotential gradient at constant height, rather than more realistically along surfaces of constant density, the misalignment of these two sorts of surfaces causes spurious mixing across density classes (Veronis, 1975). The difference of roughly eight orders of magnitude between isopycnal and diapycnal mixing in the real ocean means that small errors in the representation of isopycnal surfaces introduce significant spurious diapycnal mixing—if even one one-millionth of the isopycnal mixing is erroneously rotated into the diapycnal direction, it will overwhelm the true diapycnal mixing. More suitable choices of coordinates can help to avoid this (Griffies et al., 2000b, 2015b; Ilıcak et al., 2012).

Coordinate-free tensor formulations find application in numerical methods modeling fluid flows for other reasons as well. An important class of totally anti-symmetric tensors, *differential forms*, are especially useful for integration and discretization, particularly on unstructured meshes (Crane et al., 2013; Crane, 2018), and Cotter and Thuburn (2014) have applied these methods to the rotating shallow water equations. Åhlander et al. (2001), meanwhile, note that "the design of applications for scientific computing should be based firstly upon continuous abstractions and secondly on approximations," and show that separating software engineering concerns by the level of mathematical abstraction allows discretization to occur more naturally at each level. The literature on the Sophus software library details many of these discrete, tensor-based methods (Grant et al., 2000; Engø et al., 2001; Friis et al., 2001; Haveraaen et al., 2005; Åhlander and Otto, 2006; Haveraaen and Friis, 2009; Heinzl and Schwaha, 2011; Gilbert and Vanneste, 2023).

There is plenty of precedent for the application of tensor analysis to fluid mechanics in other domains, most obviously in relativistic fluids where spacetime itself—not just the coordinate system—is so curved as to require careful treatment. The black hole accretion study by Hawley et al. (1984) is exemplary. It is therefore natural to introduce a time derivative to non-relativistic dynamics by taking the limit $v \ll c$, where $c \approx 3 \times 10^8$ m s^{-1} is the speed of light. Maddison and Marshall (2013) take this approach to deriving the Eliassen-Palm flux tensor in time-varying coordinates. However, this introduces a speed-of-light velocity scale c that is cumbersome alongside atmospheric winds and ocean currents with mean velocities six to ten orders of magnitude smaller. We avoid this by taking a non-relativistic approach from the start, which has the added benefit of grounding the problem in familiar, flat 3D space.

Putting aside relativistic physics, introductory fluids texts (e.g., Kundu et al., 2016) often frame equations in Cartesian tensor notation with a fixed basis $\{\hat{\boldsymbol{\imath}}, \hat{\boldsymbol{\jmath}}, \hat{\boldsymbol{k}}\}$. Crucially for our purposes, partial derivatives of tensor components with respect to spatial coordinates do not immediately generalize to deforming, curvilinear coordinates, but require the added algebraic structure of the *covariant derivative*, discussed subsequently. To fully generalize component-wise tensor computations to non-orthogonal coordinates, components must be tracked with respect to both a coordinate basis $\boldsymbol{e}_i$ and its dual or reciprocal basis $\boldsymbol{e}^i$, which happen to coincide in

Cartesian coordinates; a considerable simplification.

This work builds on the rich history of advances in tensor analysis in fluid mechanics. Tensor analysis for geophysical fluids is reviewed in Griffies (2018, Chapter 18) and has been applied to the Gent-McWilliams skew flux (Griffies, 1998; Dukowicz and Smith, 1997) and to thickness-weighted averaging (Young, 2012). Oldroyd (1950) employs tensor analysis to define time derivatives for materially advected coordinates, although in quite a different sense than we do, and Hinch and Harlen (2021) provide relevant context for Oldroyd's work. Grinfeld (2009) employs tensor analysis in a fully curvilinear treatment of thin fluid films, which Grinfeld (2013) expands into the full calculus of moving surfaces. This latter text is the inspiration for the extrinsic perspective on differential geometry that we assume here, and Grinfeld's equation (16.27) for the invariant time derivative is a sort of analog to our generalization of the intrinsic derivative, but restricted to moving, embedded surfaces.

The goal of this work is three-fold. Firstly, we aim to create a primer on the tensor analysis of Euclidean space in curvilinear coordinates, to highlight the remarkable power and compactness of index notation, and to provide tensor component-based equations that can be directly translated into model code. This approach offers high levels of both abstraction and practicality, since any expression written in index notation is immediately computable. Secondly, we construct the generalized intrinsic time derivative discussed above. Finally, we use this derivative to investigate the apparent forces that arise in the general, non-inertial, deforming coordinate systems so common in GFD. These apparent forces separate cleanly into two categories based on tensor symmetries: the familiar fictitious forces arising from the rigid (translational and/or rotational) part of the coordinate transformation, and what we dub the *fantastical forces* arising from the non-rigid (straining and/or diverging) part. The fantastical forces are more subtle than the fictitious forces because they differ for covariant and contravariant representations of a tensor field.

The structure of this paper is as follows: sections 2.2 and 2.3 lay out the definitions, notation, and conventions that we employ for the tensor calculus of Euclidean space; section 2.4 derives the form of the generalized time derivative; section 2.5 applies it to the momentum equation and shows how to recover the familiar rotating equations of motion; and section 2.6 discusses generalizations of the fictitious forces that arise from non-rigid motion, provides more a abstract form of the intrinsic derivative, and discusses its connection to related work.

2.2 Preliminaries: definitions, notation, and conventions

This section introduces the definitions, notation, and conventions of tensor analysis employed throughout. Prior familiarity with tensor analysis is assumed; readers already proficient in tensor analysis using index notation can skip to section 2.4 where the GFD-specific aspects begin. For extensive treatments of this topic, the authors favor Grinfeld (2013), Carroll (2019), Itskov (2015), Aris (1962), and Ogden (1984); see also Lilly et al. (2024). For brevity's sake, many statements found readily in the literature are given without proof.

One of the goals of this work, and of this section specifically, is to be a brief introductory reference for tensor analysis and differential geometry as needed for fluid applications, in particular numerical modeling of the ocean circulation in moving coordinate systems. This leads us to make two fundamental choices: *extrinsic geometry*, meaning that the existence of flat, three-dimensional Euclidean, inertial space may be presumed, and *explicit notation*, in which we use index-based notation for tensor analysis so that mathematical expressions can be readily converted into computer code for numerical calculations. Our presentation aims not only to introduce useful abstractions but also to eschew needless ones. We occasionally refer back to equations in their symbolic form when index notation becomes onerous to interpret.

2.2.1 Space, coordinate systems, and basis vectors

In non-relativistic three-dimensional Euclidean space, the setting for GFD, time is a parameter shared by all spatial locations. A *scalar field* is a distribution of values at each point in space. A *vector field* can be visualized as a distribution of arrows, having magnitude and direction, at each point in space. Scalar and vector fields respectively are tensor fields of order zero and one. A *second-order tensor field* is a linear mapping from vectors to vectors, or a bilinear mapping from pairs of vectors to scalars, at each point in space. More generally, an nth order tensor field is a multilinear function from n vectors to scalars, although in GFD we rarely encounter tensors higher than second order. The terms "scalar," "vector," and "tensor" are understood implicitly to refer to fields rather than single values, and therefore always depend on space and time.

A *coordinate system* is a set of enumerated surfaces extending throughout space, not necessarily planar nor spatially fixed in time, that can be used to specify locations and therefore to quantify motion. These coordinate surfaces are indexed with a set of three numbers $\{x^1, x^2, x^3\}$ called the *coordinates*. When used as the argument to a function, the shorthand notation $f(x)$ will be used in place of $f(x^1, x^2, x^3)$, following Grinfeld (2013). The *position vector field* $\boldsymbol{r}(x)$ of the coordinate system is the vector field that at each coordinate location $\{x^1, x^2, x^3\}$ gives the displacement vector from the origin to that location. For notational compactness, the argument x will generally be omitted from $\boldsymbol{r}$ and other tensor fields. We shall consider x^i to refer collectively to the entire set $\{x^1, x^2, x^3\}$, and similarly for other indexed entities.

Critically, physical laws and the tensors appearing in them are not affected by the choice of coordinate systems. However, the representation of tensors as sets of components and the representation of physical laws as equations expressed in terms of these tensor components *are* affected by the choice of coordinate system. Much of the effort expended here is in deriving equations for tensor *components*, because these component equations are what we actually use for calculation in numerical models. In our experience the distinction between tensors and their components is frequently confounded in GFD, particularly when taking material derivatives, which are often applied to components alone rather than full tensors.

Differentiation of the position vector field $\boldsymbol{r}$ with respect to each coordinate defines a set of *basis vectors*

$$e_i \equiv \partial_i \boldsymbol{r} \ , \tag{2.1}$$

where $\partial_i \equiv \partial/\partial x^i$ is a shorthand for the partial derivative with respect to the ith coordinate. A basis vector is thus the tangent vector to the curve traced out by the change in position as we vary $\boldsymbol{r}$ one coordinate x^i at a time. The basis vectors need not have unit length, be orthogonal to one another, or be constant in space or time. Immediately we see the influence of extrinsic geometry here: the vector $\boldsymbol{r}$ exists independent of our representation of space as a differentiable manifold. Were we strictly intrinsic, we would have to make the more abstract choice $e_i = \partial_i$ for the basis. Singularities in the coordinate systems can be managed, for example at extrema in non-monotonic coordinates and at poles (see, e.g., Prusa, 2018), so long as there are not too many. So, coordinates imply a basis, and in casual exposition we may freely refer to either.

In order to handle so many possibilities for the basis $\boldsymbol{e}_j$, a set of *reciprocal basis vectors* $\mathbf{e}^i$ are defined such that

$$\boldsymbol{e}^i \cdot \boldsymbol{e}_j \equiv \delta^i_j \ , \tag{2.2}$$

with δ^i_j being the Kronecker delta function

$$\delta^i_j \equiv \begin{cases} 1, & i = j \\ 0, & i \neq j \,. \end{cases} \tag{2.3}$$

Unlike in Cartesian coordinates, the $\boldsymbol{e}_i$ and $\boldsymbol{e}^i$ bases are not generally orthonormal themselves. Equation (2.2) introduces a new type of joint orthonormality.

Due to the definition in equation (2.1), the basis vectors $\boldsymbol{e}_i$ will shorten when coordinates are packed more tightly – that is, they "covary" with the coordinates. The basis vectors $\boldsymbol{e}^i$ contravary with the coordinates in just such a way to make equation (2.2) hold. This justifies the names *covariant* and *contravariant*, and motivates the subscripting of covariant indices and the superscripting of contravariant indices.

Components of tensor fields also covary or contravary with the coordinates. For those familiar with tensors in Cartesian coordinates, but not general curvilinear coordinates, the distinction between these two types of components is a key new concept with critical implications for deforming coordinates.

In what follows we will make use of the partial derivatives of the basis and reciprocal basis vectors with respect to the coordinates. In flat space, these can be expressed as

$$\partial_i \boldsymbol{e}_j = \Gamma^k{}_{ij} \boldsymbol{e}_k \,, \qquad \partial_i \boldsymbol{e}^j = -\Gamma^j{}_{ik} \boldsymbol{e}^k \,, \tag{2.4}$$

where $\Gamma^k{}_{ij}$, the *Christoffel symbol of the second kind*, is defined as

$$\Gamma^k{}_{ij} \equiv \left(\partial_i \boldsymbol{e}_j\right) \cdot \boldsymbol{e}^k. \tag{2.5}$$

Thus $\Gamma^k{}_{ij}$ is the expansion coefficient for the derivative of the jth basis vector with respect to the ith coordinate that is associated with the kth basis vector. One may readily show the symmetry $\Gamma^k{}_{ij} = \Gamma^k{}_{ji}$ from (2.1) and the commutativity of partial derivatives. A readily computable expression for the Christoffel symbols will be presented shortly.

The extrinsic approach to tensor analysis offers important simplifications over the intrinsic approach common in general relativity. There, definitions may reference only the curved spacetime manifold because an extrinsic space is not observable. With an extrinsic space, however, we can think of basis vectors $\boldsymbol{e}_i$ simply as spatially and temporally varying arrows in physical space rather than abstractly as differential operators in the tangent space of the spacetime manifold. Furthermore, here the basis vectors $\boldsymbol{e}_i$ and reciprocal basis vectors $\boldsymbol{e}^i$ are elements of the same Euclidean vector space, whereas in general relativity the reciprocal basis $\boldsymbol{e}^i$ must be replaced with the dual basis $\mathrm{d}x^i$ of differential 1-forms in the cotangent space to the manifold. See section 2.4 of Carroll (2019) or section 1.4 of Ogden (1984) for further discussion.

The general, time-varying, curvilinear coordinate system x^i captures both the rotational acceleration and deformation required for GFD. In addition, we introduce a second, potentially curvilinear but rigid and inertial coordinate system y^a. On account of Galilean invariance we are free to choose an absolute reference for motion that defines this inertial coordinate system to be stationary.

A sketch is presented in Fig. 2.1, which also includes notation introduced subsequently. In order to clearly distinguish between tensor components referenced to these two systems, we adopt the convention of indexing any object as referenced from the non-inertial, deforming setting with the letters $\{i, j, k, \ell, ...\}$ and from the inertial frame with $\{a, b, c, d, ...\}$. The less common choices of letters in the latter case are intended to reflect the less common choice of an inertial coordinate system for GFD.

Let $\boldsymbol{s}$ be the position vector field associated with the y^a coordinate system, and $\boldsymbol{S} = \boldsymbol{s} - \boldsymbol{r}$ be the location of origin O_x of the x^i coordinates with respect to the origin O_y of the y^a system; see Figure 2.1. The y^a system has covariant basis vectors

$$\boldsymbol{e}_a \equiv \partial_a \boldsymbol{s} = \partial_a \boldsymbol{r} \; , \tag{2.6}$$

where $\partial_a \equiv \partial / \partial y^a$, and where the latter equality follows from the fact that $\boldsymbol{S}$ is spatially constant. Note that the basis vectors $\boldsymbol{e}_i$ and $\boldsymbol{e}_a$ are distinguished by their indices, as are the partial derivatives ∂_i and ∂_a, the Christoffel symbols $\Gamma^k{}_{ij}$ and $\Gamma^c{}_{ab}$, and so forth. While the curvilinear coordinates in the inertial y^a system may have complex spatial dependence, the time derivatives of these coordinates, their basis vectors, and any other quantities such as $\boldsymbol{s}$ and Christoffel symbols are all temporally constant. In the x^i system, the corresponding quantities may all vary in time.

2.2.2 Index notation

The extrinsic perspective allows a vector $\boldsymbol{w}$ to be equivalently represented in terms of the basis or the reciprocal basis as

$$\boldsymbol{w} = w^i \boldsymbol{e}_i = w_i \boldsymbol{e}^i \ , \tag{2.7}$$

where (2.2) is used to find the components as $w^i \equiv \boldsymbol{w} \cdot \boldsymbol{e}^i$ and $w_i \equiv \boldsymbol{w} \cdot \boldsymbol{e}_i$, called the *contravariant* and *covariant* components of $\boldsymbol{w}$, respectively. Note that we use the Einstein summation convention: any indices occurring in one upper and one lower position are understood to be summed over, so that $w^i \boldsymbol{e}_i$ means $\sum_{i=1}^{3} w^i \boldsymbol{e}_i$. For the special case of a Cartesian basis, the covariant and contravariant basis vectors are identical, and consequently so are the covariant and contravariant components of $\boldsymbol{w}$. In curvilinear coordinates, however, the index position is essential to keep track of which set of components is being considered.

Similarly, a second-order tensor $\boldsymbol{A}$ can be variously represented in terms of its contravariant, covariant, or mixed components as

$$\boldsymbol{A} = A^{ij} \boldsymbol{e}_i \otimes \boldsymbol{e}_j = A_{ij} \boldsymbol{e}^i \otimes \boldsymbol{e}^j = A^i{}_j \boldsymbol{e}_i \otimes \boldsymbol{e}^j = A_i{}^j \boldsymbol{e}^i \otimes \boldsymbol{e}_j, \tag{2.8}$$

where $\otimes$ denotes the tensor product. Each of these expressions involves a sum over nine elements, with two nested sums over three basis vectors in each sum. As with vector components, the tensor components can be found by projecting $\boldsymbol{A}$ onto the basis vectors, $A^{ij} \equiv \boldsymbol{e}^i \cdot \left(\boldsymbol{A}\boldsymbol{e}^j\right)$ and so forth, again using orthogonality (2.2) together with the defining property

$$(\boldsymbol{a} \otimes \boldsymbol{b})\, \boldsymbol{w} = \boldsymbol{a}\, (\boldsymbol{b} \cdot \boldsymbol{w}) \tag{2.9}$$

of the tensor product (see Itskov, 2015, section 1.7).

The index state of a set of tensor components—its number of indices together with their status as contravariant or covariant—is known as its *valence* (e.g., Needham, 2021, §33.1). Unlike the vector components w^i, the coordinates x^i are *not* the components of some vector field $\boldsymbol{x}$ as the notation appears to imply; they are just the numbers specifying the location of a particular point with respect to the chosen coordinate system. In particular, they are not the same as the components r^i of the position vector field $\boldsymbol{r}$, except in Cartesian coordinates.

We adopt the convention that the left-to-right order of the indices in expressions such as $A^{ij}\boldsymbol{e}_i \otimes \boldsymbol{e}_j$ must match between the components and the basis. With this convention, it becomes unnecessary to explicitly indicate the basis vectors that accompany any tensor's components, since their arrangement is evident from placement of the indices within the components. That is, the tensor component A^{ij} may be used to unambiguously refer to the entire tensor $A^{ij}\boldsymbol{e}_i \otimes \boldsymbol{e}_j$. Consequently, one need not write the basis vectors at all in evaluating tensor operations, just the relations among components. However, by the product rule the derivatives of tensors depend on both the derivatives of the components and the derivatives of the basis vectors. It follows that in order to dispense entirely with basis vectors some special machinery for expressing derivatives in terms of tensor components is needed, as introduced shortly.

2.2.3 Index juggling

The basis vectors and reciprocal basis vectors can be used to define the *metric coefficients*

$$g_{ij} \equiv \boldsymbol{e}_i \cdot \boldsymbol{e}_j, \qquad g^{ij} = \boldsymbol{e}^i \cdot \boldsymbol{e}^j \tag{2.10}$$

which are symmetric and are not equal to δ^i_j except in the special case of orthonormal basis sets. With these definitions, the contravariant and covariant components of the vector $\boldsymbol{w} = w^i\boldsymbol{e}_i = w_i\boldsymbol{e}^i$ can converted into one another. This conversion proceeds as

$$w_j g^{ji} = w_j \boldsymbol{e}^j \cdot \boldsymbol{e}^i = \boldsymbol{w} \cdot \boldsymbol{e}^i = w^j \boldsymbol{e}_j \cdot \boldsymbol{e}^i = w^j \delta^i_j = w^i \tag{2.11}$$

$$w^j g_{ji} = w^j \boldsymbol{e}_j \cdot \boldsymbol{e}_i = \boldsymbol{w} \cdot \boldsymbol{e}_i = w_j \boldsymbol{e}^j \cdot \boldsymbol{e}_i = w_j \delta^j_i = w_i \tag{2.12}$$

which together establish that

$$g^{ij}w_j = w^i, \qquad g_{ij}w^j = w_i. \tag{2.13}$$

Using the metric coefficients to convert between covariant and contravariant components is called *index raising and lowering*, *index juggling*, or *changing valence*. Note that index raising inverts index lowering, and thus

$$g^{ij}g_{jk} \equiv \delta^i_k, \tag{2.14}$$

which traditionally defines g^{ij}. The second of equations (2.10) follows from the first together with (2.14).

2.2.4 Tensor operations

When performing operations on tensors, we have the choice of working in symbolic notation with familiar operators such as $\times$, $\otimes$, and $\boldsymbol{\nabla}$, or in index notation where we represent the impact of these operation on tensor *components*. In Tables 2.1–2.3, we present translations between these two notations for common operations and identities. See section 1 of Itskov (2015) or Lilly et al. (2024) for the symbolic definitions of the tensor product $\boldsymbol{a}\otimes\boldsymbol{b}$, left operation $\boldsymbol{a}\boldsymbol{A}$, the tensor transpose $\boldsymbol{A}^T$, and the tensor trace $\mathrm{tr}\,(\boldsymbol{A})$, all of which may be defined without coordinates. Note that because $\boldsymbol{a}\cdot(\boldsymbol{A}\boldsymbol{b}) = (\boldsymbol{a}\boldsymbol{A})\cdot\boldsymbol{b}$, we may write simply $\boldsymbol{a}\boldsymbol{A}\boldsymbol{b}$.

The action of the tensor $\boldsymbol{A}$ on the vector $\boldsymbol{w}$ is represented as

$$\boldsymbol{A}\boldsymbol{w} = A^i{}_j\left(\boldsymbol{e}_i\otimes\boldsymbol{e}^j\right)w^k\boldsymbol{e}_k = A^i{}_j w^j\boldsymbol{e}_i \tag{2.15}$$

again using (2.9) and (2.2). But because the presence of the $\boldsymbol{e}_i$ can be inferred, we can write down $A^i{}_j w^j$ as an implicit representation of $\boldsymbol{A}\boldsymbol{w}$ without needing to carry out the intervening manipulations on the basis vectors. Matching an upper with a lower index in two tensor representations, as in $A^i{}_j w^j$, effects an inner product and is called *contraction*. Each contraction

Table 2.1: Common vector operations, written both in symbolic notation and in index notation, with the basis vectors associated with the index notation expressions shown in the final column. Here $\boldsymbol{\nabla} \equiv \boldsymbol{e}^i \partial_i$ denotes the familiar nabla or del operator as expressed in curvilinear coordinates, $\otimes$ denotes the tensor product, ∇_i is the covariant derivative acting on tensor components, and ε^{ijk} is the Levi-Civita or alternating tensor, all of which are defined subsequently. In later tables we will omit the final column because the basis is implied by index placement.

Name	Symbolic	Index	Basis
Inner product	$\boldsymbol{a} \cdot \boldsymbol{b}$	$a_i b^i$	—
Cross product	$\boldsymbol{a} \times \boldsymbol{b}$	$\varepsilon^{ijk} a_j b_k$	$\boldsymbol{e}_i$
Tensor product	$\boldsymbol{a} \otimes \boldsymbol{b}$	$a^i b_j$	$\boldsymbol{e}_i \otimes \boldsymbol{e}^j$
Gradient	$\boldsymbol{\nabla} \gamma$	$\nabla_i \gamma$	$\boldsymbol{e}^i$
Divergence	$\boldsymbol{\nabla} \cdot \boldsymbol{w}$	$\nabla_i w^i$	—
Curl	$\boldsymbol{\nabla} \times \boldsymbol{w}$	$\varepsilon^{ijk} \nabla_j w_k$	$\boldsymbol{e}_i$
Gradient tensor	$\boldsymbol{\nabla} \otimes \boldsymbol{w}$	$\nabla_i w^j$	$\boldsymbol{e}^i \otimes \boldsymbol{e}_j$

Table 2.2: Common vector identities involving the tensor product, written in both symbolic and index notation.

Name	Symbolic	Symbolic	Index
Tensor trace	$\mathrm{tr}\,(\boldsymbol{a} \otimes \boldsymbol{b})$	$\boldsymbol{a} \cdot \boldsymbol{b}$	$a_i b^i$
Right operation	$(\boldsymbol{a} \otimes \boldsymbol{b})\, \boldsymbol{w}$	$\boldsymbol{a}\,(\boldsymbol{b} \cdot \boldsymbol{w})$	$a^i b_j w^j$
Left operation	$\boldsymbol{w}\,(\boldsymbol{a} \otimes \boldsymbol{b})$	$(\boldsymbol{w} \cdot \boldsymbol{a})\, \boldsymbol{b}$	$w_i a^i b_j$
Transpose	$(\boldsymbol{a} \otimes \boldsymbol{b})^T$	$\boldsymbol{b} \otimes \boldsymbol{a}$	$b^i a_j$
Advection	$\boldsymbol{u}\,(\boldsymbol{\nabla} \otimes \boldsymbol{w})$	$(\boldsymbol{u} \cdot \boldsymbol{\nabla})\, \boldsymbol{w}$	$u^j \nabla_j w^i$
—	$\boldsymbol{u}\,(\boldsymbol{\nabla} \otimes \boldsymbol{w})^T$	$(\boldsymbol{\nabla} \otimes \boldsymbol{w})\, \boldsymbol{u}$	$u^j \nabla^i w_j$

involves the implicit dot product of a basis vector $\boldsymbol{e}_i$ and a reciprocal basis vector $\boldsymbol{e}^j$ using (2.2), reducing the degree of the tensor by two. Index notation readily accommodates multiple simultaneous contractions, easily identified by matching indices.

A particularly important tensor is the *identity tensor*, which in flat Euclidean space is given by

$$\boldsymbol{I} = g^{ij} \boldsymbol{e}_i \otimes \boldsymbol{e}_j = g_{ij} \boldsymbol{e}^i \otimes \boldsymbol{e}^j = \delta^i_j \boldsymbol{e}_i \otimes \boldsymbol{e}^j = \delta^j_i \boldsymbol{e}^i \otimes \boldsymbol{e}_j. \tag{2.16}$$

Its non-mixed components are the metric coefficients, while its mixed components are Kronecker delta functions. Given a flat, extrinsic space, g_{ij}, g^{ij}, and δ^i_j are all representations of $\boldsymbol{I}$ in precisely the same sense as the various representations of $\boldsymbol{A}$ in equation (2.8), and the metric $\boldsymbol{g}$ is nothing but the identity tensor $\boldsymbol{I}$. This tensor has the property that $\boldsymbol{I}\boldsymbol{w} = \boldsymbol{w}$ for all $\boldsymbol{w}$. The identity tensor is implicitly involved whenever the delta function is used in index notation, that is, $a_i \delta^i_j b^j = a_i b^i$ corresponds to the tensor equation $\boldsymbol{a}\boldsymbol{I}\boldsymbol{b} = \boldsymbol{a} \cdot \boldsymbol{b}$ with $\boldsymbol{I}$ chosen in a mixed representation. It is also implicitly involved in index juggling, since $g^{ij} w_j = w^i$ corresponds to the tensor equation $\boldsymbol{I}\boldsymbol{w} = \boldsymbol{w}$ with $\boldsymbol{I}$ chosen in a non-mixed representation. This is intuitive, because changing the representation of tensor components is an operation that does not change the tensor itself, that is, an identity operation.

Evaluation of the cross product and curl in index notation requires the introduction of an appropriate tensor operator. The *Levi-Civita symbol* ϵ_{ijk}, given by the rule

$$\epsilon_{ijk} = \epsilon^{ijk} \equiv \begin{cases} 1, & ijk \text{ an even permutation of } 123 \\ -1, & ijk \text{ an odd permutation of } 123 \\ 0, & \text{otherwise} \end{cases} \tag{2.17}$$

is used in turn to define the components of the *Levi-Civita tensor* $\boldsymbol{\varepsilon}$, also known as the *volume element*. Its covariant representation is

$$\varepsilon_{ijk} \equiv \sqrt{g}\epsilon_{ijk} \, , \tag{2.18}$$

where $g \equiv |g_{ij}|$ is the determinant of the metric components. With orthonormal basis vectors we have $g = 1$. The Levi-Civita tensor's indices may be raised in the usual way, and the contravariant components of $\boldsymbol{\varepsilon}$ are

$$\varepsilon^{ijk} = \frac{1}{\sqrt{g}}\epsilon^{ijk}. \tag{2.19}$$

Table 2.3: Operations for isolating the portions of a second-order tensor $\boldsymbol{A}$ exhibiting various types of symmetries in symbols and index notation.

Part	Symbolic	Index
Isotropic	$\frac{1}{3}\mathrm{tr}(\boldsymbol{A})\boldsymbol{I}$	$\frac{1}{3}g_{ij}A^k{}_k$
Symmetric	$\frac{1}{2}\left(\boldsymbol{A}+\boldsymbol{A}^T\right)$	$\frac{1}{2}\left(A_{ij}+A_{ji}\right) \equiv A_{(ij)}$
Skew-symmetric	$\frac{1}{2}\left(\boldsymbol{A}-\boldsymbol{A}^T\right)$	$\frac{1}{2}\left(A_{ij}-A_{ji}\right) \equiv A_{[ij]}$

The contraction of these two representations satisfies the useful identity

$$\varepsilon_{ijk}\varepsilon^{k\ell m} = \delta_i^\ell \delta_j^m - \delta_i^m \delta_j^\ell \tag{2.20}$$

which can be used to easily prove most of the triple-product identities that must be memorized or looked up for manipulation of symbolic equations.

Notation will be needed for isolating portions of a second-order tensor $\boldsymbol{A}$ exhibiting various types of symmetries, presented in Table 2.3. In symbolic notation, a tensor is said to *symmetric* if $\boldsymbol{A} = \boldsymbol{A}^T$ and *antisymmetric* or *skew-symmetric* if $\boldsymbol{A} = -\boldsymbol{A}^T$. In index notation, a tensor is symmetric if

$$A_{ij} = A_{ji}, \qquad A^i{}_j = A_j{}^i, \qquad A^{ij} = A^{ji} \tag{2.21}$$

and skew symmetric if

$$A_{ij} = -A_{ji}, \qquad A^i{}_j = -A_j{}^i, \qquad A^{ij} = -A^{ji}. \tag{2.22}$$

Using index juggling, all statements in (2.21) and (2.22) are shown to be true if any one of them is true. Note that for a symmetric tensor $\boldsymbol{A}$, there is no ambiguity in writing the mixed components as $A^i_j = A^i{}_j = A_j{}^i$, without the placeholder spaces; this is the case for the Kronecker delta δ^i_j.

This discussion has shown that explicitly writing the basis vectors is superfluous because all relevant information is already present in the placement of indices. However, rather than identify w^i and $A^i{}_j$ with a vector and second-order tensor respectively, as is sometimes done, we find it helpful to emphasize that w^i and $A^i{}_j$ are tensor *components* which only when paired with basis vectors yield the actual tensors. This underscores the fact that derivatives of the tensors involve derivatives of both the tensor components *and* the basis vectors, even if the basis vectors are not explicitly written.

2.3 Spatial derivatives in curvilinear coordinates

We would like to express not only changes in tensor representations but also spatial and temporal differentiation in component form without explicit reference to the basis vectors. This requires that a derivative be expressed in such a way that it involves an action only on the components of the tensor and not on the basis vectors. It can be shown that partial derivatives of tensor components such as $\partial_i w^j$ and $\partial_i A^j{}_k$ do not transform according to the tensor transformation law (2.24) and are thus not themselves the components of tensors. An extension of partial derivatives that accounts for changing basis vectors is thus required to express the spatial derivatives of tensors in component form. This is precisely what the Christoffel symbols defined in equations (2.4) and (2.5) express.

Though our original definitions of the Christoffel symbols are geometrically instructive, the symbols can also be calculated more straight-forwardly in terms of the metric coefficients as

$$\Gamma^i{}_{jk} = \frac{1}{2} g^{i\ell} (\partial_j g_{\ell k} + \partial_k g_{\ell j} - \partial_\ell g_{jk}) \ . \tag{2.23}$$

Under a change of basis, the components of a tensor transform according to the *tensor transformation law*

$$w^a = J^a_i w^i, \qquad w_a = J^i_a w_i, \qquad A^a{}_b = J^a_i J^j_b A^i{}_j, \tag{2.24}$$

where the *Jacobian coefficients* J^i_a and J^a_i are defined as

$$J^a_i \equiv \partial_i y^a, \qquad J^i_a \equiv \partial_a x^i \tag{2.25}$$

The transformation law (2.24) generalizes to tensors of any order, with a Jacobian contraction on each index. Note that in terms of the basis vectors, the Jacobian coefficients can also be written as[2]

$$J^a_i = \boldsymbol{e}_i \cdot \boldsymbol{e}^a, \qquad J^i_a = \boldsymbol{e}_a \cdot \boldsymbol{e}^i \ . \tag{2.26}$$

We also have, by the chain rule,

$$\boldsymbol{e}_i = J^a_i \boldsymbol{e}_a, \qquad \boldsymbol{e}_a = J^i_a \boldsymbol{e}_i, \tag{2.27}$$

meaning that J^a_i are the components of the $\boldsymbol{e}_i$ basis expanded in terms of the $\boldsymbol{e}_a$ basis, and conversely for J^i_a.

An indexed entity contains the components of a tensor *if and only if* it transforms according to (2.24). Indeed, this transformation law can be used as an alternate, equivalent definition of a tensor to the definition given above as a multilinear function on vectors, as shown in (1.6)–(1.10) of Jeevanjee (2011).

The Christoffel symbols $\Gamma^k{}_{ij}$ do not transform according to the tensor transformation law and are therefore not the components of a third-order tensor. A tensor with the same mixture of indices as $\Gamma^k{}_{ij}$ would transform according to

$$A^a{}_{bc} = J^a_i J^j_b J^k_c A^i{}_{jk} \ . \tag{2.28}$$

[2]To see this, note that the Jacobian J^i_a may be used to transform the basis vectors as $\boldsymbol{e}_a \equiv \partial_a \boldsymbol{s} = \partial_a \boldsymbol{r} = J^i_a \partial_i \boldsymbol{r} = J^i_a \boldsymbol{e}_i$. It then follows that $J^a_i = J^a_j \delta^j_i = J^a_j \left(\boldsymbol{e}_i \cdot \boldsymbol{e}^j\right) = \boldsymbol{e}_i \cdot J^a_j \boldsymbol{e}^j = \boldsymbol{e}_i \cdot \boldsymbol{e}^a$, and similarly for J^i_a.

The Christoffel symbols, however, follow the transformation law

$$\Gamma^a{}_{bc} = J^a_i J^j_b J^k_c \Gamma^i{}_{jk} + \boxed{J^a_i \frac{\partial^2 x^i}{\partial y^b \partial y^c}} \tag{2.29}$$

which differs from (2.28) in the boxed term. The reason the Christoffel symbols are not components of tensors is that $\Gamma^k{}_{ij}$, by construction according to (2.5), describes an aspect of the x^i coordinate system, namely how its basis vectors vary spatially. When we change coordinates to y^a, we are not simply changing the representation of the Christoffel symbols $\Gamma^k{}_{ij}$ but rather obtaining new quantities $\Gamma^a{}_{bc}$ that describe the spatial variations of a different set of basis vectors, the basis vectors $\boldsymbol{e}_a$ of the y^a system.

Nevertheless, the Christoffel symbols can be said to resemble tensors in the sense that the upper index and/or either one of the two lower indices will transform according to the transformation law, but both lower indices together will not. This can be understood using their definitions $\Gamma^k{}_{ij} \equiv \left(\partial_i \boldsymbol{e}_j\right) \cdot \boldsymbol{e}^k$ and $\Gamma^c{}_{ab} \equiv \left(\partial_a \boldsymbol{e}_b\right) \cdot \boldsymbol{e}^c$. The upper index k of $\Gamma^k{}_{ij}$ corresponds to the basis vectors we are expanding in; this index will therefore transform like the contravariant components of a tensor. The first lower index i corresponds to the coordinate system in which we are taking a partial derivative; this index will transform like the covariant components of a tensor. From the symmetry $\Gamma^k{}_{ij} = \Gamma^k{}_{ji}$, the second lower index can also be transformed like a tensor. Yet $\partial_i \boldsymbol{e}_j$ together does not transform like a tensor in j because this would require $\partial_i J^a_j = 0$, which is not the case in general; thus both lower indices do not simultaneously transform according to the tensor transformation law.

2.3.1 Changing representations involve the identity tensor

It builds intuition to highlight a detail that we have not seen discussed in the literature, namely the role of the identity tensor $\boldsymbol{I}$ in changing tensor representations. As discussed in section 2.2.4, in Euclidean space the action of index juggling implicitly involves the identity tensor, since $g^{ij} w_j = w^i$ corresponds to the tensor equation $\boldsymbol{I}\boldsymbol{w} = \boldsymbol{w}$ with $\boldsymbol{I} = g^{ij} \boldsymbol{e}_i \otimes \boldsymbol{e}_j$. However, the identity tensor can also be written in the form

$$\boldsymbol{I} = J^a_i \boldsymbol{e}_a \otimes \boldsymbol{e}^i = J^i_a \boldsymbol{e}_i \otimes \boldsymbol{e}^a, \tag{2.30}$$

in which case the coefficients of the basis vectors are seen to be the Jacobian coefficients. In this form it is clear that changing representations from one basis to another also involves the identity tensor, since $w^a = J^a_i w^i$ again corresponds to $\boldsymbol{I}\boldsymbol{w} = \boldsymbol{w}$ but now with $\boldsymbol{I} = J^a_i \boldsymbol{e}_a \otimes \boldsymbol{e}^i$. In both cases the effect is to express the tensor in a new representation without changing the tensor itself. Moreover, combining (2.16) with (2.30), we also see that in Euclidean space, the Kronecker delta, the metric coefficients, and the Jacobian coefficients are all different representations of the identity tensor $\boldsymbol{I}$.

This clarifies several points of ambiguity in the literature. Commonly g_{ij} is referred to as the *metric tensor*, but from our extrinsic perspective, there is no separate "metric" tensor having the g_{ij} as its covariant components apart from the identity tensor $\boldsymbol{I} = g_{ij} \boldsymbol{e}^i \otimes \boldsymbol{e}^j$. For this reason we refer to g_{ij} as the metric *coefficients* or *components*, as opposed to the metric *tensor*. At the same time, is also often said that the Jacobians are not tensors. However for our purposes the Jacobian coefficients have the same status as the metric coefficients—they are components of the identity tensor, but in a representation that uses a basis and a reciprocal basis drawn from two different coordinate system, as in (2.30). The equal status of these two sets of coefficients is also apparent if one observes that $g_{ij} \equiv \boldsymbol{e}_i \cdot \boldsymbol{e}_j$ while similarly $J^i_a = \boldsymbol{e}_a \cdot \boldsymbol{e}^i$.

2.3.2 Spatial differentiation

Taking the partial spatial derivative of a vector $\boldsymbol{w}$ with respect to the ith coordinate, we find

$$\partial_i \boldsymbol{w} = \partial_i (w^j \boldsymbol{e}_j) = \boldsymbol{e}_j \partial_i w^j + \boxed{w^j \partial_i \boldsymbol{e}_j}\,, \tag{2.31}$$

which illustrates that the components of the derivative of a tensor are not the derivatives of its components; spatial variations in the basis vectors will contribute via the boxed term, which itself is equivalent to $w^j \Gamma^k{}_{ij} \boldsymbol{e}_k$, by equation (2.4). The partial derivative $\partial_i \boldsymbol{w}$ can be rewritten as

$$\partial_i \boldsymbol{w} = \boldsymbol{e}_j \left(\partial_i w^j + \Gamma^j{}_{ik} w^k \right) \equiv \boldsymbol{e}_j \nabla_i w^j \tag{2.32}$$

Here $\nabla_i w^j$ is known as the *covariant derivative* of w^j, and has been constructed to express the action of taking the partial spatial derivative of a vector in terms of an operation on its components.

The covariant derivative of the components of a tensor takes on a different form depending upon the tensor's order and the valence of its representation. For a scalar or zero-rank tensor field we have the simple relation $\nabla_i a \equiv \partial_i a$, while for a second-order tensor $\boldsymbol{A}$ expressed in mixed component form the covariant derivative is

$$\nabla_i A^j_k \equiv \partial_i A^j_k + \Gamma^j{}_{i\ell} A^\ell_k - \Gamma^\ell{}_{ik} A^j_\ell . \tag{2.33}$$

This pattern extends in the obvious way to tensor components of different orders and valences, with a positive Christoffel term for each upper index and a negative term for each lower index. Importantly, the covariant derivative exhibits the usual properties, such as the product rule,

$$\nabla_i \left(a^j b_k \right) = a^j \nabla_i b_k + b_k \nabla_i a^j , \tag{2.34}$$

and linearity; see section 8.6 of Grinfeld (2013).

When it acts on the components of an nth order tensor, the covariant derivative produces components of an $(n+1)$th order tensor, and indeed this was the entire point of defining it this way. This means we can also define the *contravariant derivative*

$$\nabla^i \equiv g^{ij} \nabla_j \ . \tag{2.35}$$

In Table 2.1 we see how the covariant derivative is used to write various types of spatial derivatives as actions on tensor components. Importantly, when the coordinate system spans the three dimensions of Euclidean space, covariant differentiation of a tensor component corresponds to partial differentiation of the tensor itself, as is evident from fact that $\nabla_i w^j$ is the jth component of $\partial_i \boldsymbol{w}$ from (2.32); this will no longer be the case when the covariant derivative is applied along a curved manifold, such as in general relativity or along a curved surface embedded in three dimensional Euclidean space, see Chapter 11 of Grinfeld (2013).

The gradient tensor of a vector $\boldsymbol{w}$ is $\boldsymbol{\nabla} \otimes \boldsymbol{w}$ and has components $\nabla_i w^j$. A notable example is the gradient of the position vector $\boldsymbol{r}$, for which one finds

$$\boldsymbol{\nabla} \otimes \boldsymbol{r} = \boldsymbol{I}, \qquad \nabla_j r^i = \delta^i_j \,, \tag{2.36}$$

which is readily shown in Cartesian coordinates.[3]

The covariant derivative has the crucial property that its application to the metric coefficients vanishes,

$$\nabla_i g^{jk} = 0, \qquad \nabla_i g_{jk} = 0, \qquad \nabla_i \delta^j_k = 0, \tag{2.37}$$

a result known as *Ricci's theorem*, *metric compatibility*, or the *metrinilic property*. This means that we can freely raise and lower indices across the derivative. As confirmed in Appendix A, its application to the Jacobian coefficients also vanishes

$$\nabla_i J^a_j = 0, \quad \nabla_i J^j_a = 0, \quad \nabla_a J^i_b = 0, \quad \nabla_a J^b_i = 0, \tag{2.38}$$

but this had to be the case since it was designed to produce tensor components from tensor components—we have to be able to change bases through the derivative for this to be true.

It may similarly be shown that the application of the covariant derivative to the Levi-Civita

[3]In Cartesian coordinates $r^i = \{x, y, z\}$ and $\nabla_j = \partial_j$, so $\nabla_j r^i = \partial_j r^i = \delta^i_j$. It then follows from the tensor transformation law that this holds for any other coordinates y^a: $J^a_i J^j_b \delta^i_j = J^a_i J^i_b = \delta^a_b$.

tensor vanishes,

$$\nabla_\ell \varepsilon_{ijk} = 0, \qquad \nabla_\ell \varepsilon^{ijk} = 0, \tag{2.39}$$

meaning that the covariant derivative and the Levi-Civita tensor also commute.

2.3.3 Index swapping rules

In changing representations between the $\boldsymbol{e}_i$ and the $\boldsymbol{e}_a$ bases, the following rules will prove useful. Any repeated indices that generate proper tensors may be freely swapped between the $\{i, j, k\}$ and $\{a, b, c\}$ index sets, e.g.,

$$w^i \boldsymbol{e}_i = w^a \boldsymbol{e}_a, \qquad A_i{}^j \boldsymbol{e}^i \otimes \boldsymbol{e}_j = A_i{}^b \boldsymbol{e}^i \otimes \boldsymbol{e}_b \ . \tag{2.40}$$

Any contracted indices on tensor components can likewise be swapped, e.g.,

$$u^i v_i = u^a v_a, \qquad A_{ab} w^b = A_{ai} w^i. \tag{2.41}$$

For the Christoffel symbols, contractions that involve the upper index and/or one of the two lower indices may be swapped, but not those involving both lower indices:

$$\begin{aligned} \Gamma^i{}_{jk} u_i v^j w^k &= \Gamma^a{}_{jk} u_a v^j w^k = \Gamma^a{}_{bk} u_a v^b w^k \\ &= \Gamma^a{}_{jc} u_a v^j w^c \neq \Gamma^a{}_{bc} u_a v^b w^c. \end{aligned} \tag{2.42}$$

Although partial derivatives of tensor components are not in general tensor components, indices of *contracted* partial derivatives may also be swapped via

$$u^i \partial_i v^j = u^a \partial_a v^j. \tag{2.43}$$

This follows from the chain rule and the definitions (2.25), but we can also use (2.32) to rewrite expressions involving partial derivatives in terms of the covariant derivative and the Christoffel symbols, for example

$$u^i \partial_i v^j = u^i \nabla_i v^j - \Gamma^j_{\ \ ik} u^i v^k. \tag{2.44}$$

We see that swapping the i index for a only requires one of the two lower indices of the Christoffel symbol to change, and is therefore permissible.

2.4 Time derivatives in curvilinear coordinates

In order to determine the momentum equation in a generally accelerating, rotating, and deforming coordinate system, we need an analogue of the covariant derivative for temporal differentiation. That is, we need a way to compute total time derivatives of tensor fields by operating only on their components. This section introduces such a derivative, first presenting a known result for fixed coordinate systems, and then introducing a generalization that accommodates moving, deforming coordinates.

2.4.1 Frames and settings

Consider the coordinate system y^a, which we have introduced as being both rigid and inertial. In fact, both of these properties more properly pertain not to the coordinate system y^a, but rather to the *frame* in which it is embedded. We define a frame to be an imaginary, rigid lattice extending throughout space, in comparison to which Newtonian motion may be measured (see e.g., Koks, 2017). Given a non-accelerating frame, any curvilinear coordinate system that is fixed with respect to that frame will inherit its rigidity and inertiality. Thus, referring to y^a as a rigid, inertial *coordinate system* is simply a shorthand for saying that it is a coordinate system embedded within an inertial *frame*. Recall that we have employed Galilean invariance to regard this inertial frame as stationary.

The x^i coordinate surfaces, by contrast, are allowed to evolve with respect to the inertial frame according to any combination of translation, rotation, and deformation. Because these coordinates are permitted to exhibit non-rigid motion, it is not possible to fix them within any

Table 2.4: A table of different time derivatives appearing in this work. χ is a general path along which differentiation occurs. We understand the material derivative of a tensor to be taken following a fixed parcel label ξ. The intrinsic derivatives are constructed to produce components of the corresponding total derivatives acting on tensors. One further sort of time derivative, the convected derivative of Oldroyd (1950), is discussed in Appendix E and omitted here.

Name	Symbol	Argument
Total along path χ	$\frac{d}{dt}\Big\rvert^{\chi}$	Tensor
Total Material	$\frac{d}{dt} \equiv \frac{d}{dt}\Big\rvert^{\chi_\xi} \equiv \frac{d}{dt}\Big\rvert_{\xi}$	Tensor
Partial with fixed x	$\frac{\partial}{\partial t}\Big\rvert_{x}$	Either
Partial with fixed y	$\frac{\partial}{\partial t}\Big\rvert_{y}$	Either
Covariant Advection	$\nabla_{\boldsymbol{v}} \equiv v^k \nabla_k = v^c \nabla_c$	Components
Lie Advection	$\mathcal{L}_{\boldsymbol{v}}$	Components
Intrinsic	$\frac{\delta}{\delta t}\Big\rvert^{\chi}$	Components
Intrinsic Material	$\frac{\delta}{\delta t} \equiv \frac{\delta}{\delta t}\Big\rvert^{\chi_\xi} \equiv \frac{\delta}{\delta t}\Big\rvert_{\xi}$	Components

rigid frame. We instead introduce the term *setting* to indicate a deformable frame-like entity, visualizable in two dimensions as an evolving, stretching rubber sheet onto which coordinate lines are marked; in the case without deformation, a setting becomes a frame. For brevity we refer to the x^i coordinates as being within the *moving setting*.

Since the x^i coordinate surfaces are allowed to be temporally varying, it follows that the basis vectors $\boldsymbol{e}_i$, metric coefficients g_{ij} and g^{ij}, and Christoffel symbols $\Gamma^k{}_{ij}$ vary as well. Meanwhile, the y^a coordinate surfaces and hence basis vectors $\boldsymbol{e}_a$, metric coefficients g_{ab} and g^{ab}, and Christoffel symbols $\Gamma^c{}_{ab}$ are all temporally constant. The Jacobian coefficients J^a_i and J^i_a for converting between the two coordinate systems will also vary in time as the x^i coordinates do. All of these quantities are permitted to be spatially varying.

The two coordinate systems are related as follows, sketched in Fig. 2.1. The origin $O_x(t)$ of the coordinate system in the moving setting is located at position vector $\boldsymbol{S}(t)$ with respect to the origin O_y of the coordinate system in the inertial frame. Let $\boldsymbol{r}$ be a position vector with respect to the origin of the moving coordinate system O_x, and $\boldsymbol{s}$ a position vector with respect to the origin of the inertial coordinate system O_y, with $\boldsymbol{s} = \boldsymbol{r} + \boldsymbol{S}$.

It is assumed that our coordinate systems are sufficiently well-behaved that they can be related by invertible sets of differentiable functions, allowing one to translate freely between the names given to a particular point in each system. That is, we can write each coordinate system in terms of the other as

$$x^i(y,t), \qquad y^a(x,t), \tag{2.45}$$

where we suppress coordinate indices within function arguments. Differentiating each set of coordinates with the other held fixed yields two velocity fields, $\boldsymbol{\mathcal{U}}$ and $\boldsymbol{\mathcal{V}}$, having components

$$\mathcal{U}^i \equiv \left.\frac{\partial x^i}{\partial t}\right|_y, \qquad \mathcal{V}^a \equiv \left.\frac{\partial y^a}{\partial t}\right|_x. \tag{2.46}$$

At each point in space $\boldsymbol{\mathcal{U}} = \mathcal{U}^i \boldsymbol{e}_i$ is the velocity of the inertial frame as observed from the moving setting, while $\boldsymbol{\mathcal{V}} = \mathcal{V}^a \boldsymbol{e}_a$ is the velocity of the moving setting as observed from the inertial frame.

Clearly these velocity fields are equal and opposite, $\boldsymbol{\mathcal{U}} = -\boldsymbol{\mathcal{V}}$, although they both may vary in space and time. Following the tensor transformation law, each field is expressible in terms of the other basis as

$$\mathcal{U}^a \equiv J_i^a \mathcal{U}^i, \qquad \mathcal{V}^i \equiv J_a^i \mathcal{V}^a, \tag{2.47}$$

where $J_i^a \equiv \partial_i y^a$ and $J_a^i \equiv \partial_a x^i$ are the Jacobian coefficients defined earlier in (2.25), such that $\boldsymbol{\mathcal{V}} = \mathcal{V}^i \boldsymbol{e}_i = \mathcal{V}^a \boldsymbol{e}_a$, and similarly for $\boldsymbol{\mathcal{U}}$. Because the inertial coordinate system is assumed to be stationary, $\boldsymbol{\mathcal{V}}$ is the absolute velocity of the moving setting. Hereafter we use only $\boldsymbol{\mathcal{V}}$, which we name the *setting velocity field*.

Let the scalar field ξ be a label that remains constant following fluid parcels. Differentiating each set of coordinates with the label ξ held fixed yields two velocity fields characterizing the fluid motion, $\boldsymbol{u} = u^i \boldsymbol{e}_i$ and $\boldsymbol{v} = v^a \boldsymbol{e}_a$, with components given by

$$u^i \equiv \left.\frac{dx^i}{dt}\right|_\xi, \qquad v^a \equiv \left.\frac{dy^a}{dt}\right|_\xi. \tag{2.48}$$

The velocity field $\boldsymbol{u}$ is the *relative velocity* observed with respect to the moving setting while $\boldsymbol{v}$ is the *absolute velocity*. Although these velocity fields make the most sense in the setting where they are easily observed, they are vector fields and can therefore be expressed in components relative to the basis vectors of the other setting,

$$u^a \equiv J_i^a u^i, \qquad v^i \equiv J_a^i v^a. \tag{2.49}$$

These two velocity fields are related as follows: considering the x^i coordinates to be a function of parcel label and time, $x^i(\xi,t)$, we have

$$\left.\frac{d}{dt} y^a[x(\xi,t),t]\right|_\xi = J_i^a \left.\frac{dx^i}{dt}\right|_\xi + \left.\frac{\partial y^a}{\partial t}\right|_x, \tag{2.50}$$

which reduces to $v^a = u^a + \mathcal{V}^a$. Consequently

$$\boldsymbol{v} = \boldsymbol{u} + \boldsymbol{\mathcal{V}}. \tag{2.51}$$

The absolute velocity of the fluid $\boldsymbol{v}$ is thus the sum of its velocity $\boldsymbol{u}$ relative to the moving setting and the setting velocity $\boldsymbol{\mathcal{V}}$ due to the motion of the x setting itself. This is precisely what we should expect.

If the coordinate system x^i is embedded within a frame of reference rotating with the planet, then $\boldsymbol{\mathcal{V}}$ is the planetary velocity and $\boldsymbol{u}$ is the velocity relative to the planet. In cases where the x^i coordinates deform relative to the planet, for example in isopycnal or pressure coordinates, the setting velocity $\boldsymbol{\mathcal{V}}$ captures this coordinate motion as well as the planetary motion.

2.4.2 The intrinsic derivative in static frames

Next we present a standard indicial expression for the derivative along an arbitrary curve, the *intrinsic derivative*, which allows us to express the material derivative following fluid parcels as a special case. The intrinsic derivative is defined in the literature only for *static* coordinate systems and requires generalization to accommodate rotating or deforming coordinate systems x^i.

Let $\chi(t)$ be some parametrized curve, with coordinates $\chi^a(t)$ and $\chi^i(t)$ within the y^a and x^i coordinate systems respectively, and write $f[\chi(t), t]$ to denote the restriction of the field f to the curve χ. We use the notation

$$\left.\frac{df}{dt}\right|^{\chi} \equiv \frac{d}{dt} f[\chi(t), t] \tag{2.52}$$

to mean the total time derivative of f evaluated along χ, which is independent of the coordinates we use to represent χ. This notation is intended to be distinct from $df/dt|_Q$, which means that the derivative is taken with the quantity Q held at a fixed value.

The rates of change of the x^i and y^a coordinates as one moves along the curve χ specify two sets of tangent vectors, $\boldsymbol{p}[\chi(t)] = p^i \boldsymbol{e}_i$ and $\boldsymbol{q}[\chi(t)] = q^a \boldsymbol{e}_a$, called the *parametric velocities*, having components

$$p^i \equiv \left.\frac{dx^i}{dt}\right|^{\chi}, \qquad q^a \equiv \left.\frac{dy^a}{dt}\right|^{\chi}. \tag{2.53}$$

These give the apparent velocity of motion following the parameterized curve as observed with respect to the moving setting and the inertial frame, respectively. We emphasize that these are *not* material velocities—they correspond to the rate of change of a position along any chosen curve $\chi(t)$, and are in general completely independent of the velocity of the fluid in which the curve is embedded. By reasoning analogous to (2.50) and (2.51), we arrive at

$$\boldsymbol{q} = \boldsymbol{p} + \boldsymbol{\mathcal{V}}. \tag{2.54}$$

When f is considered to be a function of the y^a coordinates, $f = f[\chi^a(t), t]$, its derivative along χ is

$$\left.\frac{df}{dt}\right|^{\chi} = \left.\frac{\partial f}{\partial t}\right|_y + q^b \partial_b f \tag{2.55}$$

from the chain rule. When applied to a vector field $\boldsymbol{w}$, the total derivative along χ can be expressed as

$$\begin{aligned} \left.\frac{d\boldsymbol{w}}{dt}\right|^{\chi} &= \left.\frac{\partial \boldsymbol{w}}{\partial t}\right|_y + q^b \partial_b \boldsymbol{w} \\ &= \boldsymbol{e}_a \left(\left.\frac{\partial}{\partial t}\right|_y + q^b \nabla_b \right) w^a \end{aligned} \tag{2.56}$$

from the fact that the basis vectors $\boldsymbol{e}_a$ are temporally constant combined with the definition of the covariant derivative in (2.32). We can thus define the *intrinsic derivative*

$$\left.\frac{\delta}{\delta t}\right|^{\chi} \equiv \left(\left.\frac{\partial}{\partial t}\right|_y + q^b \nabla_b \right), \tag{2.57}$$

acting on tensor components, allowing us to write

$$\left.\frac{d\boldsymbol{w}}{dt}\right|^{\chi} = \left.\frac{\delta w^a}{\delta t}\right|^{\chi} \boldsymbol{e}_a. \tag{2.58}$$

See §7.55 of Aris (1962) or §8.9 of Grinfeld (2013) for extended discussion of this operator.

The action of the intrinsic derivative is to express the total time derivative along the curve $\chi(t)$ in static but curvilinear coordinate systems in terms of operations on tensor components alone. Put another way: when we apply the intrinsic derivative to the components of a tensor, what we are doing is taking the total time derivative of that tensor along the specified curve. The form of the intrinsic derivative given in (2.57) is independent of the order and valence of the tensor components on which it operates because this dependence is already accounted for by the covariant derivative. Finally, we reiterate that equation (2.57) is valid only for tensor components with respect to fixed basis vectors.

2.4.3 The material derivative in static frames

We now choose a curve, denoted $\chi_\xi(t)$, to follow the fluid parcel ξ, and then allow ξ to take on all possible label values, such that $\chi_\xi(t)$ specifies the paths of all fluid parcels. The total derivative along the curve $\chi_\xi(t)$ following fluid parcels for each value of ξ—that is, the *material derivative*—of some tensor quantity f is then given by

$$\left.\frac{df}{dt}\right|^{\chi_\xi} = \frac{d}{dt} f[\chi_\xi(t), t]. \tag{2.59}$$

From (2.53), the parametric velocity components p^i and q^a evaluated along the paths of fluid parcels become

$$p^i|^{\chi_\xi} \equiv \left.\frac{dx^i}{dt}\right|_\xi = u^i, \qquad q^a|^{\chi_\xi} \equiv \left.\frac{dy^a}{dt}\right|_\xi = v^a. \tag{2.60}$$

from (2.48). This emphasizes that the fluid velocities $\boldsymbol{u}$ and $\boldsymbol{v}$ are a special case of the parametric velocities $\boldsymbol{p}$ and $\boldsymbol{q}$ along a family of curves, when those curves are taken to follow fluid parcels.

We define the *material intrinsic derivative*

$$\frac{\delta}{\delta t} \equiv \left(\left.\frac{\partial}{\partial t}\right|_y + v^b \nabla_b \right) \tag{2.61}$$

Applied to a vector field $\boldsymbol{w}$, this is written in terms of the inertial y^a coordinates as

$$\left.\frac{d\boldsymbol{w}}{dt}\right|^{\chi_\xi} = \frac{\delta w^a}{\delta t} \boldsymbol{e}_a, \tag{2.62}$$

This is simply the intrinsic derivative (2.57) evaluated along fluid parcel trajectories, for which the parametric velocity $\boldsymbol{q}$ has been set to the absolute fluid velocity $\boldsymbol{v}$, and again the form (2.61) is only valid for static coordinate systems. For convenience, we define the undecorated symbol $\delta/\delta t$ to be the particular, material case of the intrinsic derivative along a curve because this version is most common in our applications. If we need to differentiate along some other path χ, we denote that explicitly by "$(\cdot)|^\chi$."

2.4.4 Velocities and settings

We pause momentarily to investigate the relationship between the vector fields $\boldsymbol{p}$ and $\boldsymbol{q}$, and to clarify the notion of a setting. As in Fig. 2.1, let $\boldsymbol{r}$ and $\boldsymbol{s}$ be the position vectors measured from the origins O_x and O_y respectively to some point in space. Due to the motion of the basis vectors, $\boldsymbol{r}$ may change even with coordinates x^i held fixed. However, on account of our choice that the inertial coordinate system y^a be embedded within a stationary frame, $\boldsymbol{s}$ may *not* change with y^a held fixed. Consequently, considering the position vectors along the curve $\chi(t)$, we see that $\boldsymbol{r}[\chi(t), t]$ is an explicit function of time but $\boldsymbol{s}[\chi(t)]$ is not.

Taking the time derivatives of these position vector along the curve $\chi(t)$ then leads to

$$\left.\frac{d\boldsymbol{r}}{dt}\right|^{\chi} = \boldsymbol{p} + \left.\frac{\partial \boldsymbol{r}}{\partial t}\right|_x, \qquad \left.\frac{d\boldsymbol{s}}{dt}\right|^{\chi} = \boldsymbol{q} \tag{2.63}$$

from $\boldsymbol{e}_i \equiv \partial_i \boldsymbol{r}$ and $\boldsymbol{e}_a \equiv \partial_a \boldsymbol{s}$, together with the definitions of $\boldsymbol{p}$ and $\boldsymbol{q}$ in (2.53). Thus the rate of change of the position vector $\boldsymbol{s}$ measured with respect to the inertial frame (which has been chosen to be stationary) is the same as the vector field $\boldsymbol{q}$ observed in that frame, but the same is not true for the moving setting. In the moving setting, an additional contribution $\partial \boldsymbol{r}/\partial t|_x$ appears due to the motion of the coordinate surfaces themselves. We name $\partial \boldsymbol{r}/\partial t|_x$ the *inherent velocity field* since it is an inherent property of the setting, not of the fluid motion. The simplest case of a non-zero inherent velocity field is that due to rigid rotation.

We may now make the following key observation with respect to settings: if two different coordinate systems have the same inherent velocity fields, they share the same setting. In this case, all coordinate locations in one coordinate system remain at the same coordinate locations in the other system even as the setting moves or deforms. These two coordinate systems can then be visualized in two dimensions as two different sets of lines on the same deformable rubber sheet. Like a frame, a setting therefore does not depend upon or imply a choice of coordinates, even if a particular coordinate system was involved in its initial specification.

The inherent velocity field $\partial \boldsymbol{r}/\partial t|_x$ is related to the setting velocity $\boldsymbol{\mathcal{V}}$, as will now be shown. Since $\boldsymbol{s} = \boldsymbol{r} + \boldsymbol{S}$, see Fig. 2.1, we can take the total derivative of this equation along curves $\chi(t)$ to yield, using (2.63) and (2.60),

$$\boldsymbol{q} = \boldsymbol{p} + \left.\frac{\partial \boldsymbol{r}}{\partial t}\right|_x + \frac{d\boldsymbol{S}}{dt}. \tag{2.64}$$

Since $\boldsymbol{S}$ is spatially constant for a given time, we also have

$$\frac{d\boldsymbol{S}}{dt} = \left.\frac{\partial \boldsymbol{S}}{\partial t}\right|_x = \left.\frac{\partial \boldsymbol{S}}{\partial t}\right|_y \tag{2.65}$$

Comparison with (2.54) then shows

$$\boldsymbol{\mathcal{V}} = \left.\frac{\partial \boldsymbol{r}}{\partial t}\right|_x + \frac{d\boldsymbol{S}}{dt} = \left.\frac{\partial \boldsymbol{s}}{\partial t}\right|_x, \tag{2.66}$$

which means that the setting velocity field $\boldsymbol{\mathcal{V}}$ consists of the inherent velocity of the moving setting $\partial \boldsymbol{r}/\partial t|_x$ plus $d\boldsymbol{S}/dt$, the velocity of the origin of the moving setting. This is equivalent to the apparent velocity of the absolute location vector $\boldsymbol{s}$ as viewed from the moving setting. In the common case that x^i and y^a have coincident origins, this reduces to $\boldsymbol{\mathcal{V}} = \partial \boldsymbol{r}/\partial t|_x = \partial \boldsymbol{s}/\partial t|_x$.

2.4.5 Transforming rates of change

In order to derive the intrinsic derivative in the moving setting we must be able to transform partial time derivatives between inertial frames and moving settings. The partial time derivative of a function f at a fixed x location is, by the chain rule,

$$\left.\frac{\partial f}{\partial t}\right|_x = \left.\frac{\partial f}{\partial t}\right|_y + \mathcal{V}^a \partial_a f \tag{2.67}$$

where f is regarded first as a function of the x^i and then of the y^a coordinates. Thus we have

$$\left.\frac{\partial}{\partial t}\right|_x = \left(\left.\frac{\partial}{\partial t}\right|_y + \mathcal{V}^b \partial_b\right) \tag{2.68}$$

where the operand field on the left-hand side is understood to depend explicitly on x while that on the right-hand side is understood to depend explicitly on y, as indicated respectively by the "$|_x$" and "$|_y$" notation. Proceeding as above but for the derivative $\partial f/\partial t|_y$, one finds

$$\left.\frac{\partial}{\partial t}\right|_y = \left(\left.\frac{\partial}{\partial t}\right|_x - \mathcal{V}^j \partial_j\right) \tag{2.69}$$

as the inverse transformation to (2.68). These relationships are a consequence only of functional dependence and therefore hold for general functions, which might be tensors of any order, their components, or even non-tensor functions like the Christoffel symbols.

While the rates of change of the basis vectors $\boldsymbol{e}_a$ at fixed y vanish, those of the basis vectors $\boldsymbol{e}_i$ at fixed x are found to be

$$\left.\frac{\partial \boldsymbol{e}_i}{\partial t}\right|_x = \boldsymbol{e}_j \nabla_i \mathcal{V}^j \ . \tag{2.70}$$

Temporal changes in $\boldsymbol{e}_i$ and spatial gradients of $\boldsymbol{\mathcal{V}}$ are then just two representations of the same phenomenon.[4] We may also note the useful fact that the temporal derivative of the setting velocity $\mathcal{V}$ at a fixed location in the inertial frame can be expressed as

$$\boldsymbol{e}^a \cdot \left.\frac{\partial \boldsymbol{\mathcal{V}}}{\partial t}\right|_y = \left.\frac{\partial \mathcal{V}^a}{\partial t}\right|_y = J^a_i \left.\frac{\partial \mathcal{V}^i}{\partial t}\right|_x . \tag{2.71}$$

Thus these follow the tensor transformation law for vector components. Notice that the coordinates held fixed during differentiation differ on either side of the second equality. This property is particular to the setting velocity $\mathcal{V}$ and is not true for tensors in general.[5] This point will be crucial when we come to the momentum equation (2.90).

2.4.6 The intrinsic derivative in moving settings

We are now able to generalize the intrinsic derivative to a rotating, deforming setting. The derivative of vector field $\boldsymbol{w}$ along a curve χ, as expressed in terms of its contravariant components in the moving coordinate system x^i, is

$$\left.\frac{d\boldsymbol{w}}{dt}\right|^{\chi} = \left(\left.\frac{\partial}{\partial t}\right|_x + p^j \partial_j\right)\left(w^i \boldsymbol{e}_i\right) = \left.\frac{\partial w^i}{\partial t}\right|_x \boldsymbol{e}_i + p^j \partial_j \boldsymbol{w} + \boxed{w^i \left.\frac{\partial \boldsymbol{e}_i}{\partial t}\right|_x} \tag{2.74}$$

---

[4]As a brief proof, we note

$$\left.\frac{\partial \boldsymbol{e}_i}{\partial t}\right|_x = \left.\frac{\partial}{\partial t}\right|_x \frac{\partial \boldsymbol{r}}{\partial x^i} = \frac{\partial}{\partial x^i} \left.\frac{\partial \boldsymbol{r}}{\partial t}\right|_x$$

just by reversing the order of the partial derivatives. Substituting from (2.66), this becomes

$$\left.\frac{\partial \boldsymbol{e}_i}{\partial t}\right|_x = \partial_i\left(\boldsymbol{\mathcal{V}} - \frac{d\boldsymbol{S}}{dt}\right) = \partial_i \boldsymbol{\mathcal{V}} = \boldsymbol{e}_j \nabla_i \mathcal{V}^j$$

using the fact that $\boldsymbol{S}$ is spatially constant together with the definition of the covariant derivative in (2.32).

[5]The first equality in (2.71) is true because the $\boldsymbol{e}_a$ are constant in time, and to verify the second equality we use (2.69) to write

$$\left.\frac{\partial \boldsymbol{\mathcal{V}}}{\partial t}\right|_y = \left.\frac{\partial}{\partial t}\right|_x \left(\mathcal{V}^i \boldsymbol{e}_i\right) - \mathcal{V}^i \partial_i \boldsymbol{\mathcal{V}} = \left.\frac{\partial \mathcal{V}^i}{\partial t}\right|_x \boldsymbol{e}_i + \mathcal{V}^i \left(\left.\frac{\partial \boldsymbol{e}_i}{\partial t}\right|_x - \boldsymbol{e}_j \nabla_i \mathcal{V}^j\right) \tag{2.72}$$

after using (2.32) in passing to the second equality; the term in parentheses then vanishes due to (2.70). Separately, we can use equation (2.68) and Table 2.6 to write, for a general vector $\boldsymbol{w}$,

$$J^a_i \left.\frac{\partial w^i}{\partial t}\right|_x = \left(\left.\frac{\partial}{\partial t}\right|_y + \mathcal{L}_{\mathcal{V}}\right) w^a \tag{2.73}$$

from which equation (2.71) follows immediately by $\mathcal{L}_{\mathcal{V}} \mathcal{V}^a = 0$. In fact, with the choice $\boldsymbol{\mathcal{V}} = \boldsymbol{v}$, equation (2.73) becomes Oldroyd (1950) equation (23) applied to vector components—see Appendix E for further discussion of that derivative and its relation to the intrinsic derivative.

using the definition of p^i in (2.53). The boxed term is of a new sort wholly absent in static frames, though common in GFD settings, and gives the contribution to the rate of change of $\boldsymbol{w}$ along $\chi(t)$ arising from the temporal variability of the basis vectors.

The intrinsic derivative of the contravariant components of a vector in a moving coordinate system is then defined as

$$\left.\frac{\delta w^i}{\delta t}\right|^{\chi} \equiv \left.\frac{\partial w^i}{\partial t}\right|_x + p^j \nabla_j w^i + \boxed{w^j \nabla_j \mathcal{V}^i} \tag{2.75}$$

which supersedes the earlier definition in (2.57). The new, boxed term emerges from the rate of change of the basis vectors in (2.74) on account of (2.70), and vanishes for any static coordinate system, recovering the form of the intrinsic derivative given earlier in (2.57). With this definition, we can express the total derivative along $\chi(t)$ in the moving coordinate system as

$$\left.\frac{d\boldsymbol{w}}{dt}\right|^{\chi} = \left.\frac{\delta w^i}{\delta t}\right|^{\chi} \boldsymbol{e}_i \tag{2.76}$$

just as was the case for the static coordinate system in (2.58).

Unlike for the static coordinate system, the expression for the intrinsic derivative in a moving coordinate system is valence-dependent. For the covariant components of a vector the generalized intrinsic derivative is

$$\left.\frac{\delta w_i}{\delta t}\right|^{\chi} \equiv \left.\frac{\partial w_i}{\partial t}\right|_x + p^j \nabla_j w_i - \boxed{w_j \nabla_i \mathcal{V}^j}\,, \tag{2.77}$$

as derived in Appendix B. In comparison with (2.75) for the contravariant components, we see that the final term appears with the opposite sign and with a different contraction of indices. As shown in Appendix B, (2.75) and (2.77) are indeed the contravariant and covariant components of the same vector $d\boldsymbol{w}/dt|^{\chi}$. Despite this, neither the first nor third terms on their right-hand sides are individually the components of the same vector. The implications of this are discussed in section 2.6.6.

For a second-order tensor $\boldsymbol{A}$ expressed in contravariant form, $\boldsymbol{A} = A^{ij}\boldsymbol{e}_i \otimes \boldsymbol{e}_j$, one finds the intrinsic derivative in a moving coordinate system to be

$$\left.\frac{\delta A^{ij}}{\delta t}\right|^{\mathcal{X}} = \left.\frac{\partial A^{ij}}{\partial t}\right|_x + p^k \nabla_k A^{ij} + A^{kj} \nabla_k \mathcal{V}^i + A^{ik} \nabla_k \mathcal{V}^j. \tag{2.78}$$

This pattern is expressed most naturally in terms of the Lie derivative along $\boldsymbol{\mathcal{V}}$, which captures all of the valence dependence in its definition. Find details in section 2.6.7.

Like the covariant spatial derivative, the intrinsic derivative obeys the tensor transformation law

$$\left.\frac{\delta w^i}{\delta t}\right|^{\mathcal{X}} = J^i_a \left.\frac{\delta w^a}{\delta t}\right|^{\mathcal{X}} \tag{2.79}$$

Separately, it is compatible with the metric, and so indices can be raised and lowered across the derivative like so

$$\left.\frac{\delta w_i}{\delta t}\right|^{\mathcal{X}} = g_{ij} \left.\frac{\delta w^j}{\delta t}\right|^{\mathcal{X}} \tag{2.80}$$

We prove this in section 2.6.7, and it is standard for the derivative in fixed frames.

The intrinsic derivative adds no complexity to time derivatives of scalars, shown in Appendix C. The added complexity of differentiating second rank tensors is shown in Appendix D using the Reynolds stress.

2.4.7 The material derivative in moving settings

The *material intrinsic derivative* following fluid parcels is then

$$\frac{\delta w^i}{\delta t} \equiv \left.\frac{\partial w^i}{\partial t}\right|_x + u^j \nabla_j w^i + \boxed{w^j \nabla_j \mathcal{V}^i}\,, \tag{2.81}$$

$$\frac{\delta w_i}{\delta t} \equiv \left.\frac{\partial w_i}{\partial t}\right|_x + u^j \nabla_j w_i - \boxed{w_j \nabla_i \mathcal{V}^j}\,, \tag{2.82}$$

found by choosing a family of curves χ_ξ as parcel trajectories relative to the coordinates such that $u^i = p^i|_\xi$ as in section 2.4.3, but retaining the boxed terms due to the moving basis.

The first two terms on the right-hand side of (2.81) give the apparent rate of change of $\boldsymbol{w}$ following the flow $\boldsymbol{u}$ as observed from within the moving setting, measuring the contravariant components of $\boldsymbol{w}$. The final term tells us that at a fixed x location, the changing basis vectors interact with the vector field $\boldsymbol{w}$ to act *as if* the setting velocity field $\boldsymbol{\mathcal{V}}$ were being advected by $\boldsymbol{w}$. We term this effect *counter-advection*.

An illuminating special case of counter-advection is that in which the vector field $\boldsymbol{w}$ is both spatially and temporally constant. In that case, temporal changes in the contravariant components w^i at fixed x locations must occur to counteract the fact that the basis vectors are also changing. The combined effect leaves the derivative of the $\boldsymbol{w}$ field unchanged.

2.5 The momentum equation in moving coordinates

The coordinate systems employed in geophysical fluid dynamics, such as isopycnal coordinates, are not often static in time. In this section we therefore develop the equations for conservation of momentum in arbitrary time-dependent coordinates using the intrinsic material derivative from the previous section, and present interpretations of the novel terms which arise. These equations are directly relevant to ocean modeling.

2.5.1 Transformation to a rotating and translating frame

To motivate the development in this section we recall the standard presentation of the momentum equation in a rotating frame, as found in many textbooks, e.g. Vallis (2017, §2.1), Gill (1982, §4.5), Pedlosky (1987, §1.5–1.6), and Batchelor (2000, §3.2). See Morin (2008, §10) for a particularly thorough treatment. Although not normally done in GFD, for generality we allow the angular velocity of the moving setting to vary in time, and we also allow the moving setting to translate with a variable velocity. With these extensions, the moving setting exhausts the possibilities of rigid motion.

As before, let the y^a coordinates be embedded in an inertial frame, denoted I, that we take to be stationary. Now let the x^i coordinate system be temporarily limited to rigid motion so that it may be considered to be embedded in a rigidly rotating and translating frame of reference, denoted R. The absolute velocity $\boldsymbol{v}$ and velocity relative to the rotating frame $\boldsymbol{u}$ are then given by

$$\boldsymbol{v} = \frac{d\boldsymbol{s}}{dt}, \qquad \boldsymbol{u} = \left(\frac{d\boldsymbol{r}}{dt}\right)_R \tag{2.83}$$

where the meaning of the notation "$(\cdot)_R$" is that the basis vectors of the rotating frame R are to be held fixed while the derivative is carried out. Note that the material derivative with the basis vectors held fixed is equivalent to the definition $\boldsymbol{u} \equiv dx^i/dt\big|_\xi \boldsymbol{e}_i$ employed previously in (2.48).

Conservation of momentum, expressed in terms of force per unit mass, appears in the inertial frame as

$$\frac{\partial \boldsymbol{v}}{\partial t} + (\boldsymbol{v} \cdot \boldsymbol{\nabla})\,\boldsymbol{v} = \boldsymbol{F} \tag{2.84}$$

where $\boldsymbol{F}$ is a generic forcing term, the details of which are not important here. In the rotating frame this becomes

$$\left(\frac{\partial \boldsymbol{u}}{\partial t}\right)_R + (\boldsymbol{u} \cdot \boldsymbol{\nabla})\,\boldsymbol{u} = \overbrace{-2\boldsymbol{\Omega} \times \boldsymbol{u}}^{\text{Coriolis}} - \overbrace{\boldsymbol{\Omega} \times (\boldsymbol{\Omega} \times \boldsymbol{r})}^{\text{centrifugal}} - \overbrace{\frac{d\boldsymbol{\Omega}}{dt}}^{\text{Euler}} \times \boldsymbol{r} - \overbrace{\frac{d^2\boldsymbol{S}}{dt^2}}^{\text{translational}} + \boldsymbol{F}\,, \tag{2.85}$$

where the first four terms on the right-hand side are *apparent* or *fictitious forces* inferred within the rotating frame.

The first two apparent forces are well known in geophysical fluid dynamics. The Coriolis force appears to accelerate the fluid perpendicular to the direction of its apparent velocity $\boldsymbol{u}$ in the rotating frame, while the centrifugal force, which appears to push fluid parcels radially outwards, is generally subsumed into the gravitational portion of $\boldsymbol{F}$. The third and fourth apparent forces are typically neglected in GFD, but we include them for completeness. The third apparent force, known as the Euler force (Marsden and Ratiu, 1999, §8.6), the azimuthal force (Morin, 2008, §10.2.4), or by no name (Batchelor, 2000, §3.2), arises due to variability in the rotation rate Ω. We experience this in rotating amusement park rides, which apparently push us backwards as a carousel begins. It is important in planetary science problems such as tidally-locked moons. The final apparent force, the translational force, arises due to variability in the translational velocity $d\boldsymbol{S}/dt$ of the moving setting, and is the familiar "g-force" one feels inside an accelerating vehicle or elevator.

To transform the momentum equation from the inertial frame to the rotating frame, we first recognize that the absolute fluid velocity is the sum of the velocity observed in the rotating frame, the velocity induced by its rotation, and the translational velocity of the origin,

$$\boldsymbol{v} = \boldsymbol{u} + \boldsymbol{\Omega} \times \boldsymbol{r} + \frac{d\boldsymbol{S}}{dt}, \tag{2.86}$$

where the second term arises from the rate of change of the basis vectors induced by $\boldsymbol{\Omega}$, see e.g. Pedlosky (1987, §1.5) or Morin (2008, §9.5, §10.1). A second differentiation shows that accelerations in the inertial frame and the rigidly translating and rotating frame are related by

$$\frac{d\boldsymbol{v}}{dt} = \left(\frac{d\boldsymbol{u}}{dt}\right)_R + \boldsymbol{\Omega} \times \boldsymbol{u} + \boldsymbol{\Omega} \times \frac{d\boldsymbol{r}}{dt} + \frac{d\boldsymbol{\Omega}}{dt} \times \boldsymbol{r} + \frac{d^2\boldsymbol{S}}{dt^2}, \tag{2.87}$$

where again the second term arises from the rotation of the basis vectors. Noting that $\boldsymbol{r} = \boldsymbol{s} - \boldsymbol{S}$ and consequently $d\boldsymbol{r}/dt = \boldsymbol{v} - d\boldsymbol{S}/dt = \boldsymbol{u} + \boldsymbol{\Omega} \times \boldsymbol{r}$ from (2.86), this becomes

$$\frac{d\boldsymbol{v}}{dt} = \left(\frac{d\boldsymbol{u}}{dt}\right)_R + 2\boldsymbol{\Omega} \times \boldsymbol{u} + \boldsymbol{\Omega} \times (\boldsymbol{\Omega} \times \boldsymbol{r}) + \frac{d\boldsymbol{\Omega}}{dt} \times \boldsymbol{r} + \frac{d^2\boldsymbol{S}}{dt^2}. \tag{2.88}$$

Finally, the time derivative appearing on the right-hand side is expanded via the chain rule as

$$\left(\frac{d\boldsymbol{u}}{dt}\right)_R = \left(\frac{\partial \boldsymbol{u}}{\partial t}\right)_R + (\boldsymbol{u} \cdot \boldsymbol{\nabla})\, \boldsymbol{u}. \tag{2.89}$$

Inserting these last two equations into (2.84) and moving terms to the right-hand-side yields

(2.85).

2.5.2 The momentum equation in a moving setting

Having presented the momentum equation appropriate for a rigidly moving frame, which includes familiar terms arising from uniform rotation as well as some less familiar terms, we use a more rigorous derivation to find a version that remains appropriate when the setting deforms. Let the x coordinates again refer to a deformable, moving setting. Applying the generalized material intrinsic derivative (2.81) to the components of the absolute velocity $\boldsymbol{v}$,

$$\frac{\delta v^i}{\delta t} = \left.\frac{\partial v^i}{\partial t}\right|_x + u^j \nabla_j v^i + v^j \nabla_j \mathcal{V}^i$$

Using $v^i = u^i + \mathcal{V}^i$,

$$\frac{\delta v^i}{\delta t} = \left.\frac{\partial u^i}{\partial t}\right|_x + u_j \nabla^j u^i + \boxed{2u_j \nabla^j \mathcal{V}^i + \mathcal{V}_j \nabla^j \mathcal{V}^i + \left.\frac{\partial \mathcal{V}^i}{\partial t}\right|_x} \tag{2.90}$$

The boxed terms are apparent forces that arise from a nonzero setting velocity $\boldsymbol{\mathcal{V}}$, and vanish otherwise. Recall that the final term does in fact contain the components of a proper vector due to (2.71).

The covariant form is different, because we use (2.77) instead of (2.81),

$$\begin{aligned}\frac{\delta v_i}{\delta t} &= \left.\frac{\partial u_i}{\partial t}\right|_x + u^j \nabla_j u_i + u^j \nabla_j \mathcal{V}_i - u^j \nabla_i \mathcal{V}_j - \mathcal{V}^j \nabla_i \mathcal{V}_j + \left.\frac{\partial \mathcal{V}_i}{\partial t}\right|_x \\ &= \left.\frac{\partial u_i}{\partial t}\right|_x + u^j \nabla_j u_i + \boxed{2u^j \nabla_{[j} \mathcal{V}_{i]} - \mathcal{V}^j \nabla_i \mathcal{V}_j + \left.\frac{\partial \mathcal{V}_i}{\partial t}\right|_x}\end{aligned} \tag{2.91}$$

In index notation, the momentum equation (per unit density) in the inertial frame is

$$\frac{\delta v^a}{\delta t} = \left.\frac{\partial v^a}{\partial t}\right|_y + v^b \nabla_b v^a = F^a, \tag{2.92}$$

the component form of (2.84), where $\boldsymbol{F}$ is the force per unit density. From (2.90) this becomes in a moving, deforming setting

$$\left.\frac{\partial u^i}{\partial t}\right|_x + u^j \nabla_j u^i = \boxed{-2u^j \nabla_j \mathcal{V}^i - \mathcal{V}^j \nabla_j \mathcal{V}^i - \left.\frac{\partial \mathcal{V}^i}{\partial t}\right|_x} + F^i. \tag{2.93}$$

The boxed terms due to the setting velocity $\boldsymbol{\mathcal{V}}$ have been moved to the right-hand side and thus categorized as apparent forces, the meaning of we will explore shortly.

Given knowledge of the forces $\boldsymbol{F}$, this form of the momentum is numerically implementable for any moving coordinate system: material, isopycnal, pressure, or any other convenient choice. It remains only to determine the form of the metric coefficients and the components of $\boldsymbol{\mathcal{V}}$ for each coordinate system, which will be done explicitly in a companion paper (Feske et al., 2026). Thus (2.93) vastly expands the scope of possibilities over those afforded by the momentum equation in a rigid frame (2.85) which already has more apparent forces than included in most GFD textbooks. The companion paper presents concrete applications of (2.93) to various common coordinate systems employed in geophysical fluid mechanics. The remainder of this paper focuses on the interpretation of this equation.

Any second-order tensor can be expanded into two portions: a symmetric part (which can be made *deviatoric* by further separating its isotropic part if desired), and an antisymmetric or "skew-symmetric" part. Applying this decomposition to a generic velocity gradient,

$$\nabla_j v^i = \overbrace{\frac{1}{2}\left(\nabla_j v^i + \nabla^i v_j\right)}^{\text{symmetric}\sim\text{strain,divergence}} + \overbrace{\frac{1}{2}\left(\nabla_j v^i - \nabla^i v_j\right)}^{\text{skew/spin}\sim\text{vorticity}} \tag{2.94}$$

These are the symmetric portion, which is associated with strain (the deviatoric part) and divergence (the isotropic part), and the antisymmetric portion, which is associated with spin and vorticity. See Table 2.3 for a comparison of symmetry operators between symbolic and index notation. When both indices are lowered, we denote symmetries concisely as

$$\nabla_j v_i = \overbrace{\nabla_{(j} v_{i)}}^{\text{symmetric}} + \overbrace{\nabla_{[j} v_{i]}}^{\text{skew}}, \tag{2.95}$$

and similarly for raised indices—again, see Table 2.3. The skew-symmetric portion consists of the same information as the curl. One may write $\boldsymbol{e}^i \cdot \boldsymbol{\nabla} \times \boldsymbol{w} = \varepsilon^{ijk} \nabla_{[j} w_{k]}$, expressing the curl of any vector $\boldsymbol{w}$ in terms of the antisymmetric part of its gradient tensor.[6] The skew-symmetric velocity tensor $\nabla_{[j} v_{k]}$ corresponding to the vorticity, i.e. the curl of the velocity, is known as the *spin tensor* (Itskov, 2015, p 61). The symmetric part $\nabla_{(j} v_{k)}$ is the *strain rate tensor*. We will refer to these operations on the setting velocity as the setting spin and setting strain rate.

With a small modification, involving adding and subtracting canceling terms, the momentum equation (2.93) achieves the alternate form

$$\begin{aligned}
\left.\frac{\partial u^i}{\partial t}\right|_x + u^j \nabla_j u^i = &- \overbrace{2 u_j \nabla^{[j} \mathcal{V}^{i]}}^{\text{generalized Coriolis}} - \overbrace{2 u_j \nabla^{(j} \mathcal{V}^{i)}}^{\text{augmented Coriolis}} \\
&- \overbrace{\left(\mathcal{V}_j - \frac{\delta S_j}{\delta t}\right) \nabla^{[j} \mathcal{V}^{i]}}^{\text{generalized centrifugal}} - \overbrace{\left(\mathcal{V}_j - \frac{\delta S_j}{\delta t}\right) \nabla^{(j} \mathcal{V}^{i)}}^{\text{augmented centrifugal}} \\
&- \overbrace{\left.\frac{\partial \mathcal{V}^i}{\partial t}\right|_x - \frac{\delta S_j}{\delta t} \nabla^{[j} \mathcal{V}^{i]}}^{\text{generalized Euler−translational}} - \overbrace{\frac{\delta S_j}{\delta t} \nabla^{(j} \mathcal{V}^{i)}}^{\text{augmented translational}} \\
&+ F^i,
\end{aligned} \tag{2.96}$$

in which the apparent forces become generalizations of the standard fictitious forces–Coriolis, centrifugal, and Euler and translational forces–all of which will be shown shortly to reduce to their familiar forms for the case of rigid motion. While this modification from (2.93) is not

[6]This is readily found using the Hodge star operator $*(\cdot)$ of differential geometry, in terms of which one finds

$$\boldsymbol{\nabla} \times \boldsymbol{\mathcal{V}} = (*d\mathcal{V}^\flat)^\sharp = \boldsymbol{e}^i \frac{1}{2} \varepsilon_i^{\ jk} \left(\nabla_j \mathcal{V}_k - \nabla_k \mathcal{V}_j\right) = \boldsymbol{e}_i \varepsilon^{ijk} \nabla_{[j} \mathcal{V}_{k]}$$

where $d\mathcal{V}^\flat$ is the exterior derivative of the 1-form associated with $\boldsymbol{\mathcal{V}}$ by the metric tensor. See, e.g., §4.2 of Marsden and Ratiu (1999), section 2.9 of Carroll (2019), section 36.5 of Needham (2021), or section 3c of Lilly et al. (2024) for further details.

necessary (nor unique) for numerical implementation, it is useful in comparing the momentum equation in a moving setting to its rigid-frame counterpart. The *augmented* versions of these forces all vanish under the case of rigid motion because they depend on the setting strain rate, but can contribute important additional effects under a general setting velocity. As these augmented terms are unfamiliar in any case, we combine them into the *fantastical* force, as

$$
\begin{aligned}
\left.\frac{\partial u^i}{\partial t}\right|_x + u^j \nabla_j u^i = &- \overbrace{2u_j \nabla^{[j}\mathcal{V}^{i]}}^{\text{generalized Coriolis}} - \overbrace{\left(\mathcal{V}_j - \frac{\delta S_j}{\delta t}\right)\nabla^{[j}\mathcal{V}^{i]}}^{\text{generalized centrifugal}} \\
&- \overbrace{\left.\frac{\partial \mathcal{V}^i}{\partial t}\right|_x - \frac{\delta S_j}{\delta t}\nabla^{[j}\mathcal{V}^{i]}}^{\text{generalized Euler−translational}} - \overbrace{\left(2u_j + \mathcal{V}_j\right)\nabla^{(j}\mathcal{V}^{i)}}^{\text{fantastical}} \\
&+ F^i.
\end{aligned} \tag{2.97}
$$

Furthermore, gathering the setting spin terms and strain rate terms separately is convenient as only the fantastical force, which depends on the setting strain rate, differs for contravariant and covariant momentum tensor representations (Table 2.5), which results from (2.75) and (2.77).

$$
\begin{aligned}
\left.\frac{\partial u_i}{\partial t}\right|_x + u^j \nabla_j u_i = &- \overbrace{2u^j \nabla_{[j}\mathcal{V}_{i]}}^{\text{generalized Coriolis}} - \overbrace{\left(\mathcal{V}^j - \frac{\delta S^j}{\delta t}\right)\nabla_{[j}\mathcal{V}_{i]}}^{\text{generalized centrifugal}} \\
&- \overbrace{\left.\frac{\partial \mathcal{V}_i}{\partial t}\right|_x - \frac{\delta S^j}{\delta t}\nabla_{[j}\mathcal{V}_{i]}}^{\text{generalized Euler−translational}} + \overbrace{\mathcal{V}^j \nabla_{(j}\mathcal{V}_{i)}}^{\text{fantastical}} + F_i.
\end{aligned} \tag{2.98}
$$

Table 2.5 presents (2.85) together with (2.97) and (2.98). The form of the fantastical force depends on whether the momentum is represented by a contravariant velocity as in (2.97) or a covariant velocity as in (2.98), because of (2.77) and (2.81). It is perhaps surprising that the different valences have such different governing equations. This will be discussed more deeply in section 2.6.

Table 2.5: Conservation of momentum in the absence of external forces. The first row shows the symbolic form in a rigid frame rotating with potentially variable angular velocity $\boldsymbol{\Omega}$ and translating with velocity $d\boldsymbol{S}/dt$. The second and third rows show the index form for a general moving, deforming setting; u^i is the relative velocity in that setting. The indexed equations are far more general because the moving coordinate system is not constrained to be rigid, but rather moves *and* deforms according to the setting velocity field $\boldsymbol{\mathcal{V}} = \mathcal{V}^i \boldsymbol{e}_i$. The indexed terms generalize those encountered in the rigid case. When we choose the rigid setting velocity $\boldsymbol{\mathcal{V}} = \boldsymbol{\mathcal{K}} = \boldsymbol{\Omega}\times\boldsymbol{r} + d\boldsymbol{S}/dt$, the lower rows reduce to the first. Additional forces $\boldsymbol{F}$ can be applied to the right-hand side.

Equation	Tendency	Advection	Coriolis	Centrifugal	Euler & Translational	Fantastical	Forces
(2.85)	$\left(\frac{\partial \boldsymbol{u}}{\partial t}\right)_R$	$+(\boldsymbol{u}\cdot\boldsymbol{\nabla})\,\boldsymbol{u} =$	$-2\boldsymbol{\Omega}\times\boldsymbol{u}$	$-\boldsymbol{\Omega}\times(\boldsymbol{\Omega}\times\boldsymbol{r})$	$-\frac{d\boldsymbol{\Omega}}{dt}\times\boldsymbol{r}-\frac{d^2\boldsymbol{S}}{dt^2}$	$+0$	$\boldsymbol{F}$
(2.97)	$\left.\frac{\partial u^i}{\partial t}\right\vert_x$	$+u^j\nabla_j u^i$	$=-2u_j\nabla^{[j}\mathcal{V}^{i]}$	$-\left(\mathcal{V}_j-\frac{\delta S_j}{\delta t}\right)\nabla^{[j}\mathcal{V}^{i]}$	$-\left.\frac{\partial \mathcal{V}^i}{\partial t}\right\vert_x-\frac{\delta S_j}{\delta t}\nabla^{[j}\mathcal{V}^{i]}$	$-\left(2u_j+\mathcal{V}_j\right)\nabla^{(j}\mathcal{V}^{i)}$	F^i
(2.98)	$\left.\frac{\partial u_i}{\partial t}\right\vert_x$	$+u^j\nabla_j u_i$	$=-2u^j\nabla_{[j}\mathcal{V}_{i]}$	$-\left(\mathcal{V}^j-\frac{\delta S^j}{\delta t}\right)\nabla_{[j}\mathcal{V}_{i]}$	$-\left.\frac{\partial \mathcal{V}_i}{\partial t}\right\vert_x-\frac{\delta S^j}{\delta t}\nabla_{[j}\mathcal{V}_{i]}$	$+\mathcal{V}^j\nabla_{(j}\mathcal{V}_{i)}$	F_i

2.5.3 Recovery of the rigid frame equation

When the moving setting is limited to rigid rotation and translation, the setting velocity components are, by equations (2.86) and (2.51),

$$\mathcal{V}^i \to \mathcal{K}^i \equiv \varepsilon^{ijk}\Omega_j r_k + \frac{\delta S^i}{\delta t}, \tag{2.99}$$

from which it follows immediately that

$$\mathcal{K}^i - \frac{\delta S^i}{\delta t} = \varepsilon^{ijk}\Omega_j r_k = \boldsymbol{e}^i\cdot(\boldsymbol{\Omega}\times\boldsymbol{r})\,. \tag{2.100}$$

We choose the label $\boldsymbol{\mathcal{K}}$ here because rigid coordinate motion is generated by *Killing vector fields*, as show in section 2.6.7. From (2.97) we see that the derivatives we need to evaluate are under rigid motions just

$$
\begin{aligned}
&\nabla^j \mathcal{K}^i = \nabla^{[j} \mathcal{K}^{i]} = \varepsilon^{i\ell k} \nabla^j \left(\Omega_\ell r_k\right) = \varepsilon^{i\ell k} \delta^j_k \Omega_\ell = \varepsilon^{i\ell j} \Omega_\ell, \\
&\nabla^{(j} \mathcal{K}^{i)} = 0 \, , \\
&\left.\frac{\partial \mathcal{K}^i}{\partial t}\right|_x = \left.\frac{\partial^2 S^i}{\partial t^2}\right|_x + \varepsilon^{ijk} \left.\frac{\partial}{\partial t}\right|_x \left(\Omega_j s_k\right) .
\end{aligned} \tag{2.101}
$$

Because the moving frame is rigid, the spatial derivatives of S^i and Ω_j are zero. The partial time derivative of r_k when holding x fixed is zero: all of the change in $\partial \boldsymbol{r}/\partial t|_x$ is encapsulated in the change of the basis vectors. Metrinilic and other properties from section 2.3.2 and Table 2.6 are also used. Shifting of indices from upper to lower position can occur later as the situation demands by the index juggling operations. Importantly, the velocity gradient tensor is antisymmetric in this case, which means that the fantastical force is zero for rigid rotation and translation in (2.97) and (2.98).

We find the apparent force terms to be

$$
\begin{aligned}
-2u_j \nabla^{[j} \mathcal{K}^{i]} &= -2u_j \varepsilon^{i\ell j} \Omega_\ell = \boldsymbol{e}^i \cdot \left(-2\boldsymbol{\Omega} \times \boldsymbol{u}\right), \\
-\left(\mathcal{K}_j - \frac{\delta S_j}{\delta t}\right) \nabla^{[j} \mathcal{K}^{i]} &= -\left(\varepsilon_{jk\ell} \Omega^k r^\ell\right) \varepsilon^{imj} \Omega_m \\
&= \left(r^i \Omega^k - r^k \Omega^i\right) \Omega_k \\
&= \boldsymbol{e}^i \cdot \left(-\boldsymbol{\Omega} \times \boldsymbol{\Omega} \times \boldsymbol{r}\right), \\
-\left(2u_j + \mathcal{K}_j\right) \nabla^{(j} \mathcal{K}^{i)} &= 0, \\
-\left.\frac{\partial \mathcal{K}^i}{\partial t}\right|_x - \frac{\delta S_j}{\delta t} \nabla^{[j} \mathcal{K}^{i]} &= -\varepsilon^{ijk} \frac{\delta \Omega_j}{\delta t} r_k - \frac{\delta^2 S^i}{\delta t^2} \\
&= \boldsymbol{e}^i \cdot \left(-\frac{d\boldsymbol{\Omega}}{dt} \times \boldsymbol{r} - \frac{d^2 \boldsymbol{S}}{dt^2}\right),
\end{aligned} \tag{2.102}
$$

and we recover the rigid frame transformation (2.85). Under arbitrary setting velocities $\boldsymbol{\mathcal{V}}$, these simplifications do not occur.

The momentum equations summarized in Table 2.5 show that both the Coriolis and centrifugal forces are closely related to advection terms, the former arising from the spin part of the advection of the setting velocity $\boldsymbol{\mathcal{V}}$ by the relative velocity $\boldsymbol{u}$ plus the spin part of the boxed term in (2.81), and the latter resembling self-advection of the spin portion of the setting velocity gradient, $\boldsymbol{\Omega}\times\boldsymbol{r}$.

The fantastical force term arises—in both the contravariant and covariant momentum equations—only when the setting velocity gradient tensor has a non-zero symmetric part, which doesn't occur under rigid rotation and translation. Finally, note the brevity index notation allows: this section is a fraction of a page long while our equivalent symbolic notation version of these proofs took over two pages.

2.6 Discussion

In this section we discuss the generalized apparent forces and the force balances in the context of the literature, especially the works of Oldroyd and Holm and their collaborators, with particular attention to comparing the generalized intrinsic derivative to related operators.

2.6.1 The apparent acceleration

We can think of observing velocity as the process of marking the coordinates of successive positions over a small time interval and taking their difference. In two dimensions the coordinates can be visualized as lines drawn on a deformable rubber sheet. If the coordinate lines are moving, this is unknown to an observer who has only these lines themselves as a reference. Similarly, acceleration is observed by a second difference of these position marks, and again, contributions to the acceleration that arise from the motion of the coordinates are invisible to an observer in the moving setting. Separately, acceleration may be measured through an accelerometer, or felt viscerally in the body. When in a moving setting, the measured, or felt accelerations that would not occur in a Newtonian rigid frame constitute the apparent forces, precisely the boxed terms in a moving setting (2.93).

The two terms on the left-hand side of (2.93) describe the acceleration observed from the moving setting as one moves with the relative velocity $\boldsymbol{u}$, and records contravariant components of velocity. The first, $\partial u^i/\partial t\big|_x$, is local rate of change of the contravariant components of velocity relative to the moving setting observed at a fixed coordinate location in that setting. The second, $u^j\nabla_j u^i$, is ith component of the advective term $\boldsymbol{e}^i \cdot (\boldsymbol{u}\cdot\boldsymbol{\nabla})\,\boldsymbol{u}$, the rate of change of relative velocity $\boldsymbol{u}$ that arises from moving through gradients of the relative velocity at the relative velocity itself. Contributions to the absolute velocity $\boldsymbol{v}$ that involve the setting velocity $\boldsymbol{\mathcal{V}}$ will not be apparent to an observer who quantifies motion based only on references to the setting coordinates. Consequently, felt accelerations that depend upon $\boldsymbol{\mathcal{V}}$ will seem to the observer to be unrelated to motion; the observer will instead conclude that these terms must be forces: the fictitious and fantastical forces.

An important point is that unlike for a rigid frame, in a deforming setting the partitioning of the material acceleration $d\boldsymbol{v}/dt$ into apparent accelerations is dependent upon whether an observer chooses to record velocity and acceleration through through contravariant or covariant components. This distinction, which appears only in the fantastical force, stems from the intrinsic material derivative—compare (2.81) and (2.82). This derivative was constructed precisely to preserve the dynamics of a vector in either representation, so it usually suffices to consider only one (we typically choose contravariant). The distinction between the contravariant and covariant representations and why they differ in the generalized intrinsic material derivative will be discussed in a geometric context in section 2.6.6.

2.6.2 The generalized Coriolis force

Table 2.5 shows that the Coriolis force is a disguised advection term arising from the relative flow $\boldsymbol{u}$ advecting the particular setting velocity $\boldsymbol{\mathcal{K}} = \boldsymbol{\Omega}\times\boldsymbol{r} + d\boldsymbol{S}/dt$. To explore the Coriolis generalization, we first mention two facts about the setting velocity of a rigidly rotating frame

(2.99):

$$\nabla^i \mathcal{K}_i = 0. \tag{2.103}$$

$$\varepsilon_{ijk} \nabla^j \mathcal{K}^k = \varepsilon_{ijk} \varepsilon^{k\ell j} \Omega_\ell = 2\Omega_i \ , \tag{2.104}$$

This velocity field is nondivergent (2.103) and has a spatially uniform vorticity (2.104). Thus the velocity gradient tensor is just the spin tensor, and the augmented apparent force is zero. Note that (2.104) is a just an application of (2.20) that results in the coefficient of 2. Because $d\boldsymbol{S}/dt$ is a spatially constant vector field, it does not contribute to any of the spatial derivatives.

The above results suggest that within a general setting, a local analogue to the standard Coriolis force can be found through an expansion of the gradient tensor of the setting velocity, $\nabla^j \mathcal{V}^i$. With this decomposition, the generalized Coriolis force then likewise consists of two parts formed from the decomposed setting velocity gradient

$$-2u^j \nabla_j \mathcal{V}^i = -2u_j \overbrace{\nabla^{[i} \mathcal{V}^{j]}}^{\text{skew/spin}} - 2u_j \overbrace{\nabla^{(i} \mathcal{V}^{j)}}^{\text{symmetric/strain}} \tag{2.105}$$

The skew-proportional term will be called the *generalized Coriolis force*. This is a Coriolis-like force that is different at every point in space, as it arises from the local spin associated with the setting velocity $\boldsymbol{\mathcal{V}}$. This term, like the standard Coriolis force, is always perpendicular to the advecting relative velocity $\boldsymbol{u}$, as $u^i u^j \nabla_{[i} \mathcal{V}_{j]} = 0$ by the symmetry of $u^i u^j$ and skew symmetry of the setting spin.[7] This implies that this term has no acceleration in the direction of $\boldsymbol{u}$ and does no work in the relative velocity's kinetic energy budget. It is proportional to the relative velocity, and thus has no effect when the fluid is fixed in relation to the coordinates. These properties resemble the ordinary Coriolis effect.

The term that depends on the symmetric portion of the velocity gradient on the right-hand side of (2.105) is quite different, and it is our first fantastical force. It will be examined in

[7] Any symmetric tensor doubly-contracted with any antisymmetric tensor is zero.

section 2.6.5 below.

A useful calculation for any vector field w_j is the divergence of its contraction with the setting spin and strain rate tensor,

$$\nabla_i \left(w_j \nabla^{[j} \mathcal{V}^{i]} \right) = \left(\nabla_i w_j \right) \left(\nabla^{[j} \mathcal{V}^{i]} \right) + w_j \nabla_i \left(\nabla^{[j} \mathcal{V}^{i]} \right), \tag{2.106}$$

$$\nabla_i \left(w_j \nabla^{(j} \mathcal{V}^{i)} \right) = \left(\nabla_i w_j \right) \left(\nabla^{(j} \mathcal{V}^{i)} \right) + w_j \nabla_i \left(\nabla^{(j} \mathcal{V}^{i)} \right). \tag{2.107}$$

The curl of these fields simplifies a bit more than the divergence because one of the two terms in the symmetrization decomposition vanishes, and the remaining one features the spin of the setting velocity.

$$\varepsilon_{mni} \nabla^n \left(w_j \nabla^{[j} \mathcal{V}^{i]} \right) = \varepsilon_{mni} \left(\nabla^n w_j \right) \left(\nabla^{[j} \mathcal{V}^{i]} \right) + w_j \nabla^j \varepsilon_{mni} \nabla^{[n} \mathcal{V}^{i]}, \tag{2.108}$$

$$\varepsilon_{mni} \nabla^n \left(w_j \nabla^{(j} \mathcal{V}^{i)} \right) = \varepsilon_{mni} \left(\nabla^n w_j \right) \left(\nabla^{(j} \mathcal{V}^{i)} \right) + \frac{1}{2} w_j \nabla^j \left(\varepsilon_{mni} \nabla^{[n} \mathcal{V}^{i]} \right). \tag{2.109}$$

When $w_j = -2u_j$ is used, (2.106) and (2.108) become the divergence and curl of the generalized Coriolis force,

$$\nabla_i \left(-2u_j \nabla^{[j} \mathcal{V}^{i]} \right) = -2 \left(\nabla_i u_j \right) \left(\nabla^{[j} \mathcal{V}^{i]} \right) - 2u_j \nabla_i \left(\nabla^{[j} \mathcal{V}^{i]} \right), \tag{2.110}$$

and

$$\varepsilon_{mni} \nabla^n \left(-2u_j \nabla^{[j} \mathcal{V}^{i]} \right) = -2\varepsilon_{mni} \left(\nabla^n u_j \right) \left(\nabla^{[j} \mathcal{V}^{i]} \right) - 2u_j \nabla^j \varepsilon_{mni} \nabla^{[n} \mathcal{V}^{i]}. \tag{2.111}$$

2.6.3 The generalized centrifugal force

The centrifugal force is also of the form of an advection term in disguise (Table 2.5). As with the Coriolis force, we can isolate a generalized centrifugal force that shares most properties with the standard centrifugal force, with the key ones being: it is proportional to the antisymmetric part of the velocity gradient tensor and it is conservative, i.e., it can be represented by the gradient of a fixed scalar field and relatedly it has no curl.

The standard rigid-frame centrifugal force has a divergence that is nonnegative and constant in space,

$$
\begin{aligned}
-\boldsymbol{\nabla}\cdot(\boldsymbol{\Omega}\times\boldsymbol{\Omega}\times\boldsymbol{r}) &= \nabla_i\left(r^i\Omega^k - r^k\Omega^i\right)\Omega_k \\
&= \Omega_k\Omega^k\delta^i_i - \Omega_k\Omega^i\delta^k_i \\
&= \Omega_k\Omega^k(3-1) \\
&= 2\Omega^k\Omega_k.
\end{aligned}
\tag{2.112}
$$

Its curl is zero,

$$
\begin{aligned}
-\boldsymbol{e}^i\cdot\boldsymbol{\nabla}\times(\boldsymbol{\Omega}\times\boldsymbol{\Omega}\times\boldsymbol{r}) &= \varepsilon^{i\ell m}\nabla_\ell\left[\left(r_m\Omega^k - r^k\Omega_m\right)\Omega_k\right] \\
&= \varepsilon^{i\ell}{}_\ell\Omega^k\Omega_k - \varepsilon^{i\ell m}\Omega_m\Omega_\ell \\
&= 0.
\end{aligned}
\tag{2.113}
$$

These properties of the standard, rigid-frame centrifugal force imply that it is a conservative force and can be written as the gradient of a potential—a crucial step in modeling and theory, because it allows the combination of the centrifugal force and gravity into the geopotential. To find the potential corresponding to the rigid centrifugal force, we begin with (2.99) and (2.101), and use these in the form of the Coriolis force from Table 2.5:

$$
\begin{aligned}
-\left(\mathcal{K}_j - \frac{\delta S_j}{\delta t}\right)\nabla^{[i}\mathcal{K}^{j]} &= -\left(\varepsilon_{jmk}\Omega^m r^k\right)\varepsilon^{i\ell j}\Omega_\ell \\
&= -\left(\varepsilon_{jmk}\Omega^m r^k_\perp\right)\varepsilon^{i\ell j}\Omega_\ell \\
&= \Omega^\ell\Omega_\ell r^i_\perp - \Omega^i \cancelto{0}{r^\ell_\perp\Omega_\ell} \\
&= \frac{1}{2}\nabla^i\left(\Omega^\ell\Omega_\ell r^j_\perp r^\perp_j\right) \\
&= \nabla^i\left(\frac{1}{2}\Omega^2 r^2_\perp\right).
\end{aligned}
\tag{2.114}
$$

Where $\boldsymbol{r}_\perp$ is defined so that $\boldsymbol{\Omega}\times\boldsymbol{r} = \boldsymbol{\Omega}\times\boldsymbol{r}_\perp$ and $\boldsymbol{\Omega}\cdot\boldsymbol{r}_\perp = 0$, and we use the identity (2.20) and $\nabla^i r_j = \delta^i_j$.

The generalized centrifugal force also has a nonnegative term in its divergence, but it is not spatially uniform. When $w_j = \left(\frac{\delta S_j}{\delta t} - \mathcal{V}_j\right)$ is used in (2.106) and (2.108), the divergence and curl of the generalized and augmented centrifugal forces can be found. The divergence is

$$\nabla_i \left(\left(\frac{\delta S_j}{\delta t} - \mathcal{V}_j \right) \nabla^{[j} \mathcal{V}^{i]} \right) = \left(\nabla_{[i} \mathcal{V}_{j]} \right) \left(\nabla^{[i} \mathcal{V}^{j]} \right) + \left(\frac{\delta S_j}{\delta t} - \mathcal{V}_j \right) \nabla_i \left(\nabla^{[j} \mathcal{V}^{i]} \right). \tag{2.115}$$

The first term is a doubly-contracted nonnegative contribution, similar to the rigid frame case. The other contribution consists of second derivatives of the setting velocity $\mathcal{V}$, picking out locations of strong curvature in the profile of $\mathcal{V}$. These terms might be important across strong fronts in isopycnal coordinates or steep topography in terrain-following coordinates. In the case of rigid rotation this effect is absent because the spin of the setting velocity is constant in space and its strain and divergence are zero—see the first two of equations (2.101).

The curl of the centrifugal force is

$$\varepsilon_{mni} \nabla^n \left[\left(\frac{\delta S_j}{\delta t} - \mathcal{V}_j \right) \nabla^{[j} \mathcal{V}^{i]} \right] = -\varepsilon_{mni} \left(\nabla^n \mathcal{V}_j \right) \left(\nabla^{[j} \mathcal{V}^{i]} \right) + \left(\frac{\delta S_j}{\delta t} - \mathcal{V}_j \right) \varepsilon_{mni} \nabla^n \nabla^{[j} \mathcal{V}^{i]}, \tag{2.116}$$

which may be nonzero for any setting with nonuniform setting velocity or spin, so the centrifugal force is not guaranteed to be conservative as it is in the rigid frame case. A Helmholtz decomposition can be used to isolate the conservative portion of this centrifugal force in (2.116), but it is not simply related to either the spin or strain rate portions of the force, as the final term in (2.116) indicates that a gradient in the spin provides a curl in the force, i.e., a non-conservative force.

2.6.4 Euler and translational force

These forces are not typically included in GFD, because translational accelerations are neglected and the rotation rate of the rigid frame is normally taken to be constant. However if they are nonzero, whether in rigid frames or deforming ones, they should be included. The augmented translational contribution cancels part of the augmented contribution from the centrifugal force in all cases, simplifying the fantastical force to be independent of $\boldsymbol{S}$.

2.6.5 The fantastical force

The fantastical force, which comprises the augmented portions of the Coriolis and centrifugal force, is unfamiliar to those accustomed only to rigid rotations and translations. As it is proportional to the symmetric part of the velocity gradient, it is only present when the setting velocity has divergence and/or strain.

$$-\left(2u_j + \mathcal{V}_j\right) \nabla^{(j}\mathcal{V}^{i)} \tag{2.117}$$

The divergence of the two contributions to the contravariant fantastical force are found from (2.107) to be

$$\nabla_i \left(-2u_j \nabla^{(j}\mathcal{V}^{i)}\right) = -2\left(\nabla_{(i}u_{j)}\right)\nabla^{(j}\mathcal{V}^{i)} - 2u_j \nabla_i \left(\nabla^{(j}\mathcal{V}^{i)}\right), \tag{2.118}$$

$$\nabla_i \left(-\mathcal{V}_j \nabla^{(j}\mathcal{V}^{i)}\right) = -\nabla_{(i}\mathcal{V}_{j)}\nabla^{(i}\mathcal{V}^{j)} - \mathcal{V}_{(j}\nabla_{i)}\left(\nabla^{(j}\mathcal{V}^{i)}\right). \tag{2.119}$$

The first term on the right hand side of (2.118) is unaffected by spin in the relative velocity. A non-positive definite contribution is the first term on the right side of (2.119), and the other three contributions are focused where the setting velocity is anomalous from its surroundings.

The curl of the two contributions to the fantastical force are found from (2.109) with $w_j = \left(-2u_j - \mathcal{V}_j\right)$ as

$$\begin{aligned}\varepsilon_{mni}\nabla^n \left(\left(-2u_j - \mathcal{V}_j\right)\nabla^{(j}\mathcal{V}^{i)}\right) = & -2\varepsilon_{mni}\left(\nabla^n u_j\right)\left(\nabla^{(j}\mathcal{V}^{i)}\right) \\ & - \frac{\varepsilon_{mni}}{2}\left(\nabla^n \mathcal{V}_j\right)\left(\nabla^j \mathcal{V}^i\right) \\ & - \left(u_j + \frac{\mathcal{V}_j}{2}\right)\nabla^j \varepsilon_{mni}\nabla^n \mathcal{V}^i.\end{aligned} \tag{2.120}$$

These results suggest there is little reason to expect the fantastical force to be zero or to be conservative for most interesting deforming coordinate systems, except when $\nabla_{(j}\mathcal{V}_{i)} = 0$. The terms proportional to u vanish for the covariant fantastical force, but the other terms remain (with the opposite sign) – see equations (2.97) and (2.98). Many other papers have used essentially the same form of the Coriolis and centrifugal forces in deforming coordinates as in rigid ones when other assumptions (e.g., hydrostasy, strong stratification) are employed (e.g., Bleck, 2002); presumably, those forces are similar when the coordinate surfaces are nearly aligned with geopotential surfaces. This paper does not examine the size of the different contributions; that will come in a later asymptotic analysis.

2.6.6 Contravariant versus covariant representations

Our discussion of the fantastical forces has repeatedly mentioned that the momentum equation in a moving setting—but not the resulting dynamics—depends upon the choice of a contravariant or covariant representation of momentum. To see this another way, we borrow a concept from continuum mechanics: the *upper* and *lower convected time derivatives*, written respectively as

$$\overset{\triangledown}{\boldsymbol{w}} = \frac{d\boldsymbol{w}}{dt} - \boldsymbol{w}\,(\boldsymbol{\nabla} \otimes \boldsymbol{v}) \tag{2.121}$$

$$\overset{\vartriangle}{\boldsymbol{w}} = \frac{d\boldsymbol{w}}{dt} + \boldsymbol{w}\,(\boldsymbol{\nabla} \otimes \boldsymbol{v})^T \tag{2.122}$$

These derive ultimately from Oldroyd (1950), and give the apparent rates of change of the vector $\boldsymbol{w}$ observed when moving at the fluid velocity $\boldsymbol{v}$. The triangles "▽" and "△" indicate the valence of the vector components to which the partial time derivative is applied, the former applies when measuring w^i or w^a, and the latter when measuring w_i or w_a. This notation is strange because, though it presents as an operation on a tensor $\boldsymbol{w}$, its form depends on the component representation of that tensor. Nonetheless, it is common in continuum mechanics (e.g., Dimitrienko, 2011; Hinch and Harlen, 2021). See Appendix E for an explicit, *component*-wise definition of these derivatives applicable to arbitrary tensor fields. Rearranging, we can write

$$\frac{d\boldsymbol{w}}{dt} = \overset{\triangledown}{\boldsymbol{w}} + \boldsymbol{w}\,(\boldsymbol{\nabla} \otimes \boldsymbol{v}) \tag{2.123}$$

$$\frac{d\boldsymbol{w}}{dt} = \overset{\vartriangle}{\boldsymbol{w}} - \boldsymbol{w}\,(\boldsymbol{\nabla} \otimes \boldsymbol{v})^T \tag{2.124}$$

Because these derivatives deal particularly with convected coordinates (which we would call *advected* or Lagrangian coordinates), we must make the particular choice $\mathcal{V} = \boldsymbol{v}$.

When these operators are applied to the local velocity $\boldsymbol{u}$, this presentation shows clearly that, depending on which set of components we measure, there are two possible partitionings of the material acceleration $d\boldsymbol{u}/dt$ into an apparent local rate of change—the first terms on the right hand side—and apparent forces, the negative of the second term. This choice is arbitrary, and does not affect the actual dynamics. The apparent forces are the same if and only if the transformation is rigid, that is, the gradient tensor of the setting velocity $\boldsymbol{\nabla} \otimes \boldsymbol{v}$ is everywhere antisymmetric. This is why we distinguish the fictitious forces (which are constructed from only the setting spin part) from the fantastical forces (which are constructed from the setting strain rate and divergence) as shown in Table 2.5.

The apparent forces arising in rigidly moving frames, being independent of the valence of the tensor's representation, are of a different nature than those which arise more generally in the presence of deformation. To understand this, consider that a moving observer will feel their total acceleration $d\boldsymbol{v}/dt$, and will not be able to viscerally distinguish between its various components. An observer standing in a rotating room, however, feels an outward acceleration, takes note of the fact that they are not in motion relative to the room, and infers the presence of a force acting outwards. In this way apparent forces are inferred from felt accelerations and measured motion together. The above result implies that when the setting is not rigid, the inference of apparent forces from felt accelerations no longer has a unique result.

2.6.7 Generalized intrinsic derivatives in terms of Lie derivatives

The Lie derivative is a potent tool in differential geometry, and appears as a generalized advection operator in the work of Holm (e.g., 2015, 2025). The intrinsic derivative, it turns out, also takes its most powerful form in terms of the Lie derivative:

$$\boxed{\left.\frac{\delta}{\delta t}\right|^{\chi} = \left(\left.\frac{\partial}{\partial t}\right|_{x} + q^j \nabla_j - \mathcal{L}_{\mathcal{V}}\right),} \tag{2.125}$$

a form which is now independent of the valence of its argument. For the contravariant components of a vector, covariant components of vector, and contravariant components of a second-order tensor, the Lie derivative is given respectively by

$$\mathcal{L}_{\mathcal{V}} w^i = \mathcal{V}^j \partial_j w^i - w^j \partial_j \mathcal{V}^i, \tag{2.126}$$

$$\mathcal{L}_{\mathcal{V}} w_i = \mathcal{V}^j \partial_j w_i + w_j \partial_i \mathcal{V}^j, \tag{2.127}$$

$$\mathcal{L}_{\mathcal{V}} A^{ij} = \mathcal{V}^k \partial_k A^{ij} - A^{kj} \partial_k \mathcal{V}^i - A^{ik} \partial_k \mathcal{V}^j. \tag{2.128}$$

The general form for the Lie derivative may be found in (B.18) of Carroll (2019), or likely in any text on differential geometry or general relativity. Due to the symmetry of the Christoffel symbols, the partial derivatives can equivalently be written as covariant derivatives. The reader may verify that equation (2.125) recovers all of the particular cases (2.75), (2.77), and (2.78). In the inertial case x becomes y, we take $\boldsymbol{\mathcal{V}} = 0$, and recover equation (2.57) as well.

As always, the choice $\boldsymbol{q} = \boldsymbol{v}$ gives the material version

$$\boxed{\frac{\delta}{\delta t} = \left(\left.\frac{\partial}{\partial t}\right|_{x} + v^j \nabla_j - \mathcal{L}_{\mathcal{V}}\right)} \tag{2.129}$$

We can see now that in the moving setting, instead of simple advection $(\boldsymbol{u} \cdot \boldsymbol{\nabla})$ by the observed velocity $\boldsymbol{u}$, each part of $\boldsymbol{u} = \boldsymbol{v} - \boldsymbol{\mathcal{V}}$ effects a different sort of advection: physical, covariant advection by the inertial fluid velocity $\boldsymbol{v}$ and Lie advection opposite the setting velocity $\boldsymbol{\mathcal{V}}$, which is the source of the apparent forces.

We might have guessed this result from the start: as implied by equations (2.45), the criterion for a well-behaved moving coordinate system x^i is that the setting velocity $\boldsymbol{\mathcal{V}}$ be a vector field that generates a diffeomorphism—that is, an invertible, one-to-one mapping—from space onto itself, as illustrated in Figure 2.2. By definition, the Lie derivative $\mathcal{L}_{\boldsymbol{\mathcal{V}}}$ is the derivative that measures how a tensor field changes under the diffeomorphism generated by $\boldsymbol{\mathcal{V}}$, and by subtracting it we undo the artifacts that this coordinate transformation introduces to tensor components.

Said another way, the observed velocity $\boldsymbol{u}$ is a transformation of space—a rearrangement of the fluid—that we can meaningfully decompose into its active part $\boldsymbol{v}$, the field along which the fluid moves, and its passive part $\boldsymbol{\mathcal{V}}$, the field along which the coordinates move through the fluid. We represent each of these transformations with a different sort of advection: the active part by familiar covariant advection $\nabla_{\boldsymbol{v}}$, and the passive part by Lie advection $\mathcal{L}_{\boldsymbol{\mathcal{V}}}$.

Geometrically meaningful expressions now tumble from the notation. The expression

$$\left.\frac{\partial}{\partial t}\right|_x - \mathcal{L}_{\boldsymbol{\mathcal{V}}} \tag{2.130}$$

measures the difference between the observed change with time at a fixed x coordinate location and the change due only to the rearrangement of coordinates induced by $\boldsymbol{\mathcal{V}}$. This operation is metric compatible because the actions of $\partial/\partial t|_x$ and $\mathcal{L}_{\boldsymbol{\mathcal{V}}}$ on the metric coefficients give the same value

$$\left.\frac{\partial g_{ij}}{\partial t}\right|_x = \mathcal{L}_{\boldsymbol{\mathcal{V}}} g_{ij} = 2\nabla_{(i}\mathcal{V}_{j)} \tag{2.131}$$

and hence (2.130) applied to g_{ij} vanishes. Together with the metric compatibility of the covariant derivative this proves metric compatibility of the generalized intrinsic derivative from (2.125),

$$\left.\frac{\delta g_{ij}}{\delta t}\right|^{\chi} = 0. \tag{2.132}$$

This property is important because it allows us to freely raise and lower indices, finally proving that

$$\left.\frac{\delta w_i}{\delta t}\right|^{\mathcal{X}} = g_{ij} \left.\frac{\delta w^j}{\delta t}\right|^{\mathcal{X}}. \tag{2.80}$$

Metric compatibility of $\delta/\delta t|^{\mathcal{X}}$ is expected because we constructed it to give components of the vector field $d\boldsymbol{w}/dt$ when acting either on w^i or w_i. Indeed, equation (2.132) could be rewritten in symbolic form as $d\boldsymbol{I}/dt = 0$, which is obviously true. Nevertheless, it is reassuring to demonstrate this property directly. See Table A1 for a compilation of derivatives of metric coefficients. We derive the same result without using Lie derivatives in Appendix B.

Equation (2.131) also means that if $\nabla_{(i}\mathcal{V}_{j)}$ vanishes—if the gradient tensor of $\boldsymbol{\mathcal{V}}$ is totally antisymmetric, which is a defining characteristic of a rigid frame (2.99)—then the derivatives in (2.130) are *separately* metric compatible, $\boldsymbol{\mathcal{V}}$ satisfies *Killing's equation*

$$\mathcal{L}_{\mathcal{V}} g_{ij} = 0, \tag{2.133}$$

and the fantastical force vanishes. The setting velocity $\boldsymbol{\mathcal{V}}$ then generates a rigid transformation of space if and only if it is a Killing vector field, motivating our choice in equation (2.99) to denote a rigid setting velocity by $\boldsymbol{\mathcal{K}}$. A Killing field is a vector field representing an isometry (a distance-preserving transformation), and in Lorentzian spacetime correspond to quantities conserved along geodesics. See §3.8 and Appendix B of Carroll (2019) for a discussion of Killing vectors and symmetries of the metric tensor.

2.7 Conclusions

In this paper, we have developed a tensor-based framework for describing geophysical fluid dynamics in general, deforming coordinate systems. Beginning from first principles in tensor analysis, we introduced a generalized intrinsic material derivative that captures the evolution of tensor components in curvilinear bases that vary arbitrarily, but continuously, in space and time. This derivative ensures consistency across covariant and contravariant representations and across inertial and non-inertial frames, providing a unified treatment of the fundamental building blocks of GFD.

The generalized intrinsic time derivative $\delta/\delta t|^{\chi}$, taking its most general form in equation (2.125), allows us to calculate the total derivative of arbitrary, space-time dependent tensor fields along any parameterized path $\chi(t)$—an integral path through an arbitrary vector field $\boldsymbol{q}$—in coordinates being deformed by an arbitrary vector field $\boldsymbol{\mathcal{V}}$. If we set $\boldsymbol{\mathcal{V}} = 0$, the generalized derivative reduces to the intrinsic time derivative discussed by Grinfeld (2013) and Aris (1962). The only constraint on $\boldsymbol{\mathcal{V}}$ is that it generate an invertible, continuously differentiable transformation of the moving coordinates x^i—that is, that it generate a *diffeomorphism* on Euclidean space. In the particular case where $\boldsymbol{q} = \boldsymbol{v}$, the fluid velocity, the intrinsic derivative reduces to the intrinsic material derivative $\delta/\delta t$.

All coordinate systems—all settings—typically used in GFD are a diffeomorphism away from an inertial, Cartesian frame. These include rotating, accelerating, neutral buoyancy, terrain-following, pressure, and tracer coordinates. Taking into account the implications of such a coordinate transformation, we have found the general form for the apparent forces that correct for the non-inertial aspects of these coordinate systems without approximation.

We applied this generalized intrinsic derivative and derived explicit expressions for all apparent accelerations arising in GFD settings. These include the familiar fictitious forces—Coriolis, centrifugal, translational, and Euler forces—as well as the additional family of terms that arise when the coordinate system is deforming, which we have termed the *fantastical* forces. Unlike fictitious forces, the fantastical forces depend on the symmetric part of the setting-velocity gradient and therefore vanish only when the setting velocity is a Killing vector field, that is, for diffeomorphisms connecting rigid frames. Their dependence on tensor valence highlights that deformation introduces qualitatively new geometric structure into the apparent dynamics.

Our results clarify the relationship between classical rotating-frame dynamics and their fully general counterparts, showing that the standard GFD equations emerge as a special case of a broader tensorial formulation. By expressing all results using index notation, we provide equations that can be directly translated into numerical model implementations, particularly those with vertical remapping, adaptive, or arbitrarily Lagrangian-Eulerian (ALE) coordinate systems.

The following statements are all logically equivalent:

1. The moving setting x is a rigid frame,
2. $\boldsymbol{\nabla} \otimes \boldsymbol{\mathcal{V}}$ is antisymmetric,
3. $\mathcal{L}_{\mathcal{V}} g_{ij} = 0$
4. $\left.\frac{\partial g_{ij}}{\partial t}\right|_x = 0$,
5. $\boldsymbol{\mathcal{V}}$ is a Killing vector field,
6. Oldroyd's upper and lower convected derivatives are equivalent,
7. The fantastical forces are zero.

In many GFD settings, these statements do not apply, and thus nonzero fantastical forces will arise. Although they may be small, they preserve exact symmetries and conservation laws under all coordinate changes.

The framework developed here lays the mathematical foundation for companion papers of this series, which will: extend these ideas to the full oceanic primitive equations including coordinate-agnostic specifications of common parameterizations and approximations; specify metric coefficients of common coordinate systems for GFD; determine coordinate-independent averaging and coarse-graining operators; provide an asymptotic scaling for the fantastical forces; and derive budgets for common higher-order invariants (vorticity, potential vorticity, energy). Together, these works aim to establish a unified, tensorial approach for next-generation ocean models, enabling more accurate representations of the physics of rotating, stratified flows in complex, time-varying geometries.

2.8 Appendix 1A: The metrinilic property for Jacobians

All the calculations here take place at fixed time, so for this purpose y^a and x^i simply represent two curvilinear coordinate systems; rules proven here hold for objects indexed in either $\{a, b, c\}$ or $\{i, j, k\}$. Tensor derivatives—that is, derivatives that act on tensor components to produce tensor components—should null out the Jacobian coefficients. Any such derivative D by definition has the property that $J_i^a D(w^i) = D(w^a)$. This is the transformation law for tensor components, and is equivalent to the statement $D(J_i^a) = 0$:

$$D(w^a) = D(J_i^a w^i) = J_i^a D(w^i). \tag{2.134}$$

In this section we show explicitly that both the covariant and Lie derivatives have this property. First we note that The basis vectors $\boldsymbol{e}_i$ are in fact covariant components of a tensor as the notation suggests: by the chain rule they transform according to the tensor transformation law $\boldsymbol{e}_a = J_a^i \boldsymbol{e}_i$, see equation (2.27). More generally, a second order tensor $\boldsymbol{A}$ has components A^{ij} so that

$$\boldsymbol{A} = A^{ij} \boldsymbol{e}_i \otimes \boldsymbol{e}_j = \boldsymbol{e}_i \otimes A^{ij} \boldsymbol{e}_j \equiv \boldsymbol{e}_i \otimes \boldsymbol{A}^i, \tag{2.135}$$

defining the covariant vector components $\boldsymbol{A}^i$ of $\boldsymbol{A}$, which by similar reasoning has covariant vector components $\boldsymbol{A}_i$.[8] By the same reasoning we can now see that the basis vectors $\boldsymbol{e}^i$ and $\boldsymbol{e}_i$ are the contravariant and covariant components of the identity $\boldsymbol{I}$ because $\boldsymbol{I} = \delta^i_{\ j} \boldsymbol{e}_i \otimes \boldsymbol{e}^j$, analogous to the final equality of (2.135):

$$\boldsymbol{I} = \delta^i_{\ j} \boldsymbol{e}_i \otimes \boldsymbol{e}^j = \boldsymbol{e}_i \otimes \boldsymbol{e}^i. \tag{2.137}$$

[8]We can see that these obey the tensor transformation law:

$$\boldsymbol{A}^a \equiv A^{ab} \boldsymbol{e}_b = J_i^a A^{ib} J_b^j \boldsymbol{e}_j = J_i^a A^{ij} \boldsymbol{e}_j \equiv J_i^a \boldsymbol{A}^i \tag{2.136}$$

which makes use of the chain rule relation (2.27).

Now we can be confident that applying index-based tensor derivatives to the basis vectors is well-defined

2.8.1 The covariant derivative

We find that

$$\nabla_j \boldsymbol{e}_i = \partial_i \boldsymbol{e}_j - \Gamma^k{}_{ij} \boldsymbol{e}_k = \Gamma^k{}_{ij} \boldsymbol{e}_k - \Gamma^k{}_{ij} \boldsymbol{e}_k = 0. \tag{2.138}$$

where we have used equation (2.4) in passing from the second expression to the third. This is not coincidence—the covariant derivative and Christoffel symbols are defined precisely to have this property. This means that we can freely write $\nabla_i \boldsymbol{a} \equiv \partial_i \boldsymbol{a}$, and we can now show that the covariant derivative satisfies the product rule across dot products of vectors:

$$\begin{aligned}\nabla_i (\boldsymbol{a} \cdot \boldsymbol{b}) &= \nabla_i \left(a_j b^j \right) \\ &= a_j \nabla_i b^j + b^j \nabla_i a_j \\ &= \boldsymbol{a} \cdot \boldsymbol{e}_j \nabla_i b^j + \boldsymbol{b} \cdot \boldsymbol{e}^j \nabla_i a_j \\ &= \boldsymbol{a} \cdot \nabla_i \boldsymbol{b} + \nabla_i \boldsymbol{a} \cdot \boldsymbol{b}.\end{aligned} \tag{2.139}$$

We also have

$$\nabla_j \boldsymbol{e}_a = J^b_j \nabla_b \boldsymbol{e}_a = 0 \tag{2.140}$$

and therefore

$$\nabla_j J^i_a = \nabla_j (\boldsymbol{e}^i \cdot \boldsymbol{e}_a) = \nabla_j \boldsymbol{e}^i \cdot \boldsymbol{e}_a + \boldsymbol{e}^i \cdot \nabla_j \boldsymbol{e}_a = 0 \tag{2.141}$$

as expected, and analogous reasoning holds for $\nabla_j J^a_i$.

2.8.2 The Lie derivative

Recalling that we can define the Lie derivative in terms of the covariant derivative, and that the Lie derivative on invariant fields is simply the directional derivative $\mathcal{L}_{\mathcal{V}} f = \mathcal{V}^i \nabla_i f$, we find that that it also satisfies the product rule over the dot product:

$$
\begin{aligned}
\mathcal{L}_{\mathcal{V}}(\boldsymbol{a}\cdot\boldsymbol{b}) &= \mathcal{L}_{\mathcal{V}}\left(a_j b^j\right) \\
&= a_j \mathcal{L}_{\mathcal{V}} b^j + b^j \mathcal{L}_{\mathcal{V}} a_j \\
&= a_j\left(\mathcal{V}^k \nabla_k b^j - \cancel{b^k \nabla_k \mathcal{V}^j}\right) \\
&\qquad + b^j\left(\mathcal{V}^k \nabla_k a_j + \cancel{a_k \nabla_j \mathcal{V}^k}\right) \\
&= \boldsymbol{a}\cdot\boldsymbol{e}_j \mathcal{V}^k \nabla_k b^j + \boldsymbol{b}\cdot\boldsymbol{e}^j \mathcal{V}^k \nabla_k a_j \\
&= \boldsymbol{a}\cdot\mathcal{V}^k \nabla_k \boldsymbol{b} + \boldsymbol{b}\cdot\mathcal{V}^k \nabla_k \boldsymbol{a} \\
&= \boldsymbol{a}\cdot\mathcal{L}_{\mathcal{V}}\boldsymbol{b} + \mathcal{L}_{\mathcal{V}}\boldsymbol{a}\cdot\boldsymbol{b}
\end{aligned}
\tag{2.142}
$$

Further, we can calculate

$$
\mathcal{L}_{\mathcal{V}}\boldsymbol{e}^i = \mathcal{V}^j \nabla_j \boldsymbol{e}^i - \boldsymbol{e}^j \nabla_j \mathcal{V}^i = -\boldsymbol{e}^j \nabla_j \mathcal{V}^i \tag{2.143}
$$

$$
\mathcal{L}_{\mathcal{V}}\boldsymbol{e}_a = \mathcal{V}^b \nabla_b \boldsymbol{e}_a + \boldsymbol{e}_b \nabla_a \mathcal{V}^b = \boldsymbol{e}_b \nabla_a \mathcal{V}^b \tag{2.144}
$$

so therefore

$$
\begin{aligned}
\mathcal{L}_{\mathcal{V}} J^i_a &= \mathcal{L}_{\mathcal{V}}(\boldsymbol{e}^i\cdot\boldsymbol{e}_a) \\
&= \mathcal{L}_{\mathcal{V}}\boldsymbol{e}^i\cdot\boldsymbol{e}_a + \boldsymbol{e}^i\cdot\mathcal{L}_{\mathcal{V}}\boldsymbol{e}_a \\
&= -\boldsymbol{e}_a\cdot\boldsymbol{e}^j \nabla_j \mathcal{V}^i + \boldsymbol{e}^i\cdot\boldsymbol{e}_b \nabla_a \mathcal{V}^b \\
&= -J^j_a \nabla_j \mathcal{V}^i + J^i_b \nabla_a \mathcal{V}^b \\
&= -\nabla_a \mathcal{V}^i + \nabla_a \mathcal{V}^i \\
&= 0
\end{aligned}
\tag{2.145}
$$

as expected, and once again analogous reasoning holds for $\mathcal{L}_{\mathcal{V}} J^a_i$. Derivatives of all useful metric-related objects can be calculated using this strategy of decomposing components of identity into dot products of basis vectors and applying the product rule. The results of all such calculations are compiled in Table 2.6. Space-time derivative commutators as applied to vector components appear in Table 2.7.

Table 2.6: A table of derivatives of the various components of the identity $\boldsymbol{I}$. Each can be derived by representing components of $\boldsymbol{I}$ as dot products of basis vectors, themselves vector-valued tensor components, and applying the product rule.

Derivative	δ^i_j	δ^a_b	g_{ij}	g_{ab}	$\boldsymbol{e}_i$	$\boldsymbol{e}^i$	$\boldsymbol{e}_a$	$\boldsymbol{e}^a$	$\boldsymbol{J}^i_a$	$\boldsymbol{J}^a_i$
∂_k	0	0	$2\Gamma_{(i,j)k}$	$2\Gamma_{(a,b)c}\boldsymbol{J}^c_k$	$\boldsymbol{e}_j\Gamma^j{}_{ik}$	$-\boldsymbol{e}^j\Gamma^i{}_{jk}$	$\boldsymbol{e}_b\Gamma^b{}_{ac}\boldsymbol{J}^c_k$	$-\boldsymbol{e}^b\Gamma^a{}_{bc}\boldsymbol{J}^c_k$	$\boldsymbol{J}^i_{ac}\boldsymbol{J}^c_k$	$\boldsymbol{J}^a_{ik}$
∂_c	0	0	$2\Gamma_{(i,j)k}\boldsymbol{J}^k_c$	$2\Gamma_{(a,b)c}$	$\boldsymbol{e}^j\Gamma^j{}_{ik}\boldsymbol{J}^k_c$	$-\boldsymbol{e}^j\Gamma^i{}_{jk}\boldsymbol{J}^k_c$	$\boldsymbol{e}_b\Gamma^b{}_{ac}$	$-\boldsymbol{e}^b\Gamma^a{}_{bc}$	$\boldsymbol{J}^i_{ac}$	$\boldsymbol{J}^a_{ik}\boldsymbol{J}^k_c$
$\frac{\partial}{\partial t}\big\|_x$	0	0	$2\nabla_{(i}\mathcal{V}_{j)}$	$\mathcal{V}^c\partial_c g_{ab}$	$\boldsymbol{e}_j\nabla_i\mathcal{V}^j$	$-\boldsymbol{e}^j\nabla_j\mathcal{V}^i$	$\boldsymbol{e}_c\Gamma^c{}_{ab}\mathcal{V}^b$	$-\boldsymbol{e}^b\Gamma^a{}_{bc}\mathcal{V}^c$	$-\boldsymbol{J}^i_b\partial_a\mathcal{V}^b$	$\boldsymbol{J}^b_i\partial_b\mathcal{V}^a$
$\frac{\partial}{\partial t}\big\|_y$	0	0	$2\partial_{(i}\mathcal{V}_{j)}$	0	$\boldsymbol{e}_j\partial_i\mathcal{V}^j$	$-\boldsymbol{e}^j\partial_j\mathcal{V}^i$	0	0	$-\boldsymbol{J}^j_a\partial_j\mathcal{V}^i$	$\boldsymbol{J}^a_j\partial_i\mathcal{V}^j$
∇_k	0	0	0	0	0	0	0	0	0	0
∇_c	0	0	0	0	0	0	0	0	0	0
$\mathcal{L}_{\mathcal{V}}$	0	0	$2\nabla_{(i}\mathcal{V}_{j)}$	$2\nabla_{(a}\mathcal{V}_{b)}$	$\boldsymbol{e}_j\nabla_i\mathcal{V}^j$	$-\boldsymbol{e}^j\nabla_j\mathcal{V}^i$	$\boldsymbol{e}_b\nabla_a\mathcal{V}^b$	$-\boldsymbol{e}^b\nabla_b\mathcal{V}^a$	0	0
$\frac{\delta}{\delta t}\big\|^{\mathcal{X}}$	0	0	0	0	0	0	0	0	0	0
$\frac{\delta}{\delta t}$	0	0	0	0	0	0	0	0	0	0

Table 2.7: A table of derivative commutators. The commutator is understood to be applied to the relevant components of the tensor in each column.

Commutator	$\boldsymbol{w}$
$\left[\frac{\partial}{\partial t}\big\rvert_x, \partial_j\right]$	0
$\left[\frac{\partial}{\partial t}\big\rvert_x, \nabla_j\right]$	$w^k \nabla_k \nabla_j \mathcal{V}^i$
$\left[\mathcal{L}_{\mathcal{V}}, \nabla_j\right]$	$w^k \nabla_k \nabla_j \mathcal{V}^i$
$\left[\frac{\delta}{\delta t}\big\rvert^{\chi}, \nabla_j\right]$	$-(\nabla_j q^k)(\nabla_k w^i)$
$\left[\frac{\delta}{\delta t}, \nabla_j\right]$	$-(\nabla_j v^k)(\nabla_k w^i)$
$\left[\frac{\partial}{\partial t}\big\rvert_y, \partial_b\right]$	0
$\left[\frac{\partial}{\partial t}\big\rvert_y, \nabla_b\right]$	0
$\left[\mathcal{L}_{\mathcal{V}}, \nabla_b\right]$	$w^c \nabla_c \nabla_b \mathcal{V}^a$
$\left[\frac{\delta}{\delta t}\big\rvert^{\chi}, \nabla_b\right]$	$-(\nabla_b q^c)(\nabla_c w^a)$
$\left[\frac{\delta}{\delta t}, \nabla_b\right]$	$-(\nabla_b v^c)(\nabla_c w^a)$

2.9 Appendix 1B: The intrinsic derivative for covariant components

Here we explicitly derive the form of the intrinsic derivative when applied to the covariant components of a vector w_i. The partial derivative $\partial_i \boldsymbol{w}$ can be rewritten as

$$\partial_i \boldsymbol{w} = \boldsymbol{e}_j \nabla_i w^j, \qquad \nabla_i w^j \equiv \partial_i w^j + \Gamma^j{}_{ik} w^k \tag{2.32}$$

$$\partial_i \boldsymbol{w} = \boldsymbol{e}^j \nabla_i w_j, \qquad \nabla_i w_j \equiv \partial_i w_j - \Gamma^k{}_{ij} w_k \tag{2.146}$$

using (2.5). Thus the covariant derivative ∇_i, viewed as an operator, takes on a different form when applied to contravariant and covariant components of a vector. The derivative of a vector along a curve χ can be written as

$$\left.\frac{d\boldsymbol{w}}{dt}\right|^{\chi} = \left.\frac{\delta w_a}{\delta t}\right|^{\chi} \boldsymbol{e}^a \tag{2.147}$$

where the intrinsic derivative of the covariant components,

$$\left.\frac{\delta w_a}{\delta t}\right|^{\chi} \equiv \left.\frac{\partial w_a}{\partial t}\right|_y + q^b \nabla_b w_a, \tag{2.148}$$

is the same as intrinsic derivative of contravariant components presented earlier in (2.57). This is because all dependence on the valence of tensor components is already accounted for by the covariant derivative.

We now need expressions for the temporal rates of change of the reciprocal basis vectors $\boldsymbol{e}^i$, and we find

$$\left.\frac{\partial \boldsymbol{e}_i}{\partial t}\right|_x = \boldsymbol{e}_j \nabla_i \mathcal{V}^j, \qquad \left.\frac{\partial \boldsymbol{e}^i}{\partial t}\right|_x = -\boldsymbol{e}^j \nabla_j \mathcal{V}^i \tag{2.149}$$

the first of which appeared earlier as (2.70). To derive the second identity, we note

$$\left.\frac{\partial}{\partial t}\left(\boldsymbol{e}^i \cdot \boldsymbol{e}_j\right)\right|_x = \left.\frac{\partial \delta^i_j}{\partial t}\right|_x = 0 \tag{2.150}$$

and consequently, from the product rule,

$$\boldsymbol{e}_j \cdot \left.\frac{\partial \boldsymbol{e}^i}{\partial t}\right|_x = -\boldsymbol{e}^i \cdot \left.\frac{\partial \boldsymbol{e}_j}{\partial t}\right|_x . \tag{2.151}$$

Combining this with (2.70) yields

$$\boldsymbol{e}_j \cdot \left.\frac{\partial \boldsymbol{e}^i}{\partial t}\right|_x = -\boldsymbol{e}^i \cdot \boldsymbol{e}_k \nabla_j \mathcal{V}^k = -\nabla_j \mathcal{V}^i \tag{2.152}$$

which is equivalent to the second identity in (2.149), as both give $-\nabla_j \mathcal{V}^i$ for the jth covariant component of $\partial \boldsymbol{e}^i / \partial t\big|_x$.

The derivative of the vector $\boldsymbol{w}$ along the curve χ in the moving setting, expressed in terms of the vector's covariant components, is then

$$\left.\frac{d\boldsymbol{w}}{dt}\right|^{\chi} = \left.\frac{\partial w_i}{\partial t}\right|_x \boldsymbol{e}^i + \left(p^j \nabla_j w_i\right) \boldsymbol{e}^i + \boxed{w_i \left.\frac{\partial \boldsymbol{e}^i}{\partial t}\right|_x} \tag{2.153}$$

which is to be compared with (2.74) in terms of the contravariant components. Again the boxed term is the new term that arises in comparison with the fixed coordinate system. From (2.149) we then obtain

$$\left.\frac{\delta w_i}{\delta t}\right|^{\chi} \equiv \left.\frac{\partial w_i}{\partial t}\right|_x + p^j \nabla_j w_i - \boxed{w_j \nabla_i \mathcal{V}^j} \tag{2.77}$$

as the covariant version of (2.75), in comparison to which the final boxed term appears with opposite sign and with a different arrangement of indices. The material version (2.77) follows from the choice $\boldsymbol{p} = \boldsymbol{u}$.

We have pointed out that, despite the fact that (2.75) and (2.77) give the contravariant and covariant components of the same vector, the same is true neither the first nor third terms on the right-hand sides considered separately. In fact on account of $\partial g_{ij} / \partial t\big|_x = 2\nabla_{(i} \mathcal{V}_{j)}$, we have

$$\left.\frac{\partial w_i}{\partial t}\right|_x - g_{ij} \left.\frac{\partial w^j}{\partial t}\right|_x = 2 w^j \nabla_{(i} \mathcal{V}_{j)} \tag{2.154}$$

by the product rule, after recognizing that $w_i = g_{ij} w^j$. The partial time derivatives $\partial w_i / \partial t|_x$ and $\partial w^i / \partial t\big|_x$ are clearly not the components of the same vector.

It is thus instructive to attempt to obtain (2.77) by lowering the index on the contravariant version. Beginning with

$$\left.\frac{\delta w^i}{\delta t}\right|^{\mathcal{X}} \equiv \left.\frac{\partial w^i}{\partial t}\right|_x + p^j \nabla_j w^i + w^j \nabla_j \mathcal{V}^i \tag{2.75}$$

we lower the i index through a contraction with g_{ij}, yielding

$$\left.\frac{\delta w_i}{\delta t}\right|^{\mathcal{X}} = g_{ij} \left.\frac{\partial w^j}{\partial t}\right|_x + p^j \nabla_j w_i + w^j \nabla_j \mathcal{V}_i. \tag{2.155}$$

Substituting the result (2.154) then leads to

$$\left.\frac{\delta w_i}{\delta t}\right|^{\mathcal{X}} = \left.\frac{\partial w_i}{\partial t}\right|_x + p^j \nabla_j w_i + w^j \left[\nabla_j \mathcal{V}_i - 2\nabla_{(j} \mathcal{V}_{i)}\right] \tag{2.156}$$

using the symmetry of $\nabla_{(i} \mathcal{V}_{j)}$ to reverse the i and j indices. A tensor minus twice its symmetric portion is equal to the negative of its own transpose. This yields

$$\left.\frac{\delta w_i}{\delta t}\right|^{\mathcal{X}} \equiv \left.\frac{\partial w_i}{\partial t}\right|_x + p^j \nabla_j w_i - w^j \nabla_i \mathcal{V}_j \tag{2.157}$$

which matches (2.77) after juggling the indices on w^j and $\mathcal{V}_j$.

2.10 Appendix 1C: Intrinsic Derivative of Scalar Field τ

The intrinsic derivative of a scalar field is particularly simple:

$$\begin{aligned} \frac{\delta \tau}{\delta t} &= \left.\frac{\partial \tau}{\partial t}\right|_y + v^b \nabla_b \tau \\ &= \left(\left.\frac{\partial}{\partial t}\right|_y + v^b \partial_b\right) \tau \end{aligned} \tag{2.158}$$

and similarly from the moving, deforming perspective

$$\begin{aligned}\frac{\delta\tau}{\delta t} &= \left.\frac{\partial\tau}{\partial t}\right|_x + v^k\nabla_k\tau - \mathcal{L}_{\mathcal{V}}\tau \\ &= \left.\frac{\partial\tau}{\partial t}\right|_x + v^k\partial_k\tau - \mathcal{V}^k\partial_k\tau \\ &= \left(\left.\frac{\partial}{\partial t}\right|_x + u^k\partial_k\right)\tau\end{aligned} \tag{2.159}$$

Thus derivatives of scalar fields are simple, advecting only by observed velocity because there is no need to consider the changing basis vectors.

2.11 Appendix 1D: Intrinsic Derivative of Reynolds Stress u^iu^j

First we note that the Lie derivative has the following properties:

$$\mathcal{L}_{\boldsymbol{A}+\boldsymbol{B}}w^i = \mathcal{L}_{\boldsymbol{A}}w^i + \mathcal{L}_{\boldsymbol{B}}w^i \tag{2.160}$$

$$\mathcal{L}_{\boldsymbol{w}}w^i = 0. \tag{2.161}$$

Then we have

$$\mathcal{L}_{\mathcal{V}}u^i = \mathcal{L}_{\boldsymbol{v}}u^i \tag{2.162}$$

and the intrinsic derivative of u^i becomes

$$\begin{aligned}\frac{\delta u^i}{\delta t} &= \left.\frac{\partial u^i}{\partial t}\right|_x + v^k\nabla_k u^i - \mathcal{L}_{\boldsymbol{v}}u^i \\ &= \left.\frac{\partial u^i}{\partial t}\right|_x + u^k\nabla_k v^i\end{aligned} \tag{2.163}$$

Because the intrinsic derivative obeys the product rule, we then find the material derivative of the Reynolds stress to be

$$\begin{aligned} \frac{\delta\left(u^i u^j\right)}{\delta t} &= \frac{\delta u^i}{\delta t} u^j + u^i \frac{\delta u^j}{\delta t} \\ &= \left.\frac{\partial\left(u^i u^j\right)}{\partial t}\right|_x + u^i u^k \nabla_k v^j + u^j u^k \nabla_k v^i \end{aligned} \tag{2.164}$$

which is symmetric in $i \leftrightarrow j$, as expected.

2.12 Appendix 1E: Oldroyd and the Intrinsic Time Derivative

The generalized intrinsic derivative lets us easily derive the expression for the convected derivative of Oldroyd (1950). Oldroyd is concerned with materially advected coordinates, and so in the following we choose the specific $\mathcal{V} = \boldsymbol{v}$. In the spirit of the rest of this paper, we prefer his original, indicial definition. This definition is preferable also because it makes clear that the upper and lower convected derivatives are not, in fact, two different derivatives of tensors, but the same derivative applied respectively to contravariant and covariant tensor *components*, in precisely the same sense as the Lie derivative or the covariant derivative. For brevity's sake, we show the derivation for the derivative as applied to vector components, however it generalizes immediately to tensors of any order. As described in the paragraph preceding Oldroyd's equation (23), the convected derivative of a vector $\boldsymbol{w} = w^i \boldsymbol{e}_i$ is nothing but the vector with components $\partial w^i / \partial t|_x$ in the moving setting. The question is: what are the inertial frame components of this vector? We treat these as tensor components by assumption, and so they transform with the Jacobian:

$$
\begin{aligned}
\frac{\mathfrak{d} w^a}{\mathfrak{d} t} &\equiv J^a_i \left.\frac{\partial w^i}{\partial t}\right|_x \\
&= J^a_i \left(\frac{\delta w^i}{\delta t} - v^k \nabla_k w^i + \mathcal{L}_{\boldsymbol{v}} w^i \right) \\
&= \frac{\delta w^a}{\delta t} - v^c \nabla_c w^a + \mathcal{L}_{\boldsymbol{v}} w^a \\
&= \left.\frac{\partial w^a}{\partial t}\right|_y + \mathcal{L}_{\boldsymbol{v}} w^a .
\end{aligned}
\tag{2.165}
$$

And there we have it—we have recovered Oldroyd's equation (23)[9]. In operator form, the convected derivative is therefore

$$
\frac{\mathfrak{d}}{\mathfrak{d} t} = \left(\frac{\delta}{\delta t} - \nabla_{\boldsymbol{v}} + \mathcal{L}_{\boldsymbol{v}} \right) \tag{2.166}
$$

and this can be applied either to inertial frame components:

$$
\frac{\mathfrak{d} w^a}{\mathfrak{d} t} = \left(\frac{\delta}{\delta t} - v^c \nabla_c + \mathcal{L}_{\boldsymbol{v}} \right) w^a = \left(\left.\frac{\partial}{\partial t}\right|_y + \mathcal{L}_{\boldsymbol{v}} \right) w^a \tag{2.167}
$$

or to moving setting components:

$$
\frac{\mathfrak{d} w^i}{\mathfrak{d} t} = \left(\frac{\delta}{\delta t} - v^k \nabla_k + \mathcal{L}_{\boldsymbol{v}} \right) w^i = \left.\frac{\partial w^i}{\partial t}\right|_x \tag{2.168}
$$

Later, coordinate-free definitions of the convected derivative, for example in Hinch and Harlen (2021), are odd because, though superficially coordinate-free, they nevertheless depend on the valence of the underlying tensor components. The "upper convected" and "lower convected" derivatives can respectively be written in terms of Oldroyd's component-wise derivative $\mathfrak{d}/\mathfrak{d}t$ like so:

[9] His formulation includes extra terms to handle the differentiation of tensor densities, all of which are zero for tensors.

$$
\begin{aligned}
\overset{\triangledown}{\boldsymbol{w}} &= \boldsymbol{e}_a \frac{\eth w^a}{\eth t} = \boldsymbol{e}_i \frac{\eth w^i}{\eth t} \\
\overset{\vartriangle}{\boldsymbol{w}} &= \boldsymbol{e}^a \frac{\eth w_a}{\eth t} = \boldsymbol{e}^i \frac{\eth w_i}{\eth t}
\end{aligned}
\tag{2.169}
$$

Notice the similarity in form here to equations (2.62) and (2.76). These two quantities are not equal because the Lie derivative, and therefore also Oldroyd's, acts on the metric coefficients to produce a non-zero tensor:

$$
\frac{\eth g_{ab}}{\eth t} = \mathcal{L}_{\boldsymbol{v}} g_{ab} = 2\nabla_{(a} v_{b)} \tag{2.170}
$$

and therefore does not commute with index juggling. We find that

$$
\overset{\vartriangle}{\boldsymbol{w}} - \overset{\triangledown}{\boldsymbol{w}} = 2\boldsymbol{e}^a w^b \nabla_{(a} v_{b)} = \boldsymbol{e}^a w^b \mathcal{L}_{\boldsymbol{v}} g_{ab}, \tag{2.171}
$$

so these derivatives coincide if and only if $\boldsymbol{v}$ is a Killing field, which would correspond physically to a rigidly translating and rotating fluid – a restrictive constraint indeed.

We have shown, for the particular case $\boldsymbol{\mathcal{V}} = \boldsymbol{v}$, that the intrinsic derivative and Oldroyd's derivative encode similar information about time-varying tensors, but they are nearly opposite in character. Oldroyd's derivative begins with the components $\partial w^i \partial t|_x$ and asserts that, when transformed as tensor components, these look a certain way in the y^a coordinates. The convected derivative is therefore constructed to produce the second form from the first, and, for vector fields, produces the components of $\partial \boldsymbol{w}/\partial t|_y + [\boldsymbol{v}, \boldsymbol{w}]$. Brackets indicate the commutator operation.

In contrast, the intrinsic derivative begins with the tensor field $d\boldsymbol{w}/dt$, and asks: what are the components of this in each of the bases $\boldsymbol{e}_i$ and $\boldsymbol{e}^i$? The derivative is therefore constructed to act on either set of components w^i or w_i and produce the components of $d\boldsymbol{w}/dt$ in the relevant basis. We prefer this latter conceptual framing because the relevant coordinate-free field $d\boldsymbol{w}/dt$ is easier to interpret than $\partial \boldsymbol{w}/\partial t|_y + [\boldsymbol{v}, \boldsymbol{w}]$.

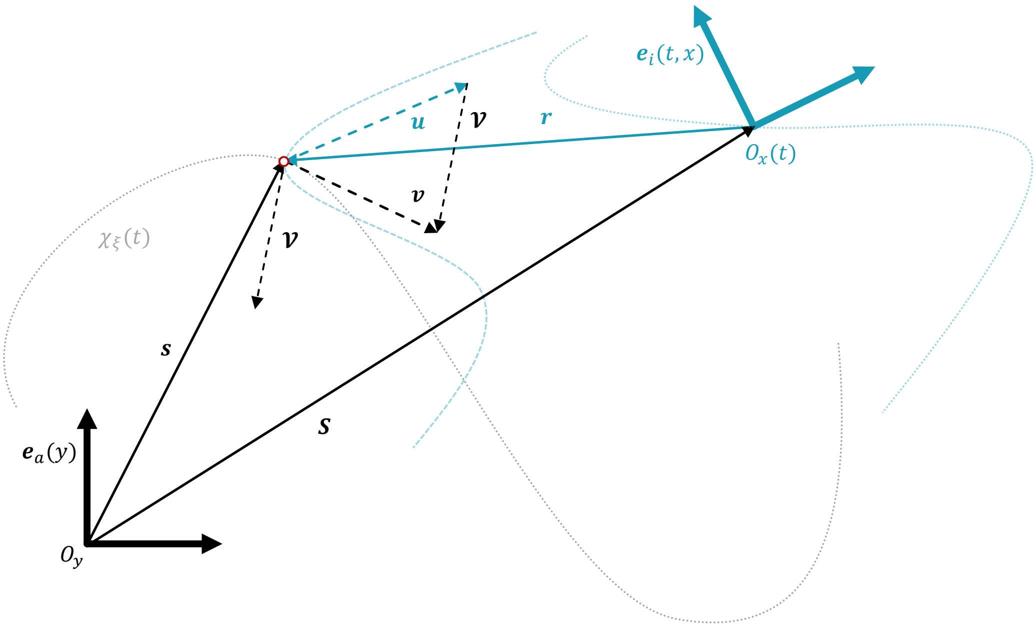

Figure 2.1: A schematic showing quantities in an inertial frame (black), chosen without loss of generality to be stationary, and a general moving, deforming coordinate system as often used in GFD (teal). Heavy solid lines indicate coordinate axes, thin solid lines are position vectors, thin dashed lines are velocity vectors, and dashed or dotted curves are trajectories. The inertial coordinate system $y^a = \{y^1, y^2, y^3\}$ has basis vectors $\boldsymbol{e}_a$ and fixed origin O_y, while the moving coordinate system $x^i = \{x^1, x^2, x^3\}$ has basis vectors $\boldsymbol{e}_i$ and moving origin $O_x(t)$, the path of which is indicated by the dotted teal curve. The instantaneous displacement at some time t_0 from the fixed origin O_y to the moving origin $O_x(t)$ is given by the vector $\boldsymbol{S}$. Addition information on this plot is not used until later sections. Then, we will consider a parameterized path $\chi_\xi(t)$, representing the time-varying position of a fluid parcel labeled ξ, the position of which at t_0 is indicated by the small white circle. The position vectors of this parcel relative to O_y and $O_x(t)$ at time t_0 are $\boldsymbol{s}$ and $\boldsymbol{r}$ respectively, which satisfy $\boldsymbol{s} = \boldsymbol{r} + \boldsymbol{S}$. At time t_0, the fluid parcel has velocity $\boldsymbol{v}$ as observed from the inertial y coordinate system and velocity $\boldsymbol{u}$ as observed from the moving, deforming x coordinate system. Through a combination of the motion of $O_x(t)$ and the internal motion and deformation of the x coordinate system, the x coordinate location occupied by the fluid parcel also traces out a curve in space, indicated by the dashed teal curve. At time t_0, the velocity of this x coordinate location as viewed from the inertial frame is the vector $\boldsymbol{\mathcal{V}}$, which is necessarily tangent to the curve. Note that $\boldsymbol{e}_i$ is a function of time *and space*, so each location in space has a potentially different basis vector set. The velocities are related by $\boldsymbol{v} = \boldsymbol{u} + \boldsymbol{\mathcal{V}}$, as shown. While we have illustrated this with an individual parcel, $\boldsymbol{v}$, $\boldsymbol{u}$, and $\boldsymbol{\mathcal{V}}$ are vector fields which add in this way at each point in the fluid.

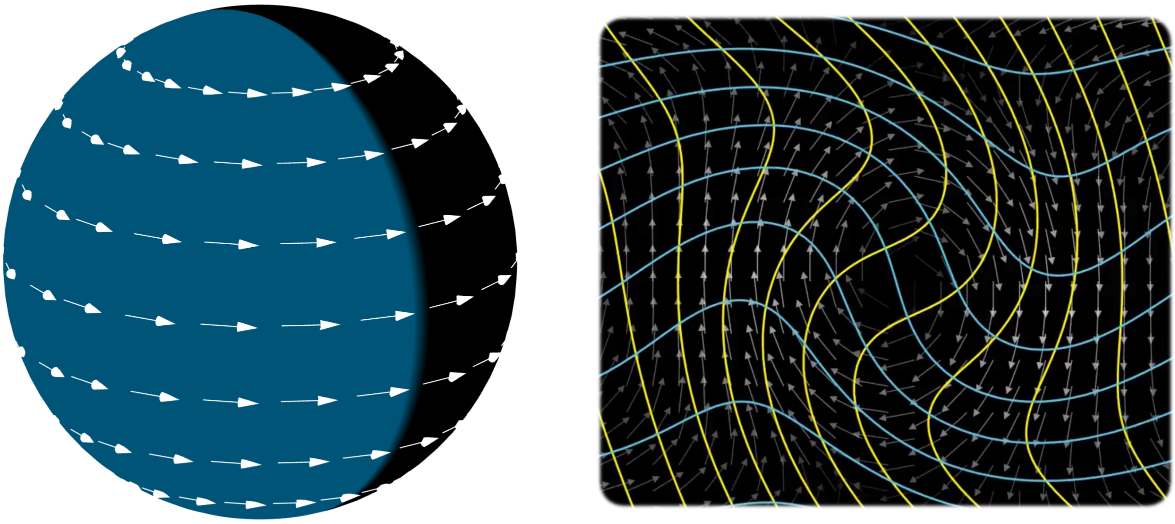

Figure 2.2: The setting velocity $\boldsymbol{\mathcal{V}}$, shown in white, is a vector field that generates a diffeomorphism of space. **Left**: $\boldsymbol{\mathcal{V}} = \boldsymbol{\Omega} \times \boldsymbol{r}$ generates rotation of the sphere. In this case, $\boldsymbol{\mathcal{V}}$ is a Killing vector field because rotation is a rigid transformation for which $\nabla_{(i}\mathcal{V}_{j)} = 0$. **Right**: A swirling and shearing diffeomorphism of the plane. Here $\nabla_{(i}\mathcal{V}_{j)} \neq 0$, and we see a straining deformation. There is no divergent deformation because this $\boldsymbol{\mathcal{V}}$ was generated from a stream function, so $\nabla_i \mathcal{V}^i = 0$. Note: these figures were generated programmatically using Matlab (left) and Python's Manim package (right) with the assistance of ChatGPT.

References

Åhlander, K., Haveraaen, M., and Munthe-Kaas, H. Z. (2001). On the role of mathematical abstractions for scientific computing. In *The Architecture of Scientific Software: IFIP TC2/WG2. 5 Working Conference on the Architecture of Scientific Software October 2–4, 2000, Ottawa, Canada*, pages 145–158. Springer.

Åhlander, K. and Otto, K. (2006). Software design for finite difference schemes based on index notation. *Future Generation Computer Systems*, 22(1-2):102–109.

Aris, R. (1962). *Vectors, tensors and the basic equations of fluid mechanics*. Courier Corporation.

Batchelor, G. (2000). *An introduction to fluid dynamics*. Cambridge University Press, Cambridge, UK.

Bleck, R. (2002). An oceanic general circulation model framed in hybrid isopycnic-cartesian coordinates. *Ocean modelling*, 4(1):55–88.

Carroll, S. M. (2019). *Spacetime and geometry*. Cambridge University Press.

Cotter, C. and Thuburn, J. (2014). A finite element exterior calculus framework for the rotating shallow-water equations. *J. Comput. Phys.*, 257:1506–1526.

Crane, K. (2018). Discrete differential geometry: An applied introduction. *Notices of the AMS, Communication*, 1153.

Crane, K., de Goes, F., Desbrun, M., and Schröder, P. (2013). Digital geometry processing with discrete exterior calculus. In *ACM SIGGRAPH 2013 Courses*, SIGGRAPH '13, New York, NY, USA. Association for Computing Machinery.

Dimitrienko, Y. I. (2011). *Nonlinear continuum mechanics and large inelastic deformations*. Springer, Dordrecht, Netherlands.

Dukowicz, J. K. and Smith, R. D. (1997). Stochastic theory of compressible turbulent fluid transport. *Physics of Fluids*, 9(11):3523–3529.

Engø, K., Marthinsen, A., and Munthe-Kaas, H. Z. (2001). Diffman: An object-oriented matlab toolbox for solving differential equations on manifolds. *Applied Numerical Mathematics*, 39(3):323–347. Themes in Geometric Integration.

Feske, J., Fox-Kemper, B., and Lilly, J. (2026). Beyond vertical coordinates: A generalized framework for ocean model equations with anisotropic diffusivity. In prep.

Fox-Kemper, B., Adcroft, A., Böning, C. W., Chassignet, E. P., Curchitser, E., Danabasoglu, G., Eden, C., England, M. H., Gerdes, R., Greatbatch, R. J., Griffies, S. M., Hallberg, R. W., Hanert, E., Heimbach, P., Hewitt, H. T., Hill, C. N., Komuro, Y., Legg, S., Le Sommer, J., Masina, S., Marsland, S. J., Penny, S. G., Qiao, F., Ringler, T. D., Treguier, A. M., Tsujino, H., Uotila, P., and Yeager, S. G. (2019). Challenges and prospects in ocean circulation models. *Front. Marine Sci.*, 6.

Friis, H. A., Johansen, T. A., Haveraaen, M., Munthe-Kaas, H., and Åsmund Drottning (2001). Use of coordinate-free numerics in elastic wave simulation. *Applied Numerical Mathematics*, 39(2):151–171.

Gibson, A. H., Hogg, A. M., Kiss, A. E., Shakespeare, C. J., and Adcroft, A. (2017). Attribution of horizontal and vertical contributions to spurious mixing in an arbitrary lagrangian–eulerian ocean model. *Ocean Modelling*, 119:45–56.

Gilbert, A. D. and Vanneste, J. (2023). A geometric look at momentum flux and stress in fluid mechanics. *Journal of Nonlinear Science*, 33(2):31.

Gill, A. E. (1982). *Atmosphere–ocean dynamics*, volume 30 of *International Geophysics Series*. Academic Press, San Diego, CA.

Grant, P. W., Haveraaen, M., and Webster, M. F. (2000). Coordinate free programming of computational fluid dynamics problems. *Scientific Programming*, 8(4):419840.

Griffies, S. (2018). *Fundamentals of ocean climate models*. Princeton university press.

Griffies, S. M. (1998). The gent–mcwilliams skew flux. *Journal of Physical Oceanography*, 28(5):831–841.

Griffies, S. M., Adcroft, A., and Hallberg, R. W. (2020). A primer on the vertical lagrangian-remap method in ocean models based on finite volume generalized vertical coordinates. *Journal of Advances in Modeling Earth Systems*, 12(10):e2019MS001954.

Griffies, S. M., Böning, C., Bryan, F. O., Chassignet, E. P., Gerdes, R., Hasumi, H., Hirst, A., Treguier, A.-M., and Webb, D. (2000a). Developments in ocean climate modelling. *Ocean Modell.*, 2(3):123–192.

Griffies, S. M., Pacanowski, R. C., and Hallberg, R. W. (2000b). Spurious diapycnal mixing associated with advection in a z-coordinate ocean model. *Monthly Weather Review*, 128(3):538–564.

Griffies, S. M., Stouffer, R. J., Adcroft, A. J., Bryan, K., Dixon, K. W., Hallberg, R., Harrison, M. J., Pacanowski, R. C., and Rosati, A. (2015a). A historical introduction to mom. *URL https://www. gfdl. noaa. gov/wp-content/uploads/2019/04/mom_history_2017*, 9.

Griffies, S. M., Winton, M., Anderson, W. G., Benson, R., Delworth, T. L., Dufour, C. O., Dunne, J. P., Goddard, P., Morrison, A. K., Rosati, A., et al. (2015b). Impacts on ocean heat from transient mesoscale eddies in a hierarchy of climate models. *Journal of Climate*, 28(3):952–977.

Grinfeld, P. (2009). Exact nonlinear equations for fluid films and proper adaptations of conservation theorems from classical hydrodynamics. *Journal of Geometry and Symmetry in Physics*, 16:1–21.

Grinfeld, P. (2013). *Introduction to tensor analysis and the calculus of moving surfaces*. Springer.

Halliwell, G. R. (2004). Evaluation of vertical coordinate and vertical mixing algorithms in the hybrid-coordinate ocean model (hycom). *Ocean Modelling*, 7(3-4):285–322.

Haveraaen, M. and Friis, H. A. (2009). Coordinate-free numerics: all your variation points for free? *International Journal of Computational Science and Engineering*, 4(4):223–230.

Haveraaen, M., Friis, H. A., and Munthe-Kaas, H. (2005). Computable scalar fields: A basis for pde software. *The Journal of Logic and Algebraic Programming*, 65(1):36–49.

Hawley, J. F., Smarr, L. L., and Wilson, J. R. (1984). A numerical study of nonspherical black hole accretion. i equations and test problems. *The Astrophysical Journal*, 277:296–311.

Heinzl, R. and Schwaha, P. (2011). A generic topology library. *Science of Computer Programming*, 76(4):324–346. Special issue on library-centric software design (LCSD 2006).

Hinch, J. and Harlen, O. (2021). Oldroyd B, and not A? *J. Non-Newton. Fluid*, 298:104668:1–7.

Holm, D. D. (2015). Variational principles for stochastic fluid dynamics. *P. Roy. Soc. Lond. A Mat.*, 471(2176):20140963:1–19.

Holm, D. D. (2025). *Geometric Mechanics-Part III: Broken Symmetry And Composition Of Maps*. World Scientific.

Ilıcak, M., Adcroft, A. J., Griffies, S. M., and Hallberg, R. W. (2012). Spurious dianeutral mixing and the role of momentum closure. *Ocean Modelling*, 45:37–58.

Itskov, M. (2015). *Tensor algebra and tensor analysis for engineers*. Springer International Publishing, Cham, Switzerland, fourth edition.

Jeevanjee, N. (2011). *An introduction to tensors and group theory for physicists*. Springer.

Koks, D. (2017). On the use of vectors, reference frames, and coordinate systems in aerospace analysis. Technical Report DST-Group-TR-3309, Defence Science and Technology Group, Australian Department of Defense.

Kundu, P. K., Cohen, I. M., and Dowling, D. R. (2016). *Fluid mechanics*. Elsevier Inc., sixth edition.

Lilly, J. M., Feske, J., Fox-Kemper, B., and Early, J. J. (2024). Integral theorems for the-gradient of a vector field, with a fluid dynamical application. *P. Roy. Soc. Lond. A Mat.*, 480(2293):20230550:1–30.

Maddison, J. R. and Marshall, D. (2013). The Eliassen-Palm flux tensor. *J. Fluid Mech.*, 729:69–102.

Marsden, J. E. and Ratiu, T. S. (1999). *Introduction to mechanics and symmetry*. Texts in Applied Mathematics. Springer, New York, NY, second edition.

McDougall, T. J. (1987). Neutral surfaces. *Journal of Physical Oceanography*, 17(11):1950–1964.

Megann, A., Chanut, J., and Storkey, D. (2022). Assessment of the z time-filtered arbitrary lagrangian-eulerian coordinate in a global eddy-permitting ocean model. *Journal of Advances in Modeling Earth Systems*, 14(11):e2022MS003056.

Morin, D. (2008). *Introduction to classical mechanics*. Cambridge University Press, Cambridge, UK.

Needham, T. (2021). *Visual Differential Geometry and Forms: A Mathematical Drama in Five Acts*. Princeton University Press.

Ogden, R. W. (1984). *Non-linear elastic deformations*. Ellis Horwood Limited, Mineola, NY.

Oldroyd, J. G. (1950). On the formulation of rheological equations of state. *Proceedings of the Royal Society of London. Series A. Mathematical and Physical Sciences*, 200(1063):523–541.

Pedlosky, J. (1987). *Geophysical fluid dynamics*. Springer-Verlang, New York, NY, second edition.

Petersen, M. R., Jacobsen, D. W., Ringler, T. D., Hecht, M. W., and Maltrud, M. E. (2015). Evaluation of the arbitrary lagrangian–eulerian vertical coordinate method in the mpas-ocean model. *Ocean Modelling*, 86:93–113.

Prusa, J. M. (2018). Computation at a coordinate singularity. *Journal of Computational Physics*, 361:331–352.

Salmon, R. (2013). An alternative view of generalized Lagrangian mean theory. *J. Fluid Mech.*, 719:165–182.

Vallis, G. K. (2017). *Atmospheric and oceanic fluid dynamics*. Cambridge University Press.

Veronis, G. (1975). The role of models in tracer studies. In *Numerical Models of the Ocean Circulation: Proceedings of a Symposium Held at Durham, New Hampshire, October 17–20, 1972*, pages 133–146. National Academy of Sciences.

Young, W. R. (2012). An exact thickness-weighted average formulation of the boussinesq equations. *Journal of Physical Oceanography*, 42(5):692–707.

CHAPTER 3

Beyond Vertical Coordinates

This chapter is a pre-print of a paper to be submitted shortly to the Journal of Physical Oceanography. I am the primary author along with Baylor Fox-Kemper and Jonathan Lilly.

Summary

Here we continue the project begun in Chapter 2—constructing a unified, coordinate-agnostic framework for geophysical fluid dynamics. Having defined time differentiation and written down the momentum equation in arbitrary coordinates, we now express the remaining fluid equations in this form along with common approximations such as the parameterization of sub-grid scale turbulent diffusion and the hydrostatic, traditional and small-slope approximations. These indicial equations, as expressed in Table 3.1, are the same for all coordinate systems, but to project them into a convenient basis we need to know the relevant metric coefficients and the setting velocity.

Section 3.5 defines basis vectors and metric coefficients for various useful coordinate systems, including isopycnal coordinates as defined in Young (2012), terrain-following coordinates as defined in Griffies (2018), and geoid-based coordinates. We also show how to define the setting velocity $\mathcal{W}$ for rotating buoyancy coordinates in section 3.3.2. Following the logic of Chapter 2,

the gradient of $\mathcal{W}$ allows us to express all of the apparent forces present in that setting, and to cleanly separate them into contributions from rotation and from the vertical motion of density surfaces. We perform this transformation in two steps, first defining $\mathcal{V} = \boldsymbol{\Omega} \times \boldsymbol{r}$ and then $\mathcal{W} = \mathcal{V} + \mathcal{U}$ for the rotating setting velocity $\mathcal{V}$ and the buoyancy setting velocity $\mathcal{U}$. The equations that express the fictitious and fantastical forces, arising respectively from $\nabla_{[j}\mathcal{W}_{i]}$ and $\nabla_{(j}\mathcal{W}_{i)}$, are completely general and work for any such two-step transformation where the first step is a rigid rotation.

Finally, we move on to sub-grid, turbulent diffusion parameterizations based on Redi (1982). The standard Redi mixing tensor effects a projection of any vector onto the neutral buoyancy surface, as pointed out by Griffies et al. (1998). This achieves isotropic diffusion within the neutral plane, but as Bachman et al. (2020) show, this is not realistic. We modify the Redi tensor to allow for anisotropic neutral diffusion and rigorously define the small-slope approximation to both the standard and anisotropic mixing tensors.

3.1 Introduction

Geophysical fluid dynamics (GFD) is the fluid dynamics of rapidly rotating, stratified flow over the topography of a rotating, spheroidal Earth with uneven surface heating. It is a non-relativistic branch of physics in the Newtonian limit of gravity, and centers on the effects of stratification, rotation, and topography, all of which break the isotropy of fluid motion and orient flow, stirring, and mixing along internal, curved surfaces.

The ocean is full of such surfaces. From the free surface of the ocean to interior surfaces of neutral buoyancy and sloping bottom topography, the dynamics of sea water are everywhere controlled by such curvature. Many of these surfaces vary in time as well as space, and all rotate along with the planet.

The ocean is also full of tensors. Physical quantities of interest in ocean physics are best modeled as tensor fields of some rank: temperature, salinity, velocity, momentum, vorticity, stress, turbulent stress, and strain rate. It is often joked that tensors “transform like tensors,” under changes of coordinates, however they do not really transform at all—their components do. This is why they are such a good model for physical reality. Though their components indeed transform in a particular way when we choose new frames of reference, those transformation rules serve only to ensure that the underlying tensor fields, and therefore the ocean state they represent, are unaffected by our choices of coordinates.

The natural calculus of tensors on curved surfaces is tensor analysis and differential geometry, and here we continue the work begun in Chapter 2 to specialize differential geometric methods to GFD in the hope that doing so will streamline communication among ocean and atmosphere models with varying configurations and illuminate some of the major existing problems.

There are three main goals of this chapter. First, we present the exact dynamical equations used in ocean modeling in a coordinate-agnostic index form. We express these along with the hydrostatic and traditional approximations, noting important simplifications for computational efficiency. Second, we provide a reference for the metric components implied by common choices of coordinates and an example of the transformation to a time-varying curvilinear setting. Finally, We show how the Redi diffusion tensor appears in this framework, how we justify the small-slope approximation geometrically, and a natural extension of the diffusion tensor to effect anisotropic diffusion in the neutral buoyancy plane. We do not fully treat eddy parameterization because a method of averaging (e.g., Bachman et al., 2020) or filtering (e.g., Aluie et al., 2018; Loose et al., 2023) is required to parameterize stirring as in Gent and McWilliams (1990) or Fox-Kemper and Ferrari (2008). We leave this for a later paper.

Unlike most other formulations of generalized coordinates, we do not restrict our attention to changing only the quasi-vertical coordinate, nor do we rely on specific discretizations, such as stacked shallow-water models. Non-inertial effects or “apparent forces” were shown in Chapter 2 to result from the transformation between the inertial frame and accelerating setting (including, but not limited to, the rotating frame). A distinct class of apparent forces results from deforming coordinate choices that oceanographers often use: isopycnal, pressure, tracer, and terrain-following (σ) coordinates.

There are many reasons to choose coordinates carefully (e.g., Chassignet et al., 2009), but until now their exposition usually begins with the hydrostatic approximation and numerical discretizations, followed by coordinate transformations, and possibly also assuming physical properties such as minimal mixing in specific directions. This procedure limits the potential accuracy of the resulting models—how does one implement numerical discretizations (e.g., Balsara and Shu, 2000) beyond the implicitly assumed approximations in the formulation of the "primitive" equations? Here we present the non-relativistic equations of motion for arbitrary choices of coordinates without approximation beyond the continuum approximation, and then apply the hydrostatic and traditional approximations afterward. Thus, numerical schemes of any order of accuracy can be built on the equations before approximations are made.

We delay until a later paper the treatment of "thickness-weighting", which is an additional step beyond coordinate transformations into eddy statistical averages (e.g., Dukowicz and Smith, 1997; Loose et al., 2023). This will require understanding what thickness-weighting means even in coordinates where "thicknesses" may have little meaning, and recognizing that density layers don't exist globally due to the non-integrable aspects of the seawater equation of state (McDougall, 1987; Jackett and McDougall, 1997; Nycander, 2011). Nonetheless, thickness-weighting underlies the formulation of quasi-Stokes drift and the parameterized streamfunctions of Gent and McWilliams (1990); Gent et al. (1995) and Fox-Kemper et al. (2008) as discussed by many (e.g., Dukowicz and Smith, 1997; Killworth, 1997; McDougall and McIntosh, 1996; Eden et al., 2007; Young, 2012; Salmon, 2013).

The structure of this work is as follows: section 3.2 introduces the relevant notation and conventions needed here that were not already introduced in section 2 of Chapter 2. Section 3.3 introduces the momentum equation and discusses its transformation first to the rotating frame, and then to a rotating, buoyancy coordinate setting. Expressions for the fictitious and fantastical forces are presented. Section 3.4 introduces common GFD approximations in tensor notation and presents the fluid equations in Table 3.1. Section 3.5 specifies basis vectors and metric coefficients for common GFD coordinate systems such as tracer, terrain-following, and geoid-based coordinates. Section 3.6 presents the Redi mixing tensor in index form, generalizes it to perform anisotropic diffusion in the neutral plane, and derives the small slope approximations to both the standard and anisotropic mixing tensors.

3.2 Definitions, Notation, and Conventions

This section extends §2 of Chapter 2 to accommodate the needs of this paper. See that section for a full treatment of the tensor analysis of Euclidean space in time-varying, curvilinear coordinates.

3.2.1 Inertial and Moving Settings

Here we briefly restate the conventions and results laid out in Chapter 2. We define two classes of coordinates: y^a in the inertial frame, and x^i in moving settings, where a "setting" is a frame-like entity that is allowed to deform – for example the Lagrangian setting deforms with a fluid. The term "frame" is then understood to capture *rigid* coordinate representations of space, and specifying that this frame is inertial implies that Newton's laws apply. These coordinate systems have origins O_y and O_x, and corresponding position vector fields $\boldsymbol{s}$ and $\boldsymbol{r}$. Tensor components indexed with the letters $\{a, b, c, d\}$ are understood to be with respect to an inertial basis $\boldsymbol{e}_a \equiv \partial_a \boldsymbol{s}$, while those indexed with the letters $\{i, j, k, \ell\}$ are understood to be with respect to a moving basis $\boldsymbol{e}_i \equiv \partial_i \boldsymbol{r}$. The basis $\boldsymbol{e}_a$ can be considered to be fixed in time, while the basis $\boldsymbol{e}_i$ cannot.

We assume coordinates to be well-behaved enough to be represented as invertible functions of one another:

$$y^a = y^a(x, t) \qquad x^i = x^i(y, t). \tag{3.1}$$

Their spatial derivatives are the components of the Jacobian transformation matrices

$$J_i^a = \frac{\partial y^a}{\partial x^i} \qquad J_a^i = \frac{\partial x^i}{\partial y^a}, \tag{3.2}$$

their partial time derivatives define the *setting velocity* $\boldsymbol{\mathcal{V}}$:

$$\mathcal{V}^a = \left.\frac{\partial y^a}{\partial t}\right|_x \qquad -\mathcal{V}^i = \left.\frac{\partial x^i}{\partial t}\right|_y, \tag{3.3}$$

where the $|_x$ notation indicates explicitly the coordinates to be held fixed. Let the scalar field ξ be a label that remains constant following fluid parcels. The total time derivatives of the coordinates with the label ξ held fixed define the observed velocities of a fluid parcel at these coordinates:

$$v^a = \left.\frac{dy^a}{dt}\right|_\xi \qquad u^i = \left.\frac{dx^i}{dt}\right|_\xi, \tag{3.4}$$

and thus $\boldsymbol{v}$ is also the absolute fluid velocity. We have $\boldsymbol{v} = \boldsymbol{u} + \boldsymbol{\mathcal{V}}$ where $\boldsymbol{\mathcal{V}}$, $\boldsymbol{v}$, and $\boldsymbol{u}$ are vector fields whose components transform freely between the y and x coordinate systems by contraction with the Jacobians, for example $\mathcal{V}^i = J_a^i \mathcal{V}^a$.

Total time derivatives of tensor quantities have components specified by the *material intrinsic derivative* $\delta/\delta t$. For moving coordinates x, this takes the form

$$\frac{\delta}{\delta t} = \left(\left.\frac{\partial}{\partial t}\right|_x + v^k \nabla_k - \mathcal{L}_{\mathcal{V}} \right), \tag{3.5}$$

where $\mathcal{L}_{\mathcal{V}}$ is a Lie derivative along the vector field $\boldsymbol{\mathcal{V}}$. Applied to an arbitrary vector field $\boldsymbol{w}$, this comes to

$$\frac{\delta w^i}{\delta t} = \left.\frac{\partial w^i}{\partial t}\right|_x + u^k \nabla_k w^i - w^k \nabla_k \mathcal{V}^i. \tag{3.6}$$

For fixed coordinates y, equations (3.5) and (3.6) reduce to the familiar form of the intrinsic derivative (Grinfeld, 2013; Aris, 1962):

$$\frac{\delta}{\delta t} = \left(\left. \frac{\partial}{\partial t} \right|_{y} + v^c \nabla_c \right), \tag{3.7}$$

and

$$\frac{\delta w^a}{\delta t} = \left. \frac{\partial w^a}{\partial t} \right|_{y} + v^c \nabla_c w^a \tag{3.8}$$

due to the properties of Lie derivatives in rigid coordinate systems—see Chapter 2, section 2.6.7. In either fixed frames or moving settings we have, by construction,

$$\frac{d\boldsymbol{w}}{dt} = \boldsymbol{e}_i \frac{\delta w^i}{\delta t} \quad \text{or} \quad \boldsymbol{e}^i \cdot \frac{d\boldsymbol{w}}{dt} = \frac{\delta w^i}{\delta t}, \tag{3.9}$$

which are equivalent. Analogous expressions hold for tensor fields of any order, and this derivative can be further generalized to follow non-material paths—see Chapter 2 section 2.4.6.

3.2.2 Time Dependence of Metric Components

The metric components presented in §3.5 are time-dependent because they are functions of the coordinates x^i which are themselves functions of time, specifying a moving setting by definition. Metric components do not, however, fully specify a moving setting. Our choice to operate in Euclidean space rather than Lorentzian 4-vector-based spacetime means that the metric tensor captures information about the spatial curvature of our coordinate surfaces at a given moment, but misses information about how those surfaces move. That information is given instead by the setting velocity $\boldsymbol{\mathcal{V}}$, as shown by (3.3).

Consider two spherical coordinate systems with the same origin, one fixed, and one rotating. For a fixed time, their respective basis vectors $\boldsymbol{e}_a$ and $\boldsymbol{e}_i$ are aligned at every point in space, and so their metric components are indistinguishable as well. The metric does not capture the rotation, and unless we specify that each coordinate point in the rotating system is moving with velocity $\mathcal{V} = \boldsymbol{\Omega} \times \boldsymbol{r}$, we completely miss the difference between these frames.

3.2.3 Matrix Representations of 2nd Order Tensors

We present the matrix forms of the metric tensors associated with various useful coordinate bases. It is important to keep in mind that the metric tensor $\boldsymbol{g} = g_{ij}\boldsymbol{e}^i\boldsymbol{e}^j$ itself[1] for flat space is in each case the same bilinear function from pairs of vectors to scalars, but its components depend on the basis vectors we choose. To be explicit about this dependence, we introduce the notation $\overset{\mathcal{B}}{\longmapsto}$ to denote a tensor's representation in the covariant basis $\mathcal{B}$, for example:

$$g_{ij} \overset{\mathcal{S}}{\longmapsto} \begin{bmatrix} r^2\,\mathrm{c}_\theta^2 & 0 & 0 \\ 0 & r^2 & 0 \\ 0 & 0 & 1 \end{bmatrix} \tag{3.10}$$

are the components g_{ij} of the metric tensor $\boldsymbol{g}$ in the covariant spherical basis $\mathcal{S}$ with radius r and latitude θ as presented in Table 3.3. It should be understood that for a tensor with covariant indices, those indices pair with the reciprocal basis of the denoted covariant basis. For example, we would write the inverse metric components as

$$g^{ij} \overset{\mathcal{S}}{\longmapsto} \begin{bmatrix} r^{-2}\,\mathrm{c}_\theta^{-2} & 0 & 0 \\ 0 & r^{-2} & 0 \\ 0 & 0 & 1 \end{bmatrix} \tag{3.11}$$

with the same $\overset{\mathcal{S}}{\longmapsto}$, even though these particular components would be contracted with the elements of $\tilde{\mathcal{S}}$. This is to avoid ambiguity with mixed tensors such as $A^i_{\ j}$. We use this same notation when we must represent a basis as an indexed set $\boldsymbol{e}_i$, for example

[1] In texts on relativity, the metric tensor is usually written as $ds^2 = g_{ij}\mathrm{d}x^i\mathrm{d}x^j$ using the dual basis of differential 1-forms $\mathrm{d}x^i$. Since we always work within a flat, 3D, Euclidean embedding space, we lose nothing by representing the dual basis of 1-forms instead as the reciprocal vector basis $\boldsymbol{e}^i$, which is considerably less abstract and easier to picture.

$$\boldsymbol{e}_i \overset{\mathcal{S}}{\longmapsto} [r\,\mathrm{c}_\theta\,\hat{\boldsymbol{\lambda}}, r\hat{\boldsymbol{\theta}}, \hat{\boldsymbol{r}}] \tag{3.12}$$

When an indexed object makes reference to two different bases, as for a Jacobian matrix, we include a basis indicator below the arrow as well. For example, the Jacobian that transforms vector components v^i in the 2D polar coordinate frame $\mathcal{P}$ to components $v^{i'}$ in the 2D Cartesian frame C is denoted by

$$J_i^{i'} \overset{\mathcal{P},C}{\longmapsto} \begin{bmatrix} \mathrm{c}_\theta & -r\,\mathrm{s}_\theta \\ \mathrm{s}_\theta & r\,\mathrm{c}_\theta \end{bmatrix} \tag{3.13}$$

The two horizontal or quasi-horizontal basis vectors of basis $\mathcal{B}$ form the sub-basis $\mathcal{B}_h$. For example, the pullback onto a density surface given by equation (3.62)

$$Z_\alpha^i \overset{C,\tilde{\mathcal{Y}}_h}{\longmapsto} \begin{bmatrix} 1 & 0 \\ 0 & 1 \\ L_x & L_y \end{bmatrix}$$

projects onto the quasi-horizontal surface basis $\tilde{\mathcal{Y}}_h$ of the ambient basis $\tilde{\mathcal{Y}}$.

There are many notations for matrix representations across various texts, and some choose a simple equals sign in place of our arrow, however this leaves the choice of basis implicit. We wish to emphasize that any matrix representation is valid only in a particular basis, and always to make that choice explicit.

Throughout, bases will be named by a script letter and defined as an ordered set of vectors: $\mathcal{B} = \{\boldsymbol{a}, \boldsymbol{b}, \boldsymbol{c}\}$. A tilde will denote the reciprocal basis like so: $\tilde{\mathcal{B}}$. Whether we choose $\mathcal{B}$ or $\tilde{\mathcal{B}}$ to be the covariant basis $\boldsymbol{e}_i$ is arbitrary, and a matter only of taste or convention. This choice, however, constrains the choice of the contravariant basis to be the dual set $\boldsymbol{e}^i = \boldsymbol{e}_j g^{ji}$. We always present the basis vectors in the indexed order used for contractions: $\mathcal{B} = \{\boldsymbol{e}_1, \boldsymbol{e}_2, \boldsymbol{e}_3\}$. The quasi-horizontal subset $\{\boldsymbol{e}_1, \boldsymbol{e}_2\}$ of the basis $\mathcal{B}$ is denoted $\mathcal{B}_h$.

3.2.4 Surfaces

Finally, we will need some tools for dealing with vector fields constrained to lie on two-dimensional surfaces embedded within three-dimensional space. Imagine a continuously indexed collection of non-intersecting but potentially curved and moving surfaces.[2] A good example is surfaces of constant density in the ocean. In what follows, it suffices to consider only one such surface.

Given a two-dimensional surface, we first create projection operators that act normal or tangent to the surface, as illustrated in Fig. 3.1. Let $\boldsymbol{n} = n^i \boldsymbol{e}_i = n_i \boldsymbol{e}^i$ be the unit normal vector field, and define the *normal projection* operator $\boldsymbol{N}$ as the tensor having components

$$N^i_j = n^i n_j. \tag{3.14}$$

The projection of some vector field $\boldsymbol{w}$ onto $\boldsymbol{n}$ is then a vector with components $N^i_j w^j = n^i n_j w^j$, meaning that it is the normal vector $\boldsymbol{n}$ scaled by the dot product $n_j w^j$. Similarly, the *transverse projection* operator $\boldsymbol{T}$, also called the *orthogonal projection*, is the tensor having components

$$T^i_j \equiv \delta^i_j - N^i_j. \tag{3.15}$$

Because δ^i_j represents the identity tensor, the action of this operator on a vector field is to remove its normal projection, yielding a vector field everywhere tangent to the surface.

In addition to the coordinates x^i and y^a that span three-dimensional space, we will also make use of coordinates restricted to the surface. Tensor components on the surface are indexed with Greek letters $\{\alpha, \beta, \gamma, \delta\}$ that run over the set $\{1, 2\}$, following Grinfeld (2013). We denote 2D surface coordinates by s^α, and define corresponding basis vectors $\boldsymbol{s}_\alpha \equiv \partial_\alpha \tilde{\boldsymbol{r}}$, where the tilde is used to denote tensors that are limited to the surface or the components thereof. There exist Jacobian-like transformation matrices between the surface and ambient coordinates, which we

[2] That is, a time-varying *foliation* of $\mathbb{R}^3$.

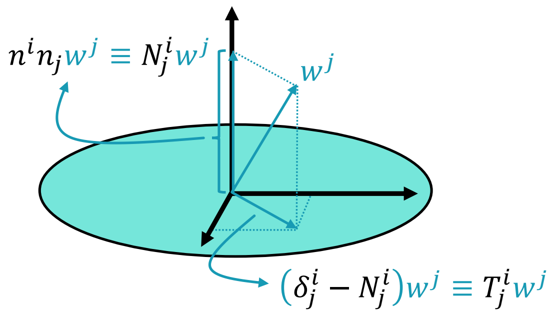

Figure 3.1: Visualization of the normal and transverse projection operators acting on the components of a vector $\boldsymbol{w}$.

denote as

$$Z^i_\alpha \equiv \frac{\partial x^i}{\partial s^\alpha}, \qquad Z^\alpha_i \equiv g_{ij} Z^j_\beta g^{\beta\alpha} \tag{3.16}$$

This is called the *shift tensor* by Grinfeld (2013), but is more often referred to as the *pullback matrix* — see Appendix A of Carroll (2019). The second equation requires the definition of the contravariant surface metric components $g^{\alpha\beta}$ given in equation (3.20).

Z^i_α differs from a standard Jacobian J^i_a because it transforms to and from a lower-dimensional subspace, and so information is lost when moving from the ambient to the surface basis. Another interpretation will be given momentarily. Analogous to Jacobians, the two shift tensors are a sort of inverse of one another, always satisfying

$$Z^\alpha_i Z^i_\beta = \delta^\alpha_\beta, \tag{3.17}$$

however because Z^i_α can have a rank of at most two, $Z^i_\alpha Z^\alpha_j \neq \delta^i_{\ j}$.

The shift tensor operates on the ambient basis to recover the surface basis,

$$\boldsymbol{s}_\alpha = Z^i_\alpha \boldsymbol{e}_i, \qquad \boldsymbol{s}^\alpha = Z^\alpha_i \boldsymbol{e}^i \tag{3.18}$$

but note that the ambient basis vectors cannot be recovered from the surface basis vectors. The metric coefficients of the surface basis are then again defined as $g_{\alpha\beta} \equiv \boldsymbol{s}_\alpha \cdot \boldsymbol{s}_\beta$, but these can also be calculated by "pulling back" the ambient metric components using the shift tenor like so:

$$g_{\alpha\beta} = Z^i_\alpha Z^j_\beta g_{ij} \tag{3.19}$$

As in the case of the ambient basis, we again define the contravariant metric components by

$$g^{\alpha\gamma} g_{\gamma\beta} = \delta^\alpha_\beta \tag{3.20}$$

Two successive applications of the shift tensor project an ambient vector onto the plane and then recover the ambient components of that projection, which is to say that we can write the transverse projection operator T^i_j as

$$T^i_j = Z^i_\alpha Z^\alpha_j, \tag{3.21}$$

as will now be shown. A general vector field $\boldsymbol{w}$, projected onto the surface, becomes

$$\tilde{w}^i \equiv T^i_j w^j, \tag{3.22}$$

resulting in a version of that vector that is limited to the surface. Alternatively, using the shift tensor, we have[3]

$$\tilde{w}^\alpha \equiv Z^\alpha_j w^j, \qquad \tilde{w}^i = Z^i_\alpha \tilde{w}^\alpha \tag{3.23}$$

with the first operation transforming the vector into its surface representation and thus projecting it into the surface, and the second operation transforming the projected vector back into its ambient representation. Combining these two equations and comparison with (3.22) then yields (3.21).

Similar to the ambient case, $g^{\alpha\beta}$, $g_{\alpha\beta}$, δ^α_β, Z^i_α, and Z^α_i can all be represented as the components

[3]This justifies the use of the tilde notation. $\tilde{\boldsymbol{w}} = w^\alpha \boldsymbol{e}_\alpha$ is the surface projection of $\boldsymbol{w} = w^i \boldsymbol{e}_i$, and in general these are different vectors because $\boldsymbol{w}$ will have a non-zero component normal to the surface.

of one set of basis vectors in terms of another, that is, as dot products of basis vector sets:

$$g_{\alpha\beta} \equiv \boldsymbol{s}_\alpha \cdot \boldsymbol{s}_\beta \qquad \delta^\alpha_\beta = \boldsymbol{s}^\alpha \cdot \boldsymbol{s}_\beta \qquad g^{\alpha\beta} = \boldsymbol{s}^\alpha \cdot \boldsymbol{s}^\beta$$
$$Z^i_\alpha = \boldsymbol{e}^i \cdot \boldsymbol{s}_\alpha \qquad Z^\alpha_i = \boldsymbol{s}^\alpha \cdot \boldsymbol{e}_i \tag{3.24}$$

This makes it easy to show that, also in analogy to the ambient case, all are components of the same transverse projection tensor $\boldsymbol{T}$ with different choices of representation. This is similar to how the identity tensor components in different representations of the ambient basis can appear as $\delta^a_b = \boldsymbol{e}^a \cdot \boldsymbol{e}_b$ or $g_{ab} = \boldsymbol{e}_a \cdot \boldsymbol{e}_b$, for example. The coefficients $g^{\alpha\beta}$, $g_{\alpha\beta}$, and δ^α_β are the contravariant, covariant, and mixed components of the transverse projection operator when it is represented in terms of the surface basis vectors,

$$\boldsymbol{T} = g^{\alpha\beta}\boldsymbol{s}_\alpha \otimes \boldsymbol{s}_\beta = g_{\alpha\beta}\boldsymbol{s}^\alpha \otimes \boldsymbol{s}^\beta = \delta^\alpha_\beta \boldsymbol{s}_\alpha \otimes \boldsymbol{s}^\beta \tag{3.25}$$

while Z^i_α and Z^α_i are its components when represented in terms of one surface and one ambient basis vector,

$$\boldsymbol{T} = Z^i_\alpha \boldsymbol{e}_i \otimes \boldsymbol{s}^\alpha = Z^\alpha_i \boldsymbol{s}_\alpha \otimes \boldsymbol{e}^i. \tag{3.26}$$

In terms of a tensor operation, (3.21) is simply $\boldsymbol{T} = \boldsymbol{T}\boldsymbol{T}$, reflecting the idempotent property of projection operators. It is also true that $\boldsymbol{N} = \boldsymbol{N}\boldsymbol{N}$. Unlike the identity tensor, the transverse projection tensor and the normal projection tensor are not full rank and thus not invertible, which is why the ambient basis cannot be recovered from the surface basis or the normal direction alone.

3.3 Fluid Equations

The following assumes the reader is familiar with the intrinsic derivative $\delta/\delta t$, and its application to the case of moving frames presented in sections 4f and 4g of Chapter 2. The inviscid momentum equation in terms of the generalized material intrinsic derivative is

$$\frac{\delta v^i}{\delta t} = -\frac{1}{\rho}\nabla^i p - \nabla^i g, \tag{3.27}$$

which is equivalent to

$$\left.\frac{\partial u^i}{\partial t}\right|_x + u^j \nabla_j u^i = -2u^j \nabla_j \mathcal{V}^i - \mathcal{V}^j \nabla_j \mathcal{V}^i - \left.\frac{\partial \mathcal{V}^i}{\partial t}\right|_x - \frac{1}{\rho}\nabla^i p - \nabla^i g \tag{3.28}$$

when expressed in terms of the measured velocity $\boldsymbol{u}$, where the left hand side is the observed acceleration of a fluid parcel, $-2u^j \nabla_j \mathcal{V}^i$ is the Coriolis-like acceleration, $-\mathcal{V}^j \nabla_j \mathcal{V}^i$ is the centrifugal-like acceleration (assuming O_x and O_y always coincide), and $\partial \mathcal{V}^i / \partial t|_x$ is the Euler-like acceleration. Here the scalar field g is the gravitational potential. Because in uniform rotation the centrifugal force is conservative, we would normally combine g with the centrifugal potential to define a geopotential Φ, however for arbitrarily moving coordinates x, $(\boldsymbol{\mathcal{V}} \cdot \boldsymbol{\nabla})\boldsymbol{\mathcal{V}}$ is not necessarily irrotational, and so we choose to leave the terms separate here.

Given a particular moving setting, the apparent force terms that arise are then determined by the gradient tensor of the setting velocity, $\boldsymbol{\nabla} \otimes \boldsymbol{\mathcal{V}}$, which governs both the Coriolis-like and centrifugal-like forces, and by $\partial \mathcal{V}^i / \partial t|_x$, which governs the Euler-like terms. We will now show the explicit forms that these terms take in some familiar settings. We choose to show the matrix form of $\nabla_j \mathcal{V}_i$ rather than $\nabla_j \mathcal{V}^i$ because lowering the index makes the symmetries more obvious.

3.3.1 The Rotating Frame

We can apply these definitions to the rotating transformation and see that we recover familiar results. The coordinates y^a and x^i become

$$y^a(t,x) \overset{\mathcal{S}}{\longmapsto} \begin{pmatrix} \varphi(t,\lambda) \\ \theta \\ r \end{pmatrix} = \begin{pmatrix} \lambda + \Omega t \\ \theta \\ r \end{pmatrix}, \qquad x^i(t,y) \overset{\mathcal{S}}{\longmapsto} \begin{pmatrix} \lambda(t,\varphi) \\ \theta \\ r \end{pmatrix} = \begin{pmatrix} \varphi - \Omega t \\ \theta \\ r \end{pmatrix} \tag{3.29}$$

where Ω is the angular velocity of the rotating coordinate system, and we call the inertial azimuthal coordinate φ to distinguish it from the longitude λ as measured on the rotating Earth. In that case, the Jacobians have the particularly simple form $J^i_a = \delta^i_a$ and $J^a_i = \delta^a_i$ because we are in spherical coordinates in both frames, but in general such Jacobians will be functions of both space and time. The setting velocity field $\mathcal{V}$ is then given by

$$\mathcal{V}^a \overset{\mathcal{S}}{\longmapsto} \begin{bmatrix} \Omega \\ 0 \\ 0 \end{bmatrix} \tag{3.30}$$

Because the purely rotating transformation is rigid, we expect to find that $\boldsymbol{\nabla} \otimes \boldsymbol{\mathcal{V}}$ is antisymmetric, and indeed we do:

$$\begin{aligned} \nabla_j \mathcal{V}_i &\overset{\mathcal{S}}{\longmapsto} r^2 \mathrm{c}^2_\theta \Omega \begin{bmatrix} 0 & -\mathrm{t}_\theta & 1/r \\ \mathrm{t}_\theta & 0 & 0 \\ -1/r & 0 & 0 \end{bmatrix} \\ &\overset{\mathcal{C}}{\longmapsto} \qquad \Omega \begin{bmatrix} 0 & -1 & 0 \\ 1 & 0 & 0 \\ 0 & 0 & 0 \end{bmatrix} \end{aligned} \tag{3.31}$$

With both indices lowered, these components do not form a normal matrix in the sense of linear algebra, which would have one upper and one lower index. We must note explicitly then that i indexes rows and j columns in our representation, as would have been the case for the true matrix $\nabla_j \mathcal{V}^i$.

The tensor $\boldsymbol{\nabla} \otimes \boldsymbol{\mathcal{V}}$ effects a cross product with $\boldsymbol{\Omega}$,[4] and so contraction with $-2u^j$ recovers the standard Coriolis force $-2\boldsymbol{\Omega} \times \boldsymbol{u}$. Further, $\boldsymbol{\mathcal{V}}$ has the same components as $\boldsymbol{\Omega} \times \boldsymbol{r}$, and so contraction of $\boldsymbol{\nabla} \otimes \boldsymbol{\mathcal{V}}$ with $\mathcal{V}^j$ recovers the standard centrifugal force $\boldsymbol{\Omega} \times \boldsymbol{\Omega} \times \boldsymbol{r}$.[5]

We also find that

$$\left.\frac{\partial \mathcal{V}^i}{\partial t}\right|_x \overset{\mathcal{S}}{\longmapsto} \begin{bmatrix} 0 \\ 0 \\ 0 \end{bmatrix} \tag{3.32}$$

and so the Euler force is zero in this case, which we expected because the rotation rate of the Earth is constant.

3.3.2 The Rotating Buoyancy Setting

Consider how this looks for a slightly more complicated coordinate transformation: inertial spherical to rotating spherical-based buoyancy coordinates. In this case we will do the transformation in two parts, first transforming the inertial spherical setting y to the rotating spherical setting x as before, and then further transforming x to the rotating buoyancy setting z, where $z^p = (\tilde{\lambda}, \tilde{\theta}, \tilde{b})$ and buoyancy $\tilde{b} = b(t, \lambda, \theta, r)$ is a function of space and time. We index objects in the z setting with $\{p, q, r\}$. In principle one could do this transformation directly from y, however it is impractical to represent buoyancy as a function of fixed, celestial longitude φ, and more natural to represent it as a function of terrestrial longitude λ. In the transformation from x to z we follow along closely with §2 of Young (2012), making the necessary adjustments for spherical coordinates. The coordinate systems are related as

[4] Contraction with the j index of $\nabla_j \mathcal{V}_i$ effects $\boldsymbol{\Omega} \times \_$ while contraction with the i index effects $\_ \times \boldsymbol{\Omega}$.
[5] See Appendix A for a list of useful objects in spherical coordinates.

$$y^a(x,t) = \begin{pmatrix} \varphi(\lambda,t) = \lambda + \Omega t \\ \theta \\ r \end{pmatrix} \quad x^i(y,t) = \begin{pmatrix} \lambda(\varphi,t) = \varphi - \Omega t \\ \theta \\ r \end{pmatrix}$$

$$x^i(z,\tilde{t}) = \begin{pmatrix} \lambda \\ \theta \\ r = \varrho(\tilde{\lambda},\tilde{\theta},\tilde{b},\tilde{t}) \end{pmatrix} \quad z^p(x,t) = \begin{pmatrix} \tilde{\lambda} \\ \tilde{\theta} \\ \tilde{b} = b(\lambda,\theta,r,t) \end{pmatrix} \tag{3.33}$$

Note that ϱ is not density, but the name of the functional form of the coordinate r when represented as a function of z^p. Compare to Young's equation (25). We name the rotating buoyancy setting velocity $\boldsymbol{\mathcal{W}}$. Our goal is to find the form of $\boldsymbol{\nabla} \otimes \boldsymbol{\mathcal{W}}$ in spherical coordinates x^i and compare it to equation (3.31); see Appendix B for the full calculations. Following Young (2012), we define the symbols

$$\sigma \equiv \frac{1}{\partial_r b}$$

$$L_\lambda \equiv -\sigma \partial_\lambda b$$

$$L_\theta \equiv -\sigma \partial_\theta b \tag{3.34}$$

$$\omega \equiv -\sigma \left. \frac{\partial b}{\partial t} \right|_x$$

and the components of $\boldsymbol{\mathcal{W}}$ are

$$\mathcal{W}^a \stackrel{\mathcal{S}}{\longmapsto} \begin{bmatrix} \Omega \\ 0 \\ \omega \end{bmatrix} \tag{3.35}$$

Ultimately, we find that

$$\nabla_j \mathcal{W}_i \xmapsto{\mathcal{S}} \begin{bmatrix} 0 & 0 & 0 \\ 0 & 0 & 0 \\ \partial_\lambda \omega & \partial_\theta \omega & \partial_r \omega \end{bmatrix} + r^2\,\mathrm{c}_\theta^2\,\Omega \begin{bmatrix} 0 & -\mathrm{t}_\theta & 1/r \\ \mathrm{t}_\theta & 0 & 0 \\ -1/r & 0 & 0 \end{bmatrix} + \omega \begin{bmatrix} rc_\theta^2 & 0 & 0 \\ 0 & r & 0 \\ 0 & 0 & 0 \end{bmatrix} \tag{3.36}$$

which in buoyancy coordinates looks like

$$\begin{aligned} \nabla_q \mathcal{W}_p \xmapsto{\mathcal{B}} & \begin{bmatrix} L_\lambda\partial_\lambda\omega + L_\lambda^2\partial_r\omega & L_\lambda\partial_\theta\omega + L_\lambda L_\theta\partial_r\omega & \sigma L_\lambda\partial_r\omega \\ L_\theta\partial_\lambda\omega + L_\lambda L_\theta\partial_r\omega & L_\theta\partial_\theta\omega + L_\theta^2\partial_r\omega & \sigma L_\theta\partial_r\omega \\ \sigma\partial_\lambda\omega + \sigma L_\lambda\partial_r\omega & \sigma\partial_\theta\omega + \sigma L_\theta\partial_r\omega & \sigma^2\partial_r\omega \end{bmatrix} \\ & + r^2\,\mathrm{c}_\theta^2\,\Omega \begin{bmatrix} 0 & L_\theta/r - \mathrm{t}_\theta & \sigma/r \\ \mathrm{t}_\theta - L_\theta/r & 0 & 0 \\ -\sigma/r & 0 & 0 \end{bmatrix} \\ & + \omega \begin{bmatrix} rc_\theta^2 & 0 & 0 \\ 0 & r & 0 \\ 0 & 0 & 0 \end{bmatrix} \end{aligned} \tag{3.37}$$

We present the decomposition into its symmetric (deforming) and antisymmetric (rigid) parts in spherical coordinates x^i to allow direct comparison to equation (3.31):

$$\nabla_{(j} \mathcal{W}_{i)} \xmapsto{\mathcal{S}} \frac{1}{2} \begin{bmatrix} 0 & 0 & \partial_\lambda \omega \\ 0 & 0 & \partial_\theta \omega \\ \partial_\lambda \omega & \partial_\theta \omega & 2\partial_r \omega \end{bmatrix} + \omega \begin{bmatrix} rc_\theta^2 & 0 & 0 \\ 0 & r & 0 \\ 0 & 0 & 0 \end{bmatrix} \tag{3.38}$$

$$\nabla_{[j} \mathcal{W}_{i]} \xmapsto{\mathcal{S}} \frac{1}{2} \begin{bmatrix} 0 & 0 & -\partial_\lambda \omega \\ 0 & 0 & -\partial_\theta \omega \\ \partial_\lambda \omega & \partial_\theta \omega & 0 \end{bmatrix} + r^2\,\mathrm{c}_\theta^2\,\Omega \begin{bmatrix} 0 & -\mathrm{t}_\theta & 1/r \\ \mathrm{t}_\theta & 0 & 0 \\ -1/r & 0 & 0 \end{bmatrix} \tag{3.39}$$

This final term is identical to the components of $\boldsymbol{\nabla} \otimes \boldsymbol{\mathcal{V}}$ in equation (3.31) because it is the part of $\boldsymbol{\nabla} \otimes \boldsymbol{\mathcal{W}}$ due purely to rotation.

In terms of the measured fluid velocity $\boldsymbol{w} \equiv \boldsymbol{e}_p dz^p/dt$, the *local Coriolis force* will have components $2w^j \nabla_{[j} \mathcal{W}_{i]}$. Just like the standard Coriolis force, this apparent force will act perpendicular to measured velocity because $w^i w^j \nabla_{[j} \mathcal{W}_{i]} = 0$.[6] See Chapter 2 sections 5b and 6b for a full discussion of the local Coriolis force.

Similarly, there will be an analog of the centrifugal force with components $\mathcal{W}^j \nabla_{[j} \mathcal{W}_{i]}$ that acts perpendicular to $\boldsymbol{\mathcal{W}}$. The two copies of $\boldsymbol{\mathcal{W}}$ in this expression ensure that, like the standard centrifugal force, its value does not depend on the sign of $\boldsymbol{\mathcal{W}}$ — centrifugal force is directed outward whichever way the merry-go-round spins.

Although these apparent forces are analogous to the Coriolis force $2u^j \nabla_j \mathcal{V}_i$ and centrifugal force $\mathcal{V}^j \nabla_j \mathcal{V}_i$, they are not identical. In equation (3.101), we introduce the velocity field $\boldsymbol{\mathcal{U}}$ — the velocity of the z setting as viewed from the x setting — defined so that $\boldsymbol{\mathcal{W}} = \boldsymbol{\mathcal{V}} + \boldsymbol{\mathcal{U}}$, which also gives $\boldsymbol{w} = \boldsymbol{u} - \boldsymbol{\mathcal{U}}$. See Table 3.5 for the names of all relative setting velocities. We can use this to decompose the apparent force terms

$$2w^j \nabla_{[j} \mathcal{W}_{i]} = \boxed{2u^j \nabla_j \mathcal{V}_i} + 2\left(u^j \nabla_{[j} \mathcal{U}_{i]} - \mathcal{U}^j \nabla_{[j} \mathcal{W}_{i]}\right) \tag{3.40}$$

where the left-hand side is the local, generalized Coriolis force, the boxed term is the standard Coriolis force, and the other two terms are unnamed. Similarly we have

$$\mathcal{W}^j \nabla_{[j} \mathcal{W}_{i]} = \boxed{\mathcal{V}^j \nabla_j \mathcal{V}_i} + \mathcal{V}^j \nabla_{[j} \mathcal{U}_{i]} + \mathcal{U}^j \nabla_{[j} \mathcal{W}_{i]} \tag{3.41}$$

where the left-hand side is the generalized centrifugal force, the boxed term is the standard centrifugal force, and the other two terms are unnamed. Furthermore, the symmetric part of $\boldsymbol{\nabla} \otimes \boldsymbol{\mathcal{W}}$ will produce unnamed fantastical force

$$\left(2w^j + \mathcal{W}^j\right) \nabla_{(j} \mathcal{W}_{i)} \tag{3.42}$$

[6] The double contraction of a symmetric tensor such as $w^i w^j$ with an antisymmetric tensor is identically zero.

related to the deformation of the buoyancy setting as the buoyancy surfaces undulate. This fantastical term is expected to be small compared to the boxed terms of (3.40)-(3.41) if $\mathcal{V}^j\mathcal{V}_j \gg \mathcal{U}^j\mathcal{U}_j$.

We also have a non-zero generalized Euler force in this case:

$$J^i_p \left.\frac{\partial \mathcal{W}^p}{\partial t}\right|_z \tag{3.43}$$

We presented this in rotating spherical coordinates x^i to facilitate comparison with the previous section, but these expressions can be recast in rotating buoyancy coordinates z^p using the Jacobians in equations (3.104) and (3.105).

Finally note that, although the matrix representations we present in this section are specific to rotating spherical buoyancy coordinates, the indexed expressions (3.40) - (3.42) are entirely general, and apply to any setting velocity $\mathcal{W}$ laid on top of rotating spherical coordinates.

3.4 Common Approximations

While it is nice to have the exact equations in tensor form, it is useful to write down common approximations as well.

3.4.1 Perfect Fluids in an Accelerating or Rotating Frame

We summarize the equations of motion for geophysical fluid dynamics in covariant form in Table 3.1.

3.4.2 Ocean Primitive Equations

Hydrostatic Balance

Hydrostatic balance is an important simplification that allows the pressure gradient equation to be separable. In general, solving for the pressure field is a three-dimensional partial differential

Table 3.1: Rotating fluid equations in symbolic and index notations. We have the absolute fluid velocity $\boldsymbol{v} = \boldsymbol{u} + \boldsymbol{\mathcal{V}}$, where $\boldsymbol{u}$ is the fluid velocity as measured locally in the moving setting, and $\boldsymbol{\mathcal{V}}$ is the absolute velocity of the moving setting. Setting velocity $\boldsymbol{\mathcal{V}}$ is $\Omega\bar{\varphi} = \Omega r c_\theta \hat{\varphi}$ in the case of pure rotation. This choice for $\boldsymbol{\mathcal{V}}$, or indeed any choice for which $\nabla_{(j}\mathcal{V}_{i)} = 0$, results in a conservative Coriolis-like term $\mathcal{V}^j \nabla_j \mathcal{V}^i$ which could be absorbed into the gravitational potential g, however this is not the case for general $\boldsymbol{\mathcal{V}}$—see section 2.6.3. The tracer transport equation can be used either for salinity S or potential temperature Θ. κ_τ is the isotropic background diffusivity of the relevant tracer τ, and \$ is the anisotropic Redi tensor—see section 3.6.2. To close this equation set we must also include an equation of state $b = b(S, \Theta, p)$.

	Symbolic	Index
Continuity	$\partial_t \rho + \boldsymbol{\nabla} \cdot (\rho \boldsymbol{v}) = 0$	$\left.\frac{\partial \rho}{\partial t}\right\rvert_x + \nabla_i(\rho[u^i + \mathcal{V}^i]) = 0$
Momentum	$\frac{D\boldsymbol{u}}{Dt} + 2\boldsymbol{\Omega} \times \boldsymbol{u} = -\frac{1}{\rho}\boldsymbol{\nabla} p - \boldsymbol{\nabla}\Phi$	$\left.\frac{\partial u^i}{\partial t}\right\rvert_x + u^j \nabla_j u^i + 2u^j \nabla_j \mathcal{V}^i + \mathcal{V}^j \nabla_j \mathcal{V}^i + \left.\frac{\partial \mathcal{V}^i}{\partial t}\right\rvert_x = -\frac{1}{\rho}\nabla^i p - \nabla^i g$
Incompressibility	$\boldsymbol{\nabla} \cdot \boldsymbol{v} = 0$	$\nabla_i \left(u^i + \mathcal{V}^i\right) = 0$
Tracer transport	$\frac{D\tau}{Dt} = \boldsymbol{\nabla} \cdot \boldsymbol{R} \cdot \boldsymbol{\nabla}\tau$	$\frac{D\tau}{Dt} = \nabla_i \left[\left(\kappa_\tau g^{ij} + \$^{ij}\right) \nabla_j \tau\right]$

equation, but with the hydrostatic approximation it becomes a system of one ODE and one two-dimensional PDE, which is computationally favorable. To reap this benefit we must choose a compatible coordinate system – one where the vertical direction aligns with the acceleration due to effective gravity $\boldsymbol{g} = -\nabla\Phi$, [7] where we define the geopotential Φ to be the sum of the gravitational potential and the centrifugal potential. In height coordinates (for height z defined in terms of the geopotential) we have the usual form of the hydrostatic balance

$$\partial_z p = -\rho g \tag{3.44}$$

From this scalar equation, we can deduce a vector equation by recognizing that, as clarified by Stewart and McWilliams (2022), in any orthogonal coordinate system with the vertical defined by $\nabla\Phi$, we have $-g\hat{\boldsymbol{k}} = -\boldsymbol{\nabla}\Phi$:

$$\hat{\boldsymbol{k}}\partial_z p = \rho\boldsymbol{\nabla}\Phi \tag{3.45}$$

where $\hat{\boldsymbol{k}}$ is the vertical unit vector defined by $\hat{\boldsymbol{k}} = \nabla\Phi/|\nabla\Phi|$. To write this equation in covariant form, we project ∇p onto $\hat{\boldsymbol{k}}$ using

$$k^i k_j \equiv \frac{\nabla^i\Phi\nabla_j\Phi}{\nabla^k\Phi\nabla_k\Phi}. \tag{3.46}$$

Hydrostatic balance then becomes

$$k^i k_j \nabla^j p = \rho\nabla^i\Phi, \tag{3.47}$$

which is valid in any curvilinear coordinate system whatever – not only in orthogonal coordinates with one basis vector oriented vertically, as in equation (3.45).

Table 3.2 shows that the coordinate settings defining the vertical along $\hat{\boldsymbol{k}}$ result in simpler

[7] It is conventional in geodetics to use the positive gradient $\boldsymbol{g} = \nabla\Phi$ so that the geopotential as decreasing with increasing radius (Hughes and Bingham, 2006), however we follow the oceanographer's and the physicist's convention.

representations of hydrostatic balance, whereas in Young's basis $\mathcal{Y}$ (see section 3.5.1), the expression is convoluted because we are forced to use pressure derivatives with respect to the tracer concentration τ, the proxy for height. We therefore prefer to orient our vertical direction along the geopotential gradient, as in Young's dual basis $\tilde{\mathcal{Y}}$.

Inviscid Momentum Equation and the Traditional Approximation

We begin by writing the inviscid momentum equation, where we make the choice

$$F^i = -\frac{1}{\rho}\nabla^i p - \nabla^i \Phi. \tag{3.48}$$

Recognizing that here we have $d\mathbf{\Omega}/dt = 0$ and $\boldsymbol{S} = \mathbf{0}$ for all time, and the rigid frame velocity

$$\begin{aligned} \mathcal{V}^i &= \varepsilon^{ijk}\Omega_j r_k \\ &\rightarrow \nabla^j \mathcal{V}^i = \varepsilon^{i\ell j}\Omega_\ell \\ &\rightarrow \left.\frac{\partial \mathcal{V}^i}{\partial t}\right|_x = 0, \end{aligned} \tag{3.49}$$

we can manipulate $\delta v^i/\delta t = F^i$ to find

$$\left.\frac{\partial u^i}{\partial t}\right|_x + u^j \nabla_j u^i + 2\varepsilon^{i\ell j}\Omega_\ell u_j = F^i. \tag{3.50}$$

Compare this to Vallis (2017) Equation (2.43).[8] Inserted into (3.50), the exact relations

$$\begin{aligned} u^k &\overset{\mathcal{S}}{\longmapsto} \left(\frac{u}{r\,\mathrm{c}_\theta}, \frac{v}{r}, w\right) \\ \Omega_j &\overset{\mathcal{S}}{\longmapsto} \left(0, \Omega r\,\mathrm{c}_\theta, \Omega\,\mathrm{s}_\theta\right), \end{aligned} \tag{3.51}$$

recover Vallis' non-hydrostatic equations (2.47), including all components of the Coriolis force.[9]

To make the traditional approximation, we can neglect the radial component of velocity and

[8] Recognize here that by D/Dt, Vallis means $\left(\partial/\partial t|_x + u^j\nabla_j\right)$, which is not the true material derivative, but the apparent material derivative in the rotating frame.

[9] See Appendix A for useful relations in spherical coordinates

Table 3.2: The hydrostatic approximation represented in various coordinate systems. The reader may confirm that in each case we have $\boldsymbol{e}_i k^i = \hat{\boldsymbol{k}}$, $k_i k^i = 1$, and $\boldsymbol{e}_i k^i k_j \nabla^j p = \hat{\boldsymbol{k}} \partial_z p$. When the basis has a true vertical basis vector, its component representation of the gravitational force is nonzero only in that direction. Otherwise it is a linear combination of all basis directions. Normally we would write covariant components as row vectors, but we write them here as column vectors simply to save space. The final expression of $k^i k_j \nabla^j p$ for the rotated orthogonal basis $\mathcal{RO}$ is left to the reader to derive, for it would not fit in this table.

Basis	$\boldsymbol{e}_i$	k^i	k_j	$\nabla^j p$	$k^i k_j \nabla^j p = \rho \nabla^i \Phi$
$\mathcal{C}$	$\begin{bmatrix} \hat{\boldsymbol{i}} \\ \hat{\boldsymbol{j}} \\ \hat{\boldsymbol{k}} \end{bmatrix}$	$\begin{bmatrix} 0 \\ 0 \\ 1 \end{bmatrix}$	$\begin{bmatrix} 0 \\ 0 \\ 1 \end{bmatrix}$	$\begin{bmatrix} \partial_x p \\ \partial_y p \\ \partial_z p \end{bmatrix}$	$\begin{bmatrix} 0 \\ 0 \\ \partial_z p \end{bmatrix}$
$\mathcal{Y}$	$\begin{bmatrix} \hat{\boldsymbol{i}} \\ \hat{\boldsymbol{j}} \\ \boldsymbol{\nabla}\tau \end{bmatrix}$	$\begin{bmatrix} L_x \\ L_y \\ \sigma \end{bmatrix}$	$\begin{bmatrix} 0 \\ 0 \\ \frac{1}{\sigma} \end{bmatrix}$	$\begin{bmatrix} \partial_x p + L_x \partial_z p \\ \partial_y p + L_y \partial_z p \\ \sigma \partial_z p \end{bmatrix}$	$\begin{bmatrix} L_x \partial_z p \\ L_y \partial_z p \\ \sigma \partial_z p \end{bmatrix}$
$\tilde{\mathcal{Y}}$	$\begin{bmatrix} \hat{\boldsymbol{i}} + L_x \hat{\boldsymbol{k}} \\ \hat{\boldsymbol{j}} + L_y \hat{\boldsymbol{k}} \\ \sigma \hat{\boldsymbol{k}} \end{bmatrix}$	$\begin{bmatrix} 0 \\ 0 \\ \frac{1}{\sigma} \end{bmatrix}$	$\begin{bmatrix} L_x \\ L_y \\ \sigma \end{bmatrix}$	$\begin{bmatrix} \partial_x p \\ \partial_y p \\ \frac{1}{\sigma}\left(-L_x \partial_x p - L_y \partial_y p + \partial_z p\right) \end{bmatrix}$	$\frac{1}{\sigma} \begin{bmatrix} 0 \\ 0 \\ \partial_z p \end{bmatrix}$
$\mathcal{SO}$	$\begin{bmatrix} \hat{\boldsymbol{i}} \\ \hat{\boldsymbol{j}} \\ \sigma \hat{\boldsymbol{k}} \end{bmatrix}$	$\begin{bmatrix} 0 \\ 0 \\ \frac{1}{\sigma} \end{bmatrix}$	$\begin{bmatrix} 0 \\ 0 \\ \sigma \end{bmatrix}$	$\begin{bmatrix} \partial_x p \\ \partial_y p \\ \frac{\partial_z p}{\sigma} \end{bmatrix}$	$\frac{1}{\sigma} \begin{bmatrix} 0 \\ 0 \\ \partial_z p \end{bmatrix}$
$\mathcal{RO}$	$\begin{bmatrix} \hat{\boldsymbol{i}} + L_x \hat{\boldsymbol{k}} \\ -\frac{L_x L_y}{\sigma} \hat{\boldsymbol{i}} + \frac{1+L_x^2}{\sigma} \hat{\boldsymbol{j}} + \frac{L_y}{\sigma} \hat{\boldsymbol{k}} \\ \nabla\tau \end{bmatrix}$	$\begin{bmatrix} \frac{L_x}{1+L_x^2} \\ \frac{L_y}{\sigma \lvert \boldsymbol{\nabla}\tau \rvert^2 (1+L_x^2)} \\ \frac{1}{\sigma \lvert \boldsymbol{\nabla}\tau \rvert^2} \end{bmatrix}$	$\begin{bmatrix} L_x \\ \frac{L_y}{\sigma} \\ \frac{1}{\sigma} \end{bmatrix}$	$\begin{bmatrix} \dfrac{\partial_x p + L_x \partial_z p}{1 + L_x^2} \\ \dfrac{-L_x L_y \partial_x p + (1 + L_x^2) \partial_y p + L_y \partial_z p}{\sigma \lvert \boldsymbol{\nabla}\tau \rvert^2 (1 + L_x^2)} \\ \dfrac{\boldsymbol{\nabla}\tau \cdot \boldsymbol{\nabla} p}{\lvert \boldsymbol{\nabla}\tau \rvert^2} \end{bmatrix}$	$\cdots$

the the non-radial components of rotation by replacing u^k and Ω_j by

$$\begin{aligned} u^k - r^k r_j u^j = \tilde{u}^k &\overset{\mathcal{S}}{\longmapsto} \left(\frac{u}{r\,\mathrm{c}_\theta}, \frac{v}{r}, 0\right), \\ r_j r^k \Omega_k = \tilde{\Omega}_j &\overset{\mathcal{S}}{\longmapsto} (0, 0, \Omega\,\mathrm{s}_\theta)\,. \end{aligned} \tag{3.52}$$

To an approximation as good as the radial traditional one itself, the radial components can be removed by removal of the vertical unit vector $\boldsymbol{k}$ defined to lie along the geopotential gradient in the previous section.

$$\begin{aligned} u^k - k^k k_j u^j &\approx \tilde{u}^k, \\ k_j k^k \Omega_k &\approx \tilde{\Omega}_j\,. \end{aligned} \tag{3.53}$$

This equation is useful if greater care is being paid to the vertical direction than is typical in spherical coordinates, e.g., when using a reference ellipsoid. Indeed, in such a case it is unclear whether the traditional approximation is truly based on the radial or vertical direction—the main idea is to simplify the vertical or radial momentum equation and remove the vertical or radial velocity contributions to the Coriolis terms in the horizontal equation, so the form of the traditional approximation should be chosen accordingly.

Inserting these components into (3.50) yields

$$\left.\frac{\partial \tilde{u}^i}{\partial t}\right|_x + \tilde{u}^j \nabla_j \tilde{u}^i + 2\varepsilon^{i\ell j}\tilde{\Omega}_\ell \tilde{u}_j = F^i\,. \tag{3.54}$$

From here, assuming hydrostatic balance as defined in the previous section, and making the shallow water approximation recovers the primitive equations, given by Vallis in equations (2.50).

There are real forces that are neglected in this approximation, and the Coriolis force no longer quite represents the operation of a rotating planet. Nonetheless, (3.54) can be expressed in any coordinate system after this approximation is made.

3.5 Useful Bases and Their Metric Coefficients

Metric tensors for simple geometries appear in Table 3.3. We will immediately move on to discussing more complicated bases specialized for geophysical fluid dynamics.

3.5.1 Tracer Coordinates

For any scalar field τ we can define coordinates based on its gradient – density coordinates, buoyancy coordinates, pressure coordinates, etc. In this section, we follow Griffies et al. (1998) and Bachman et al. (2020) in defining the slope vector $\boldsymbol{L} = -\nabla_h \tau / \partial_z \tau$ as the horizontal components of the tracer concentration gradient scaled by the vertical component. See Figure 3.2.

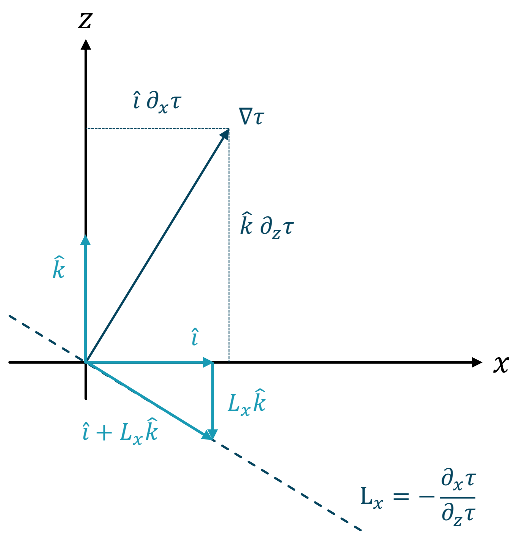

Figure 3.2: Definition of the x-component of the slope vector $\boldsymbol{L} = L_x \hat{\boldsymbol{\imath}} + L_y \hat{\boldsymbol{\jmath}}$. The y-component is defined analogously as $L_y = -\partial_y \tau / \partial_z \tau$. The ith basis vector in the iso-surface of τ is the projection of the ith Cartesian basis vector onto that surface along $\hat{\boldsymbol{k}}$.

Young's Basis $\mathcal{Y}$ and Dual Basis $\tilde{\mathcal{Y}}$

In this section we show the basis vectors and metric tensors based on a general tracer concentration τ. If we choose τ to represent buoyancy, we recover the bases defined in Young (2012), and so we call these bases Young's basis $\mathcal{Y}$ and Young's dual basis $\tilde{\mathcal{Y}}$. Once again

Table 3.3: Metric tensors for simple geometries. ν is geocentric co-latitude, θ is geocentric latitude, and Θ is geodetic latitude. α and μ are parameters defined so that for the oblate spheroid that best approximates the Earth (say, the GRS80 reference ellipsoid), $\alpha\cosh\mu$ is the equatorial radius of Earth, and $\alpha\sinh\mu$ is the polar radius of Earth. As elsewhere, s_θ, c_θ, and ch_μ denote $\sin\theta$, $\cos\theta$, and $\cosh\theta$, respectively. a is the radius of the toroidal coordinates' reference circle.

Geometry	$\boldsymbol{e}_i$	g_{ij}
Cartesian	$\begin{bmatrix}\hat{\boldsymbol{\imath}} & \hat{\boldsymbol{\jmath}} & \hat{\boldsymbol{k}}\end{bmatrix}$	$\begin{bmatrix}1 & 0 & 0\\ 0 & 1 & 0\\ 0 & 0 & 1\end{bmatrix}$
Cylindrical	$\begin{bmatrix}\hat{\boldsymbol{\imath}} & r\hat{\boldsymbol{\lambda}} & \hat{\boldsymbol{k}}\end{bmatrix}$	$\begin{bmatrix}1 & 0 & 0\\ 0 & r^2 & 0\\ 0 & 0 & 1\end{bmatrix}$
Spherical (co-latitude ν)	$\begin{bmatrix}\hat{\boldsymbol{r}} & r\hat{\boldsymbol{\nu}} & r\,\mathrm{s}_\nu\hat{\boldsymbol{\lambda}}\end{bmatrix}$	$\begin{bmatrix}1 & 0 & 0\\ 0 & r^2 & 0\\ 0 & 0 & r^2\,\mathrm{s}_\nu^2\end{bmatrix}$
Spherical (latitude θ)	$\begin{bmatrix}r\,\mathrm{c}_\theta\hat{\boldsymbol{\lambda}} & r\hat{\boldsymbol{\theta}} & \hat{\boldsymbol{r}}\end{bmatrix}$	$\begin{bmatrix}r^2\,\mathrm{c}_\theta^2 & 0 & 0\\ 0 & r^2 & 0\\ 0 & 0 & 1\end{bmatrix}$
Oblate Spheroidal	$\begin{bmatrix}\alpha\,\mathrm{ch}_\mu\,\mathrm{c}_\Theta\hat{\boldsymbol{\lambda}} & \alpha\sqrt{\mathrm{ch}_\mu^2-\mathrm{c}_\Theta^2}\,\hat{\boldsymbol{\Theta}} & \alpha\sqrt{\mathrm{ch}_\mu^2-\mathrm{c}_\Theta^2}\,\hat{\boldsymbol{\mu}}\end{bmatrix}$	$\alpha^2\begin{bmatrix}\mathrm{ch}_\mu^2\,\mathrm{c}_\Theta^2 & 0 & 0\\ 0 & \mathrm{ch}_\mu^2-\mathrm{c}_\Theta^2 & 0\\ 0 & 0 & \mathrm{ch}_\mu^2-\mathrm{c}_\Theta^2\end{bmatrix}$
Toroidal	$\begin{bmatrix}\frac{a}{\mathrm{ch}_\tau-\mathrm{c}_\sigma}\hat{\boldsymbol{\sigma}} & \frac{a}{\mathrm{ch}_\tau-\mathrm{c}_\sigma}\hat{\boldsymbol{\tau}} & \frac{a\,\mathrm{sh}_\tau}{\mathrm{ch}_\tau-\mathrm{c}_\sigma}\hat{\boldsymbol{\phi}}\end{bmatrix}$	$\frac{a^2}{(\mathrm{ch}_\tau-\mathrm{c}_\sigma)^2}\begin{bmatrix}1 & 0 & 0\\ 0 & 1 & 0\\ 0 & 0 & \mathrm{sh}_\tau^2\end{bmatrix}$

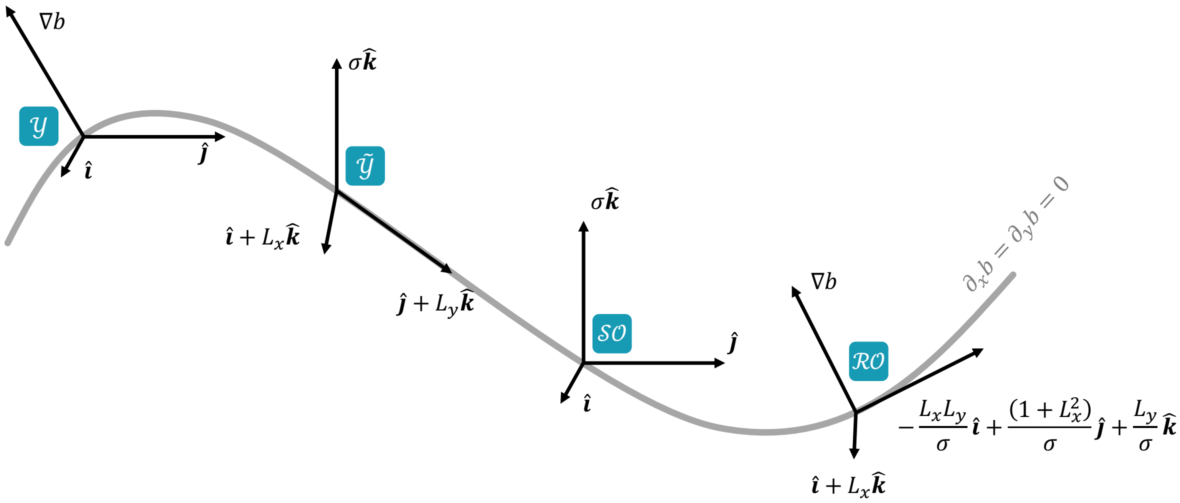

Figure 3.3: Visualization of the four definitions of tracer coordinates discussed in section 3.5.1, showing Young's basis $\mathcal{Y}$, Young's dual basis $\tilde{\mathcal{Y}}$, scaled orthogonal coordinates $\mathcal{SO}$, and rotated orthogonal coordinates $\mathcal{RO}$.

following Young's §2, we define

$$\begin{aligned} \sigma &\equiv \frac{1}{\partial_z \tau} \\ L_x &\equiv -\sigma \partial_x \tau \\ L_y &\equiv -\sigma \partial_y \tau \end{aligned} \tag{3.55}$$

which are analogous to equations (3.34). $[\,L_x \;\; L_y \;\; 0\,]$ are components of the slope vector $\boldsymbol{L}$:

$$\boldsymbol{L} = L_x \hat{\boldsymbol{\imath}} + L_y \hat{\boldsymbol{\jmath}} \tag{3.56}$$

See Figure 3.2 for a geometric definition of $\boldsymbol{L}$. In terms of $\boldsymbol{L}$, the tracer gradient is

$$\boldsymbol{\nabla}\tau = -\frac{L_x}{\sigma}\hat{\boldsymbol{\imath}} - \frac{L_y}{\sigma}\hat{\boldsymbol{\jmath}} + \frac{1}{\sigma}\hat{\boldsymbol{k}} \tag{3.57}$$

and its squared magnitude becomes

$$|\boldsymbol{\nabla}\tau|^2 = \frac{L_x^2 + L_y^2 + 1}{\sigma^2} = \frac{L^2+1}{\sigma^2} \tag{3.58}$$

Choosing $\tilde{\mathcal{Y}}$ to be the covariant basis, we have

$$\begin{aligned} \boldsymbol{e}^i &\xmapsto{\tilde{\mathcal{Y}}} \begin{bmatrix} \hat{\boldsymbol{\imath}} \\ \hat{\boldsymbol{\jmath}} \\ \nabla\tau \end{bmatrix} \\ \boldsymbol{e}_i &\xmapsto{\tilde{\mathcal{Y}}} \begin{bmatrix} \hat{\boldsymbol{\imath}} + L_x\hat{\boldsymbol{k}} & \hat{\boldsymbol{\jmath}} + L_y\hat{\boldsymbol{k}} & \sigma\hat{\boldsymbol{k}} \end{bmatrix} \end{aligned} \tag{3.59}$$

Compare this to equations (38) - (41) in Young (2012). We can immediately write down the metric components $g_{ij} = \boldsymbol{e}_i \cdot \boldsymbol{e}_j$

$$g_{ij} \xmapsto{\tilde{\mathcal{Y}}} \begin{bmatrix} 1+L_x^2 & L_xL_y & \sigma L_x \\ L_xL_y & 1+L_y^2 & \sigma L_y \\ \sigma L_x & \sigma L_y & \sigma^2 \end{bmatrix} \tag{3.60}$$

and inverse metric components $g^{ij} = \boldsymbol{e}^i \cdot \boldsymbol{e}^j$

$$g^{ij} \xmapsto{\tilde{\mathcal{Y}}} \begin{bmatrix} 1 & 0 & -L_x/\sigma \\ 0 & 1 & -L_y/\sigma \\ -L_x/\sigma & -L_y/\sigma & |\boldsymbol{\nabla}\tau|^2 \end{bmatrix} \tag{3.61}$$

Geometrically, the two quasi-horizontal basis vectors of $\tilde{\mathcal{Y}}$ are a projection of $\hat{\boldsymbol{\imath}}$ and $\hat{\boldsymbol{\jmath}}$ onto isosurfaces of τ (see Figure 3.2), and so we could have arrived at them by pulling back the Cartesian basis $\boldsymbol{e}_{i'} \xmapsto{C} \begin{bmatrix} \hat{\boldsymbol{\imath}} & \hat{\boldsymbol{\jmath}} & \hat{\boldsymbol{k}} \end{bmatrix}$ onto those isosurfaces using the proper shift tensor—see section 3.2.4. Choosing the shift tensor

$$Z_{\alpha}^{i'} \xmapsto{C,\tilde{\mathcal{Y}}_h} \begin{bmatrix} 1 & 0 \\ 0 & 1 \\ L_x & L_y \end{bmatrix} \tag{3.62}$$

we find that

$$\boldsymbol{s}_{\alpha} = \boldsymbol{e}_{i'} Z_{\alpha}^{i'} \xmapsto{\tilde{\mathcal{Y}}_h} \begin{bmatrix} \hat{\boldsymbol{\imath}} + L_x \hat{\boldsymbol{k}} & \hat{\boldsymbol{\jmath}} + L_y \hat{\boldsymbol{k}} \end{bmatrix} \tag{3.63}$$

and so we have recovered the quasi-horizontal sub-basis of $\tilde{\mathcal{Y}}$. We use this method again to define the surface metric on the geoid in section 3.5.2. The pullback matrix containing the components of the shift tensor is essentially a Jacobian matrix that takes ambient Cartesian coordinates to surface tracer coordinates. The full 3D Jacobian for the transformation from Cartesian to tracer coordinates is closely related to the pullback matrix:

$$J_{i}^{i'} \xmapsto{C,\mathcal{Y}} \begin{bmatrix} 1 & 0 & 0 \\ 0 & 1 & 0 \\ L_x & L_y & \sigma \end{bmatrix} \tag{3.64}$$

Compare this to the Jacobian matrix in equation (3.105).

Scaled Orthogonal basis $\mathcal{SO}$

If we would like to preserve orthogonality as well as the standard horizontal directions, we can scale the vertical basis vector by the z-component of the gradient, giving us the covariant basis

$$\boldsymbol{e}_i \overset{\mathcal{SO}}{\longmapsto} \begin{bmatrix} \hat{\boldsymbol{\imath}} & \hat{\boldsymbol{\jmath}} & \sigma\hat{\boldsymbol{k}} \end{bmatrix} \tag{3.65}$$

and the metric components

$$g_{ij} \overset{\mathcal{SO}}{\longmapsto} \begin{bmatrix} 1 & 0 & 0 \\ 0 & 1 & 0 \\ 0 & 0 & \sigma^2 \end{bmatrix} \qquad g^{ij} \overset{\mathcal{SO}}{\longmapsto} \begin{bmatrix} 1 & 0 & 0 \\ 0 & 1 & 0 \\ 0 & 0 & 1/\sigma^2 \end{bmatrix} \tag{3.66}$$

Rotated Orthogonal Basis $\mathcal{RO}$

If we do not need to preserve the usual horizontal directions, it makes sense to define an orthogonal coordinate system using the full tracer gradient. Choosing $\nabla\tau$ to define the quasi-vertical direction, we choose the other two directions to be orthogonal vectors in the tangent plane to the iso-surface of the tracer. Choose $\boldsymbol{e}_1 = \hat{\boldsymbol{\imath}} + L_x\hat{\boldsymbol{k}}$ from Young's dual basis, which is orthogonal to $\nabla\tau$ by construction. Although $\hat{\boldsymbol{\jmath}} + L_y\hat{\boldsymbol{k}}$ is also orthogonal to $\nabla\tau$, it is not orthogonal to our chosen $\boldsymbol{e}_1$. We therefore simply choose $\boldsymbol{e}_2 = \boldsymbol{e}_3 \times \boldsymbol{e}_1$ to give the basis

$$\boldsymbol{e}_i \overset{\mathcal{RO}}{\longmapsto} \begin{bmatrix} \hat{\boldsymbol{\imath}} + L_x\hat{\boldsymbol{k}} & -\frac{L_xL_y}{\sigma}\hat{\boldsymbol{\imath}} + \frac{1+L_x^2}{\sigma}\hat{\boldsymbol{\jmath}} + \frac{L_y}{\sigma}\hat{\boldsymbol{k}} & \boldsymbol{\nabla}\tau \end{bmatrix} \tag{3.67}$$

which gives us the metric components

$$\begin{aligned} g_{ij} &\overset{\mathcal{RO}}{\longmapsto} \begin{bmatrix} 1+L_x^2 & 0 & 0 \\ 0 & (1+L_x^2)|\boldsymbol{\nabla}\tau|^2 & 0 \\ 0 & 0 & |\boldsymbol{\nabla}\tau|^2 \end{bmatrix} \\ g^{ij} &\overset{\mathcal{RO}}{\longmapsto} \begin{bmatrix} \frac{1}{1+L_x^2} & 0 & 0 \\ 0 & \frac{1}{(1+L_x^2)|\boldsymbol{\nabla}\tau|^2} & 0 \\ 0 & 0 & \frac{1}{|\boldsymbol{\nabla}\tau|^2} \end{bmatrix} \end{aligned} \tag{3.68}$$

If normalized, this basis coincides exactly with the basis given by Griffies (2018) in eqs. (6.8)-(6.10). As for any orthonormal basis, this normalized version of $\mathcal{RO}$ has metric components $g_{ij} = \delta_{ij}$, just as with the Cartesian or height coordinates. This emphasizes the fact that choosing metric components does not specify a particular coordinate system, but specifies it *up to some rotation*.

3.5.2 The Geoid Basis $\mathcal{G}$

The geoid is a surface of constant gravitational potential coinciding with the ocean's time-averaged surface, and that potential field is represented by the spherical harmonic expansion

$$V(\lambda, \theta, r) = -\frac{GM}{r}\sum_{\ell=0}^{\infty}\sum_{m=-\ell}^{\ell}\left(\frac{R_0}{r}\right)^{\ell} C_{\ell m} Y_{\ell m}(\theta + \frac{\pi}{2}, \lambda) \tag{3.69}$$

where $Y_{\ell m}$ are the spherical harmonics of degree ℓ and order m, $C_{\ell m}$ are their coefficients, G is the gravitational constant, M is the mass of the Earth, and R_0 is a reference radius – see Wieczorek (2015) §10.05.2.2 equation (19). [10]

The geopotential Φ is then given by

$$\Phi = V + \phi \tag{3.70}$$

for the centrifugal potential $\phi = -(\Omega^2 r^2 \cos^2\theta)/2$. Effective gravitational force, as usual, is the negative gradient of geopotential

$$\boldsymbol{g} = -\nabla\Phi \tag{3.71}$$

We find ourselves in precisely the same situation as with the tracer coordinates in section 3.5.1: we have a scalar field, we wish to use its gradient to define "up," and we must define "east" and "north" within the tangent plane to the scalar field's isosurfaces. In analogy with section 3.5.1,

[10] As in section 3.4.2, we reverse the geodetic sign convention used in Wieczorek (2015).

we will pull back an ambient basis to define a surface basis $\mathcal{G}_h$ tangent to the geoid. In this case we pull back the covariant spherical basis $\mathcal{S}$ rather than the Cartesian basis $\mathcal{C}$, and we construct the shift tensor Z^i_α analogously to equation (3.62) – see Figure 3.4:

$$Z^i_\alpha \overset{\mathcal{S},\mathcal{G}_h}{\longmapsto} \begin{bmatrix} 1 & 0 \\ 0 & 1 \\ L_\lambda & L_\theta \end{bmatrix} \tag{3.72}$$

where the slope vector is now defined exactly as it was in equation (3.34).[11] The slope vector has covariant components

$$\begin{aligned} L_i &\overset{\mathcal{S}}{\longmapsto} \begin{bmatrix} L_\lambda & L_\theta & 0 \end{bmatrix} \\ \boldsymbol{L} &= L_\lambda \frac{\hat{\boldsymbol{\lambda}}}{r\,\mathrm{c}_\theta} + L_\theta \frac{\hat{\boldsymbol{\theta}}}{r} \end{aligned} \tag{3.73}$$

We find surface basis vectors $\mathcal{G}_h$ to be

$$\boldsymbol{e}_\alpha = \boldsymbol{e}_i Z^i_\alpha \overset{\mathcal{G}_h}{\longmapsto} \{\bar{\boldsymbol{\lambda}} + L_\lambda \bar{\boldsymbol{r}}, \bar{\boldsymbol{\theta}} + L_\theta \bar{\boldsymbol{r}}\} \tag{3.74}$$

and the surface metric components to be

$$g_{\alpha\beta} = g_{ij} Z^i_\alpha Z^j_\beta \overset{\mathcal{G}_h}{\longmapsto} \begin{bmatrix} r^2 c_\theta^2 + L_\lambda^2 & L_\lambda L_\theta \\ L_\lambda L_\theta & r^2 + L_\theta^2 \end{bmatrix} \tag{3.75}$$

Notice that this is a correction to the spherical metric that is quadratic in the components of $\boldsymbol{L}$, so if $\boldsymbol{L} \to 0$ this recovers the surface metric on the sphere. By pulling back the spherical metric tensor, we have essentially shrink-wrapped an initially spherical surface tightly around the geoid.

We promote the surface basis $\mathcal{G}_h$ to an ambient basis $\mathcal{G}$ by including the geopotential gradient

[11] Notice that the shift tensor in equation (3.72) is just the first two columns of the Jacobian matrix in equation (3.105).

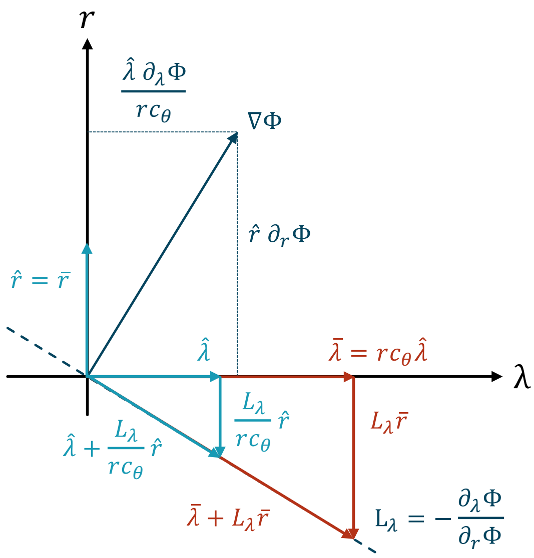

Figure 3.4: Definition of the λ-component of the slope vector $\boldsymbol{L}$. The θ-component is defined analogously as $L_\theta = -\partial_\theta \Phi / \partial_r \Phi$. The ith basis vector in the iso-surface of Φ is the projection of the ith spherical basis vector onto that surface along $\hat{\boldsymbol{r}}$.

as the vertical direction, giving us

$$\mathcal{G} = \{\bar{\boldsymbol{\lambda}} + L_\lambda \bar{\boldsymbol{r}}, \bar{\boldsymbol{\theta}} + L_\theta \bar{\boldsymbol{r}}, \nabla\Phi\} \tag{3.76}$$

and metric components

$$g_{ij} \xmapsto{\mathcal{G}} \begin{bmatrix} r^2 c_\theta^2 + L_\lambda^2 & L_\lambda L_\theta & 0 \\ L_\lambda L_\theta & r^2 + L_\theta^2 & 0 \\ 0 & 0 & |\nabla\Phi|^2 \end{bmatrix} \tag{3.77}$$

for 3D space. These metric components with respect to the geoid can be made arbitrarily precise by keeping more terms in the spherical harmonic expansion of $V(\lambda, \theta, r)$. For another approach to defining a metric based on the geoid, see Kopeikin (2016) equations 13-19.

3.5.3 The Terrain-following Basis $\mathcal{T}$

Near the bottom of the ocean sea floor topography controls the dynamics, and it makes sense to orient our basis accordingly. Following the definition given in Griffies (2018) equation (6.1), we define the parameter σ so that

$$\sigma = \frac{z-\eta}{H+\eta} \tag{3.78}$$

where $\eta = \eta(x,y,t)$ is the vertical displacement from the average sea-surface height $z = 0$, and $H = H(x,y)$ is the depth of the sea floor with the bottom at $z = -H$. We then have $\sigma \in [-1,0]$, as the reader may confirm. We define the basis

$$\mathcal{T} = \{\hat{\boldsymbol{\imath}}, \hat{\boldsymbol{\jmath}}, \nabla\sigma\} \tag{3.79}$$

and the metric components are therefore

$$g_{ij} \overset{\mathcal{T}}{\longmapsto} \begin{bmatrix} 1 & 0 & \hat{\boldsymbol{\imath}}\cdot\nabla\sigma \\ 0 & 1 & \hat{\boldsymbol{\jmath}}\cdot\nabla\sigma \\ \hat{\boldsymbol{\imath}}\cdot\nabla\sigma & \hat{\boldsymbol{\jmath}}\cdot\nabla\sigma & \nabla\sigma\cdot\nabla\sigma \end{bmatrix} \tag{3.80}$$

which becomes

$$g_{ij} \overset{\mathcal{T}}{\longmapsto} \begin{bmatrix} 1 & 0 & \partial_x\sigma \\ 0 & 1 & \partial_y\sigma \\ \partial_x\sigma & \partial_y\sigma & |\nabla\sigma|^2 \end{bmatrix} \tag{3.81}$$

referenced to the locally Cartesian coordinates (x,y,z).

3.6 Turbulence Parameterizations

In this section we will show that the usual Redi isoneutral diffusion tensor $R^i_j = \kappa T^i_j$, which is isotropic in the neutral plane, can be made fully anisotropic by introducing a second projection. We denote this fully anisotropic form as $\$$. Further, we derive the small-slope approximation to both $\boldsymbol{R}$ and $\$$ by first splitting the projection operator into the pullback and inverse pullback $T^i_j = Z^i_\alpha Z^\alpha_j$ and taking the small-slope limit of these objects individually.

3.6.1 The Redi Tensor

The Redi isoneutral diffusion tensor (Redi, 1982) can be written as a scaled projection operator:

$$R^i_j = \kappa T^i_j = \kappa(\delta^i_j - n^i n_j) = \kappa Z^i_\alpha Z^\alpha_j \tag{3.82}$$

for isoneutral, quasi-horizontal diffusivity κ, dianeutral unit vector $\hat{\boldsymbol{n}}$, and shift tensor Z^i_α defined in section 3.2.4. See Figure 3.5. $\boldsymbol{R}$ has eigenvalues $(\kappa, \kappa, 0)$, and is diagonalized in the rotated orthogonal basis $\mathcal{RO}$, depicted in Figure 3.3d. The identical eigenvalues in both quasi-horizontal directions shows that the effected diffusion is isotropic in the local isopycnal plane. Decomposition into shift tensors will become useful in making the small slope approximation in section section 3.6.3. Table 3.4 shows the form that R^i_j takes when projected into various bases under the assumption that the dianeutral direction is the diapycnal direction $n^i = \nabla^i \rho / \sqrt{\nabla^k \rho \nabla_k \rho}$.

We can effect fully three dimensional diffusion by adding an isotropic background diffusion with coefficient μ:

$$(R_{3D})^i_j = \kappa T^i_j + \mu \delta^i_j \tag{3.83}$$

which has eigenvalues $(\kappa + \mu, \kappa + \mu, \mu)$. In the limit that $\mu \ll \kappa$, the isotropic diffusivity μ is overwhelmed in the neutral plane, and only contributes meaningfully in the dianeutral direction, so that $\boldsymbol{R}_{3D}$ approaches

$$(R_{3D})^i_j \approx \kappa T^i_j + \mu N^i_j \tag{3.84}$$

with eigenvalues $\approx (\kappa, \kappa, \mu)$, recovering Griffies et al. (1998) equation (1).

3.6.2 Transverse Anisotropic Form

The usual Redi diffusion tensor is transverse isotropic—that is, isotropic in the neutral plane. However, diffusion in the ocean is strongly anisotropic within this plane; Bachman et al. (2020) provide a quantification of the anisotropy using the eddy-resolving ocean model Parallel Ocean Program Version 2 (POP2), showing that the ratio of major to minor eigenvalues of the diffusion tensor is about 7.22 on average, with the larger eigenvalue tending to orient along the direction of average fluid velocity. In order to reliably parameterize diffusion, we must capture this anisotropy in our eddy transfer tensor. How can we do this while maintaining the covariant representation of the tensor? The answer turns out to be straightforward. We name the new, anisotropic diffusion tensor $\$$. Whereas we defined $\boldsymbol{R}$ as a simple scaled projection, we define $\$$ as the double projection

$$\$^i_j = T^i_k S^k_\ell T^\ell_j \tag{3.85}$$

where the symmetric tensor S holds empirical information about the 3D diffusivity, but in general has eigenvalues (κ, λ, ν) and, like $\boldsymbol{R}$, is diagonalized in $\mathcal{RO}$. The choice $S^k_\ell = \kappa\delta^k_\ell$ recovers equation (3.82). Whereas $\boldsymbol{R}$ has eigenvalues $(\kappa, \kappa, 0)$, $\$$ has eigenvalues $(\kappa, \lambda, 0)$ – the symmetry in the neutral plane has been broken. See figure 3.5 for a comparison of the geometric operations of $\boldsymbol{R}$ and $\$$.

If we want a fully 3D anisotropic diffusion tensor we again add an isotropic background diffusion:

Table 3.4: The Redi tensor projected into various density coordinate systems, increasingly aligned with its eigenbasis (its principal axes). The individual components of $\boldsymbol{R}$ are more physically meaningful the greater this alignment, seen best in the $\mathcal{RO}$ basis. Hydrostatic models might still prefer Young's Dual basis $\tilde{\mathcal{Y}}$ because it permits a vertically separable momentum equation, as shown in Table 3.2. The reader may confirm that in each case we have $\boldsymbol{e}_i \nabla^i \tau = \boldsymbol{\nabla}\tau$. We define $n^i \equiv \nabla^i \tau / |\boldsymbol{\nabla}\tau|$ and $L^2 \equiv |\boldsymbol{L}|^2 = L_x^2 + L_y^2$ is the squared magnitude of the slope vector. κ is quasi-horizontal diffusivity. Components are presented in terms of the geometric objects σ, L, and $\boldsymbol{\nabla}\tau$ for brevity and to encourage physical intuition, but these can be readily expressed in terms of the components of $\boldsymbol{L}$ according to equations (3.55) - (3.58). See Figure 3.3 for geometric depictions of these coordinate systems.

$\boldsymbol{e}_i$	$\nabla^i \tau$	$R^{ij} = \kappa\left(g^{ij} - n^i n^j\right)$
$\mathcal{C}$	$\begin{bmatrix} -L_x/\sigma \\ -L_y/\sigma \\ 1/\sigma \end{bmatrix}$	$\frac{\kappa}{\sigma^2 \|\boldsymbol{\nabla}\tau\|^2} \begin{bmatrix} L_y^2+1 & -L_x L_y & L_x \\ -L_x L_y & L_x^2+1 & L_y \\ L_x & L_y & L^2 \end{bmatrix}$
$\mathcal{SO}$	$\begin{bmatrix} -L_x/\sigma \\ -L_y/\sigma \\ 1/\sigma^2 \end{bmatrix}$	$\frac{\kappa}{\sigma^2 \|\boldsymbol{\nabla}\tau\|^2} \begin{bmatrix} L_y^2+1 & -L_x L_y & L_x/\sigma \\ -L_x L_y & L_x^2+1 & L_y/\sigma \\ L_x/\sigma & L_y/\sigma & L^2/\sigma^2 \end{bmatrix}$
$\mathcal{Y}$	$\begin{bmatrix} 0 \\ 0 \\ 1 \end{bmatrix}$	$\kappa \begin{bmatrix} L_x^2+1 & L_x L_y & \sigma L_x \\ L_x L_y & L_y^2+1 & \sigma L_y \\ \sigma L_x & \sigma L_y & L^2/\|\boldsymbol{\nabla}\tau\|^2 \end{bmatrix}$
$\tilde{\mathcal{Y}}$	$\begin{bmatrix} -L_x/\sigma \\ -L_y/\sigma \\ \|\boldsymbol{\nabla}\tau\|^2 \end{bmatrix}$	$\frac{\kappa}{\sigma^2 \|\boldsymbol{\nabla}\tau\|^2} \begin{bmatrix} L_y^2+1 & -L_x L_y & 0 \\ -L_x L_y & L_x^2+1 & 0 \\ 0 & 0 & 0 \end{bmatrix}$
$\mathcal{RO}$	$\begin{bmatrix} 0 \\ 0 \\ 1 \end{bmatrix}$	$\frac{\kappa}{L_x^2+1} \begin{bmatrix} 1 & 0 & 0 \\ 0 & 1/\|\boldsymbol{\nabla}\tau\|^2 & 0 \\ 0 & 0 & 0 \end{bmatrix}$

$$(\$_{3D})^i_j = \$^i_j + \mu\delta^i_j \approx \$^i_j + \mu N^i_j \tag{3.86}$$

in analogy to equations (3.83) and (3.84). Once again, the precise tensor has eigenvalues $(\kappa + \mu, \lambda + \mu, \mu)$, which is approximately (κ, λ, μ) in the limit where isoneutral diffusion overwhelms dianeutral diffusion: $\mu \ll \kappa, \lambda$.

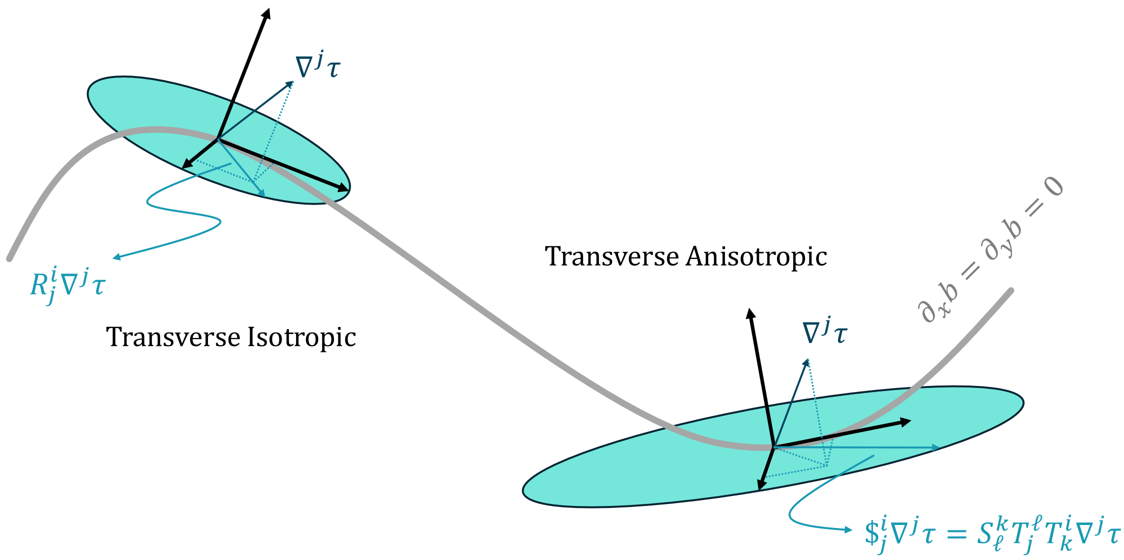

Figure 3.5: The geometric operations performed by the transverse isotropic Redi diffusion tensor $\boldsymbol{R}$ and the transverse-anisotropic diffusion tensor \$. Whereas $\boldsymbol{R}$ performs a simple orthogonal projection onto the neutral surface scaled by the local diffusivity, \$ allows us the freedom to rotate the projection within the neutral plane, biasing diffusion towards the direction of the largest eigenvector.

3.6.3 Small Slope Approximation

In the following, we use a tilde to denote the small-slope approximation of a tensor. For example, the Redi tensor $\boldsymbol{R}$ has the small-slope approximation $\tilde{\boldsymbol{R}}$.

Oceanic flow along neutral surfaces covers considerably greater distances horizontally than vertically. Because of this extreme aspect ratio, it is often reasonable to assume that the slopes of neutral surfaces are small, and we normally encounter the Redi diffusion tensor in its small slope limit – see, for example, Griffies et al. (1998). So far we have discussed the covariant representation of the full diffusion tensor, but we can perform a similar analysis of its small slope limit.

Recall from equation (3.21) that we can decompose the projection operator into the pullback and inverse pullback: $T^i_j = Z^i_\alpha Z^\alpha_j$, where

$$
\begin{aligned}
Z^i_\alpha &\overset{C,\tilde{\mathcal{Y}}_h}{\longmapsto} \begin{bmatrix} 1 & 0 \\ 0 & 1 \\ L_x & L_y \end{bmatrix} \\
Z^\alpha_j &\overset{\tilde{\mathcal{Y}}_h,C}{\longmapsto} \frac{1}{1+L^2} \begin{bmatrix} 1+L_y^2 & -L_xL_y & L_x \\ -L_xL_y & 1+L_x^2 & L_y \end{bmatrix}
\end{aligned}
\tag{3.87}
$$

satisfying equation (3.17), $Z^\alpha_i Z^i_\beta = \delta^\alpha_\beta$. Taking terms quadratic in the small slopes to zero, we arrive at

$$
\tilde{Z}^\alpha_i \overset{\tilde{\mathcal{Y}},C}{\longmapsto} \begin{bmatrix} 1 & 0 & L_x \\ 0 & 1 & L_y \end{bmatrix}
\tag{3.88}
$$

We can now rewrite $\tilde{\boldsymbol{R}}$ as

$$
\tilde{R}^i_j \equiv \kappa Z^i_\alpha \tilde{Z}^\alpha_j \equiv \kappa \tilde{T}^i_j \overset{C}{\longmapsto} \kappa \begin{bmatrix} 1 & 0 & L_x \\ 0 & 1 & L_y \\ L_x & L_y & L^2 \end{bmatrix}
\tag{3.89}
$$

where the second equality defines the small-slope projection operator $\tilde{\boldsymbol{T}}$. Compare this to Griffies et al. (1998) equation (3) with $A_I = 1$ and $A_D = 0$. The approximation to $\$$ follows immediately:

$$
\tilde{\$}^i_j \equiv \tilde{T}^i_k S^k_\ell \tilde{T}^\ell_j .
\tag{3.90}
$$

3.7 Summary & Discussion

Tensor analysis lets us benefit from convenient coordinate systems without being bound to them, and uses a simple algebra for manipulating equations in generalized, time-varying, curvilinear coordinates. Because we are always manipulating tensor quantities, we maintain the geometric intuition of invariant tensor equations in an algebraically workable form.

This work has furthered the project, begun in Chapter 2, of developing a unified, tensorial framework for geophysical fluid dynamics. We present a general formulation of parameterized tracer diffusion that allows for anisotropic dianeutral diffusion. We use this, together with the generalized intrinsic time derivative to express the exact fluid equations for continuity, momentum, incompressibility, and tracer transport. We also show how to make common simplifications such as hydrostatic balance and the traditional and small slope approximations. These equations appear together in Table3.1.

We also present basis vectors and metric tensor coefficients for common GFD settings including spherical, oblate spheroidal, geoid, terrain-following, and tracer coordinates. Such coordinates build useful geometries into the equations naturally. Further, we defined the setting velocity $\boldsymbol{\mathcal{W}}$ for the transformation from spherical to rotating-isopycnal coordinates, performing the transformation in two steps: static spherical $\rightarrow$ rotating spherical $\rightarrow$ rotating isopycnal. By expressing the transformation in index-notation, we arrived at general expressions for both fictitious and fantastical forces in such 2-step transformations.

The next step in this project will describe coordinate-independent methods of spatiotemporal averaging. This will allow operations such as parameterized advection and thickness-weighted averaging, and could also extend to convolution filters for coarse-graining in arbitrary geometries, analogous to the methods of Aluie et al. (2018) on the sphere.

3.8 Appendix 2A: Useful Objects in Spherical Coordinates

$$\boldsymbol{e}_i = \begin{bmatrix} \bar{\boldsymbol{\lambda}} & \bar{\boldsymbol{\theta}} & \bar{\boldsymbol{r}} \end{bmatrix} = \begin{bmatrix} rc_\theta\hat{\boldsymbol{\lambda}} & r\hat{\boldsymbol{\theta}} & \hat{\boldsymbol{r}} \end{bmatrix}, \quad \boldsymbol{e}^i = \begin{bmatrix} \bar{\boldsymbol{\lambda}}/r^2c_\theta^2 \\ \bar{\boldsymbol{\theta}}/r^2 \\ \bar{\boldsymbol{r}} \end{bmatrix} = \begin{bmatrix} \hat{\boldsymbol{\lambda}}/rc_\theta \\ \hat{\boldsymbol{\theta}}/r \\ \hat{\boldsymbol{r}} \end{bmatrix} \tag{3.91}$$

$$g_{ij} = \begin{bmatrix} r^2c_\theta^2 & 0 & 0 \\ 0 & r^2 & 0 \\ 0 & 0 & 1 \end{bmatrix}, \quad g^{ij} = \begin{bmatrix} 1/r^2c_\theta^2 & 0 & 0 \\ 0 & 1/r^2 & 0 \\ 0 & 0 & 1 \end{bmatrix} \tag{3.92}$$

$$\varepsilon_{ijk} = r^2c_\theta\epsilon_{ijk}, \qquad \varepsilon^{ijk} = \epsilon^{ijk}/r^2c_\theta \tag{3.93}$$

$$\Gamma^{\varphi}{}_{jk} = \begin{bmatrix} 0 & -t_\theta & 1/r \\ -t_\theta & 0 & 0 \\ 1/r & 0 & 0 \end{bmatrix}, \quad \Gamma^{\theta}{}_{jk} = \begin{bmatrix} s_\theta c_\theta & 0 & 0 \\ 0 & 0 & 1/r \\ 0 & 1/r & 0 \end{bmatrix}, \quad \Gamma^{r}{}_{jk} = \begin{bmatrix} -rc_\theta^2 & 0 & 0 \\ 0 & -r & 0 \\ 0 & 0 & 0 \end{bmatrix} \tag{3.94}$$

$$\Omega_j = \begin{bmatrix} 0 & \Omega rc_\theta & \Omega s_\theta \end{bmatrix}, \qquad \Omega^j = \begin{bmatrix} 0 \\ \Omega c_\theta/r \\ \Omega s_\theta \end{bmatrix} \tag{3.95}$$

$$r_k = \begin{bmatrix} 0 & 0 & r \end{bmatrix}, \qquad r^k = \begin{bmatrix} 0 \\ 0 \\ r \end{bmatrix} \tag{3.96}$$

3.9 Appendix 2B: The Transformation to Rotating Buoyancy Coordinates

In this appendix we flesh out transformation from the inertial, spherical setting y to the rotating, buoyancy setting z using the intermediate rotating, spherical setting x. The transformation from the rotating spherical to the rotating buoyancy setting follows along close with §2 of Young (2012). Our ultimate goal is to calculate the components of the gradient tensor $\boldsymbol{\nabla} \otimes \boldsymbol{\mathcal{W}}$ where $\boldsymbol{\mathcal{W}}$ is the setting velocity for z, and to decompose it into its symmetric (deforming) and antisymmetric (rigid) parts. We present the components $\nabla_j \mathcal{W}_i$ so that they may be compared directly to the components $\nabla_j \mathcal{V}_i$ in equation (3.31), and for completeness we also present the components $\nabla_q \mathcal{W}_p$, although they are rather inscrutable.

Define two moving settings x and z indexed respectively by the sets $\{i, j, k, \ldots\}$ and $\{p, q, r \ldots\}$, along with the inertial setting y indexed by $\{a, b, c, \ldots\}$:

$$y^a(x,t) = \begin{pmatrix} \varphi(\lambda, t) = \lambda + \Omega t \\ \theta \\ r \end{pmatrix} \quad x^i(y,t) = \begin{pmatrix} \lambda(\varphi, t) = \varphi - \Omega t \\ \theta \\ r \end{pmatrix}$$
$$x^i(z,\tilde{t}) = \begin{pmatrix} \lambda \\ \theta \\ r = \varrho(\tilde{\lambda}, \tilde{\theta}, \tilde{b}, \tilde{t}) \end{pmatrix} \quad z^p(x,t) = \begin{pmatrix} \tilde{\lambda} \\ \tilde{\theta} \\ \tilde{b} = b(\lambda, \theta, r, t) \end{pmatrix} \tag{3.33}$$

where ϱ is *not* a density, but rather the name of the function that returns a radius when fed buoyancy coordinates. Analogous to Young's (21) - (24) we can define

$$
\begin{aligned}
\partial_\lambda &= \partial_{\tilde\lambda} + \frac{\partial b}{\partial \lambda}\partial_{\tilde b} \\
\partial_\theta &= \partial_{\tilde\theta} + \frac{\partial b}{\partial \theta}\partial_{\tilde b} \\
\partial_r &= \frac{\partial b}{\partial r}\partial_{\tilde b} \\
\left.\frac{\partial}{\partial t}\right|_x &= \left.\frac{\partial}{\partial t}\right|_z + \left.\frac{\partial b}{\partial t}\right|_x \partial_{\tilde b}
\end{aligned}
\tag{3.97}
$$

where the final equality follows because b is a function of time, but $\tilde\lambda$ and $\tilde\theta$ are not. Analogous to (26) - (27) we have

$$
\sigma(\tilde\lambda,\tilde\theta,\tilde b,\tilde t) \equiv \frac{\partial \varrho}{\partial \tilde b} = \frac{1}{\partial_r b}
\tag{3.98}
$$

and analogous to (28) we have

$$
\begin{aligned}
\frac{\partial \varrho}{\partial \tilde\lambda} &= -\sigma \partial_\lambda b \equiv L_\lambda \\
\frac{\partial \varrho}{\partial \tilde\theta} &= -\sigma \partial_\theta b \equiv L_\theta \\
\left.\frac{\partial \varrho}{\partial t}\right|_z &= -\sigma \left.\frac{\partial b}{\partial t}\right|_x \equiv \omega(x,t)
\end{aligned}
\tag{3.99}
$$

where the first two expressions give the components of the slope vector $\boldsymbol{L} = (L_\lambda, L_\theta, 0)$; the subscripts *do not* indicate partial differentiation, which we never denote with subscripts. We have named the final expression ω for two reasons: it looks a bit like a w, and represents the thickness-weighted quasi-vertical velocity of a buoyancy surface; it rides along with Ω in the components of $\mathcal{W}$, as we will see shortly. The important thing is that it is a function of the coordinates $x^i = (\lambda, \theta, r)$. As usual we define the x setting velocity $\mathcal{V}$ by

$$
\mathcal{V}^a = \left.\frac{\partial y^a}{\partial t}\right|_x \overset{S}{\longmapsto} \begin{bmatrix} \Omega \\ 0 \\ 0 \end{bmatrix}
\tag{3.100}
$$

To define the z setting velocity $\mathcal{W}$, we first define $\mathcal{U}$ so that

Table 3.5: The names given to the various setting velocities. Velocities that are derivatives of y^a *or* that hold y fixed are absolute, while the others are relative. Notice that the table is antisymmetric, so we only need three unique labels for the interaction of three settings. Indices are omitted here.

	y	x	z
$\frac{\partial}{\partial t}\big\rvert_y$	$\cdot$	$-\mathcal{V}$	$-\mathcal{W}$
$\frac{\partial}{\partial t}\big\rvert_x$	$\mathcal{V}$	$\cdot$	$-\mathcal{U}$
$\frac{\partial}{\partial t}\big\rvert_z$	$\mathcal{W}$	$\mathcal{U}$	$\cdot$

$$\mathcal{U}^i \equiv \left.\frac{\partial x^i}{\partial t}\right\rvert_z \overset{S}{\longmapsto} \begin{bmatrix} 0 \\ 0 \\ \omega \end{bmatrix} \tag{3.101}$$

Then $\boldsymbol{\mathcal{W}}$ has components

$$\begin{aligned} \mathcal{W}^a &\equiv \left.\frac{\partial y^a(t,x(z,t))}{\partial t}\right\rvert_z \\ &= \left.\frac{\partial y^a}{\partial t}\right\rvert_x + \left.\frac{\partial y^a}{\partial x^i}\frac{\partial x^i}{\partial t}\right\rvert_z \\ &= \mathcal{V}^a + J_i^a \mathcal{U}^i \\ \boldsymbol{\mathcal{W}} &= \boldsymbol{\mathcal{V}} + \boldsymbol{\mathcal{U}} \end{aligned} \tag{3.102}$$

which should not surprise us. The change $\boldsymbol{\mathcal{W}}$ from $y \to z$ is just the sum of the changes $\boldsymbol{\mathcal{V}}$ from $y \to x$ and $\boldsymbol{\mathcal{U}}$ from $x \to z$. See table 3.5 for a summary of the names given to all the relative setting velocities.

The Jacobian J_i^a is

$$J_i^a = \frac{\partial y^a}{\partial x^i} \overset{\mathcal{S},\mathcal{S}}{\longmapsto} \begin{bmatrix} \frac{\partial\varphi}{\partial\lambda} & \frac{\partial\varphi}{\partial\theta} & \frac{\partial\varphi}{\partial r} \\ \frac{\partial\theta}{\partial\lambda} & \frac{\partial\theta}{\partial\theta} & \frac{\partial\theta}{\partial r} \\ \frac{\partial r}{\partial\lambda} & \frac{\partial r}{\partial\theta} & \frac{\partial r}{\partial r} \end{bmatrix} = \begin{bmatrix} 1 & 0 & 0 \\ 0 & 1 & 0 \\ 0 & 0 & 1 \end{bmatrix} = \delta_i^a \tag{3.103}$$

which means that tensor components in the two spherical coordinate systems y and x look the same. Components of $\boldsymbol{\mathcal{W}}$ are then

$$\mathcal{W}^a \overset{\mathcal{S}}{\longmapsto} \begin{bmatrix} \Omega \\ 0 \\ \omega \end{bmatrix} \tag{3.35}$$

We now want to calculate $\nabla_q \mathcal{W}_p$, and we will do it as $\nabla_q \mathcal{W}_p = J_p^i J_q^j \nabla_j \mathcal{W}_i$ since we know the Christoffel symbols for spherical coordinates x and would rather not calculate them for z. The Jacobians J_i^p and J_p^i are

$$J_i^p = \frac{\partial z^p}{\partial x^i} \overset{\mathcal{B},\mathcal{S}}{\longmapsto} \begin{bmatrix} 1 & 0 & 0 \\ 0 & 1 & 0 \\ -\sigma^{-1} L_\lambda & -\sigma^{-1} L_\theta & \sigma^{-1} \end{bmatrix} \tag{3.104}$$

$$J_p^i = \frac{\partial x^i}{\partial z^p} \overset{\mathcal{S},\mathcal{B}}{\longmapsto} \begin{bmatrix} 1 & 0 & 0 \\ 0 & 1 & 0 \\ L_\lambda & L_\theta & \sigma \end{bmatrix} \tag{3.105}$$

As a sanity check, the reader may confirm that we have $J_i^p J_q^i = \delta_q^p$ and $J_p^i J_j^p = \delta_j^i$. The components $\mathcal{W}_i = g_{ij} J_a^j \mathcal{W}^a$ are

$$
\begin{aligned}
\mathcal{W}_i &= g_{ij} J^j_a \mathcal{W}^a \\
&= g_{ij} \delta^j_a \mathcal{W}^a \\
&\overset{\mathcal{S}}{\longmapsto} \begin{bmatrix} r^2\,\mathrm{c}_\theta^2 & 0 & 0 \\ 0 & r^2 & 0 \\ 0 & 0 & 1 \end{bmatrix} \begin{bmatrix} 1 & 0 & 0 \\ 0 & 1 & 0 \\ 0 & 0 & 1 \end{bmatrix} \begin{bmatrix} \Omega \\ 0 \\ \omega \end{bmatrix} \\
&= \begin{bmatrix} r^2\,\mathrm{c}_\theta^2 & 0 & 0 \\ 0 & r^2 & 0 \\ 0 & 0 & 1 \end{bmatrix} \begin{bmatrix} \Omega \\ 0 \\ \omega \end{bmatrix} \\
&= \begin{bmatrix} r^2\,\mathrm{c}_\theta^2\,\Omega \\ 0 \\ \omega \end{bmatrix}
\end{aligned}
\tag{3.106}
$$

We calculate the components $\nabla_j \mathcal{W}_i$ where since both indices are lowered we choose explicitly to let i index rows and j columns:

$$
\begin{aligned}
\nabla_j \mathcal{W}_i &= \partial_j \mathcal{W}_i - \Gamma^k{}_{ji} \mathcal{W}_k \\
&= \partial_j \mathcal{W}_i - \Gamma^1{}_{ji} \mathcal{W}_1 - \Gamma^3{}_{ji} \mathcal{W}_3
\end{aligned}
$$

$$
\overset{\mathcal{S}}{\longmapsto} \begin{bmatrix} 0 & -2r^2\,\mathrm{c}_\theta\,\mathrm{s}_\theta\,\Omega & 2r\,\mathrm{c}_\theta^2\,\Omega \\ 0 & 0 & 0 \\ \partial_\lambda\omega & \partial_\theta\omega & \partial_r\omega \end{bmatrix} - r^2\,\mathrm{c}_\theta^2\,\Omega \begin{bmatrix} 0 & -\mathrm{t}_\theta & 1/r \\ -\mathrm{t}_\theta & 0 & 0 \\ 1/r & 0 & 0 \end{bmatrix} - \omega \begin{bmatrix} -rc_\theta^2 & 0 & 0 \\ 0 & -r & 0 \\ 0 & 0 & 0 \end{bmatrix}
\tag{3.107}
$$

$$
= \begin{bmatrix} 0 & 0 & 0 \\ 0 & 0 & 0 \\ \partial_\lambda\omega & \partial_\theta\omega & \partial_r\omega \end{bmatrix} + r^2\,\mathrm{c}_\theta^2\,\Omega \begin{bmatrix} 0 & -\mathrm{t}_\theta & 1/r \\ \mathrm{t}_\theta & 0 & 0 \\ -1/r & 0 & 0 \end{bmatrix} + \omega \begin{bmatrix} rc_\theta^2 & 0 & 0 \\ 0 & r & 0 \\ 0 & 0 & 0 \end{bmatrix}
$$

where the final manipulation serves only to simplify subsequent calculations. Decomposing $\boldsymbol{\nabla} \otimes \boldsymbol{\mathcal{W}}$ into its symmetric (deforming) and antisymmetric (rigid) parts, we find that

$$\nabla_{(j}\mathcal{W}_{i)} \overset{\mathcal{S}}{\longmapsto} \frac{1}{2}\begin{bmatrix} 0 & 0 & \partial_\lambda\omega \\ 0 & 0 & \partial_\theta\omega \\ \partial_\lambda\omega & \partial_\theta\omega & 2\partial_r\omega \end{bmatrix} + \omega \begin{bmatrix} rc_\theta^2 & 0 & 0 \\ 0 & r & 0 \\ 0 & 0 & 0 \end{bmatrix} \tag{3.38}$$

$$\nabla_{[j}\mathcal{W}_{i]} \overset{\mathcal{S}}{\longmapsto} \frac{1}{2}\begin{bmatrix} 0 & 0 & -\partial_\lambda\omega \\ 0 & 0 & -\partial_\theta\omega \\ \partial_\lambda\omega & \partial_\theta\omega & 0 \end{bmatrix} + r^2\mathrm{c}_\theta^2\Omega \begin{bmatrix} 0 & -\mathrm{t}_\theta & 1/r \\ \mathrm{t}_\theta & 0 & 0 \\ -1/r & 0 & 0 \end{bmatrix} \tag{3.39}$$

The second term in the antisymmetric part is identical to the components of $\nabla_j\mathcal{V}_i$ in equation (3.31) because this is the part of the rotating buoyancy transformation that comes from pure rotation. For the sake of completeness we can calculate the components $\nabla_q\mathcal{W}_p$ as

$$\nabla_q\mathcal{W}_p = J_p^i\nabla_j\mathcal{W}_iJ_q^j$$

$$\overset{\mathcal{B}}{\longmapsto} \begin{bmatrix} 1 & 0 & L_\lambda \\ 0 & 1 & L_\theta \\ 0 & 0 & \sigma \end{bmatrix} \left\{ \begin{bmatrix} 0 & 0 & 0 \\ 0 & 0 & 0 \\ \partial_\lambda\omega & \partial_\theta\omega & \partial_r\omega \end{bmatrix} + r^2\mathrm{c}_\theta^2\Omega \begin{bmatrix} 0 & -\mathrm{t}_\theta & 1/r \\ \mathrm{t}_\theta & 0 & 0 \\ -1/r & 0 & 0 \end{bmatrix} + \omega \begin{bmatrix} rc_\theta^2 & 0 & 0 \\ 0 & r & 0 \\ 0 & 0 & 0 \end{bmatrix} \right\} \begin{bmatrix} 1 & 0 & 0 \\ 0 & 1 & 0 \\ L_\lambda & L_\theta & \sigma \end{bmatrix}$$

$$= \begin{bmatrix} L_\lambda\partial_\lambda\omega + L_\lambda^2\partial_r\omega & L_\lambda\partial_\theta\omega + L_\lambda L_\theta\partial_r\omega & \sigma L_\lambda\partial_r\omega \\ L_\theta\partial_\lambda\omega + L_\lambda L_\theta\partial_r\omega & L_\theta\partial_\theta\omega + L_\theta^2\partial_r\omega & \sigma L_\theta\partial_r\omega \\ \sigma\partial_\lambda\omega + \sigma L_\lambda\partial_r\omega & \sigma\partial_\theta\omega + \sigma L_\theta\partial_r\omega & \sigma^2\partial_r\omega \end{bmatrix} + r^2\mathrm{c}_\theta^2\Omega \begin{bmatrix} 0 & L_\theta/r - \mathrm{t}_\theta & \sigma/r \\ \mathrm{t}_\theta - L_\theta/r & 0 & 0 \\ -\sigma/r & 0 & 0 \end{bmatrix} + \omega \begin{bmatrix} rc_\theta^2 & 0 & 0 \\ 0 & r & 0 \\ 0 & 0 & 0 \end{bmatrix} \tag{3.108}$$

Notice that even though J_p^i and J_q^j represent the same Jacobian matrix in the above calculation, we have transposed the matrix representation of J^i_p. This is because $\nabla_j \mathcal{W}_i$ is not a normal matrix — both its indices are lowered. In order to use ordinary matrix multiplication to contract with the lowered index on $\mathcal{W}_i$, we've had to transpose J^i_p. The decomposition of $\boldsymbol{\nabla} \otimes \boldsymbol{\mathcal{W}}$ in rotating buoyancy coordinates is

$$\nabla_{(q}\mathcal{W}_{p)} \overset{\mathcal{B}}{\longmapsto} \begin{bmatrix} L_\lambda \partial_\lambda \omega + L_\lambda^2 \partial_r \omega & \frac{L_\lambda \partial_\theta \omega + L_\theta \partial_\lambda \omega}{2} + L_\lambda L_\theta \partial_r \omega & \frac{\sigma \partial_\lambda \omega}{2} + \sigma L_\lambda \partial_r \omega \\ \frac{L_\lambda \partial_\theta \omega + L_\theta \partial_\lambda \omega}{2} + L_\lambda L_\theta \partial_r \omega & L_\theta \partial_\theta \omega + L_\theta^2 \partial_r \omega & \frac{\sigma \partial_\theta \omega}{2} + \sigma L_\theta \partial_r \omega \\ \frac{\sigma \partial_\lambda \omega}{2} + \sigma L_\lambda \partial_r \omega & \frac{\sigma \partial_\theta \omega}{2} + \sigma L_\theta \partial_r \omega & \sigma^2 \partial_r \omega \end{bmatrix} + \omega \begin{bmatrix} r c_\theta^2 & 0 & 0 \\ 0 & r & 0 \\ 0 & 0 & 0 \end{bmatrix} \tag{3.109}$$

$$\begin{aligned} \nabla_{[q}\mathcal{W}_{p]} \overset{\mathcal{B}}{\longmapsto} \frac{1}{2} & \begin{bmatrix} 0 & L_\lambda \partial_\theta \omega - L_\theta \partial_\lambda \omega & -\sigma \partial_\lambda \omega \\ -L_\lambda \partial_\theta \omega + L_\theta \partial_\lambda \omega & 0 & -\sigma \partial_\theta \omega \\ \sigma \partial_\lambda \omega & \sigma \partial_\theta \omega & 0 \end{bmatrix} \\ + r^2 \mathrm{c}_\theta^2 \Omega & \begin{bmatrix} 0 & L_\theta / r & (\sigma - 1)/r \\ -L_\theta / r & 0 & 0 \\ -(\sigma - 1)/r & 0 & 0 \end{bmatrix} \\ + r^2 \mathrm{c}_\theta^2 \Omega & \begin{bmatrix} 0 & -\mathrm{t}_\theta & 1/r \\ \mathrm{t}_\theta & 0 & 0 \\ -1/r & 0 & 0 \end{bmatrix} \end{aligned} \tag{3.110}$$

It is likely that the slopes L_λ and L_θ are small, and that terms quadratic in these slopes are negligible, in analogy to the small-slope approximation presented in Griffies et al. (1998).

References

Aluie, H., Hecht, M., and Vallis, G. K. (2018). Mapping the energy cascade in the north atlantic ocean: The coarse-graining approach. *Journal of Physical Oceanography*, 48(2):225 – 244.

Aris, R. (1962). *Vectors, tensors and the basic equations of fluid mechanics*. Courier Corporation.

Bachman, S. D., Fox-Kemper, B., and Bryan, F. O. (2020). A diagnosis of anisotropic eddy diffusion from a high-resolution global ocean model. *Journal of Advances in Modeling Earth Systems*, 12(2):e2019MS001904.

Balsara, D. S. and Shu, C.-W. (2000). Monotonicity preserving weighted essentially non-oscillatory schemes with increasingly high order of accuracy. *Journal of Computational Physics*, 160(2):405–452.

Carroll, S. M. (2019). *Spacetime and geometry*. Cambridge University Press.

Chassignet, E., Hurlburt, H., Metzger, E. J., Smedstad, O., Cummings, J., Halliwell, G., Bleck, R., Baraille, R., Wallcraft, A., Lozano, C., Tolman, H., Srinivasan, A., Hankin, S., Cornillon, P., Weisberg, R., Barth, A., He, R., Werner, F., and Wilkin, J. (2009). US GODAE: Global ocean prediction with the HYbrid Coordinate Ocean Model (HYCOM). *Oceanography*, 22(2):64–75.

Dukowicz, J. K. and Smith, R. D. (1997). Stochastic theory of compressible turbulent fluid transport. *Physics of Fluids*, 9(11):3523–3529.

Eden, C., Greatbatch, R. J., and Willebrand, J. (2007). A diagnosis of thickness fluxes in an eddy-resolving model. *Journal of physical oceanography*, 37(3):727–742.

Fox-Kemper, B. and Ferrari, R. (2008). Parameterization of mixed layer eddies. Part II: Prognosis and impact. *J. Phys. Oceanogr.*, 38:1166–1179.

Fox-Kemper, B., Ferrari, R., and Hallberg, R. W. (2008). Parameterization of mixed layer eddies. Part I: Theory and diagnosis. *J. Phys. Oceanogr.*, 38(6):1145–1165.

Gent, P. R. and McWilliams, J. C. (1990). Isopycnal mixing in ocean circulation models. *Journal of Physical Oceanography*, 20(1):150–155.

Gent, P. R., Willebrand, J., McDougall, T. J., and McWilliams, J. C. (1995). Parameterizing eddy-induced tracer transports in ocean circulation models. *Journal of Physical Oceanography*, 25(4):463–474.

Griffies, S. (2018). *Fundamentals of ocean climate models*. Princeton university press.

Griffies, S. M., Gnanadesikan, A., Pacanowski, R. C., Larichev, V. D., Dukowicz, J. K., and Smith, R. D. (1998). Isoneutral diffusion in a z-coordinate ocean model. *Journal of Physical Oceanography*, 28(5):805–830.

Grinfeld, P. (2013). *Introduction to tensor analysis and the calculus of moving surfaces*. Springer.

Hughes, C. and Bingham, R. (2006). An oceanographer's guide to goce and the geoid. *Ocean Science Discussions*, 3(5):1543–1568.

Jackett, D. R. and McDougall, T. J. (1997). A neutral density variable for the world's oceans. *Journal of Physical Oceanography*, 27(2):237–263.

Killworth, P. D. (1997). On the parameterization of eddy transfer part i. theory. *Journal of Marine Research*, 55(6):1171–1197.

Kopeikin, S. M. (2016). Reference ellipsoid and geoid in chronometric geodesy. *Frontiers in Astronomy and Space Sciences*, 3:5.

Loose, N., Marques, G. M., Adcroft, A., Bachman, S., Griffies, S. M., Grooms, I., Hallberg, R. W., and Jansen, M. F. (2023). Comparing two parameterizations for the restratification effect of mesoscale eddies in an isopycnal ocean model. *J. Adv. Model. Earth Sy.*, 15(12).

McDougall, T. J. (1987). Neutral surfaces. *Journal of Physical Oceanography*, 17(11):1950–1964.

McDougall, T. J. and McIntosh, P. C. (1996). The temporal-residual-mean velocity. part i: Derivation and the scalar conservation equations. *Journal of Physical Oceanography*, 26(12):2653–2665.

Nycander, J. (2011). Energy conversion, mixing energy, and neutral surfaces with a nonlinear equation of state. *Journal of Physical Oceanography*, 41(1):28–41.

Redi, M. H. (1982). Oceanic isopycnal mixing by coordinate rotation. *Journal of Physical Oceanography*, 12(10):1154–1158.

Salmon, R. (2013). An alternative view of generalized lagrangian mean theory. *Journal of Fluid Mechanics*, 719:165–182.

Stewart, A. L. and McWilliams, J. C. (2022). Gravity is vertical in geophysical fluid dynamics. *Scientific Reports*, 12(1):6029.

Vallis, G. K. (2017). *Atmospheric and oceanic fluid dynamics*. Cambridge University Press.

Wieczorek, M. A. (2015). Gravity and topography of the terrestrial planets. *Treatise on geophysics*, 10:165–206.

Young, W. R. (2012). An exact thickness-weighted average formulation of the boussinesq equations. *Journal of Physical Oceanography*, 42(5):692–707.

CHAPTER 4

The Gradient Tensor Theorem: Proof, Utility, and Limitations

This chapter covers material published as Lilly et al. (2024). Below, I highlight my main contributions to the published work, which appear in section 4d.

Summary

Integral theorems relating quantities on the boundary of a region to quantities on the interior are common in vector analysis and field theories, and geophysical fluid dynamics is no exception. Such relationships are of practical relevance in observational oceanography: a ship may trace out a set of closed curves and, from those measurements alone, infer the state of the entire enclosed region—see figure 4.1.

This work discusses the old-but-rarely-discussed result

$$\int\int\int_{\mathcal{V}} \boldsymbol{\nabla} \otimes \boldsymbol{u} dV = \int\int_{\mathcal{A}} \boldsymbol{n} \otimes \boldsymbol{u} dA \tag{4.1}$$

which is due to Gibbs (1884). It is a kind of generalization of similar theorems relating boundary

integrals to volume integrals, such as the divergence and Kelvin-Stokes theorems, which show up respectively as the trace and antisymmetric part of (4.1). The translation to index notation admits a straight-forward proof:

$$
\begin{aligned}
\int\int\int_{\mathcal{V}} \boldsymbol{\nabla}\otimes\boldsymbol{u}dV &= \int\int\int_{\mathcal{V}} \left(\nabla_i u_j\right)\boldsymbol{e}^i\otimes\boldsymbol{e}^j dV \\
&= \int\int\int_{\mathcal{V}} \nabla_i\left(u_j\boldsymbol{e}^i\otimes\boldsymbol{e}^j\right) dV \\
&= \int\int_{\mathcal{A}} n_i u_j \boldsymbol{e}^i\otimes\boldsymbol{e}^j dA \\
&= \int\int_{\mathcal{A}} \boldsymbol{n}\otimes\boldsymbol{u}dA
\end{aligned}
\tag{4.2}
$$

where the first equality is simply a translation from symbolic to tensor notation, and the second relies on the metric compatibility of the basis vectors: $\nabla_i\boldsymbol{e}^j = 0$. The third is an application of the generalized divergence theorem

$$
\int\int\int_{\mathcal{V}} \boldsymbol{\nabla}\cdot\boldsymbol{T}dV = \int\int_{\mathcal{A}} \boldsymbol{n}\cdot\boldsymbol{T}dA,
\tag{4.3}
$$

found in Grinfeld (2013) as equation (12.6.7), and the final equality is a translation back to symbolic notation. Decomposing $\boldsymbol{\nabla}\otimes\boldsymbol{u}$ into its antisymmetric, trace, and trace-free symmetric parts as in table 2.3, we find

$$
\int\int\int_{\mathcal{V}} \left(\nabla_{[i}u_{j]}\right)\boldsymbol{e}^i\otimes\boldsymbol{e}^j dV = \int\int_{\mathcal{A}} n_{[i}u_{j]}\boldsymbol{e}^i\otimes\boldsymbol{e}^j dA
\tag{4.4}
$$

$$
\int\int\int_{\mathcal{V}} \left(\nabla_k u^k\right) dV = \int\int_{\mathcal{A}} n_k u^k dA
\tag{4.5}
$$

$$
\int\int\int_{\mathcal{V}} \left(\nabla_{(i}u_{j)} - \frac{1}{3}g_{ij}\nabla_k u^k\right)\boldsymbol{e}^i\otimes\boldsymbol{e}^j dV = \int\int_{\mathcal{A}} \left(n_{(i}u_{j)} - \frac{1}{3}g_{ij}n_k u^k\right)\boldsymbol{e}^i\otimes\boldsymbol{e}^j dA
\tag{4.6}
$$

which are, respectively, the Kelvin-Stokes theorem, the divergence theorem, and a third theorem regarding strain rates on the boundary. It is this last relation that should surprise us for, because it is a relation between purely symmetric tensors, it cannot be captured by the standard Generalized Stokes Theorem

$$\int_{\Omega} \mathrm{d}\omega = \int_{\partial\Omega} \omega, \tag{4.7}$$

relating the differential form $\mathrm{d}\omega$ over a volume to the form ω on the boundary. Differential forms are, by definition, purely antisymmetric tensors, and so while equations (4.4) and (4.5) are special cases of (4.7), (4.6) is not. Then there must be an assumption implicit in the proof (4.2); we now show that that assumption is the flatness of the ambient space.

Recall from section 3.2.4 that we use Greek letters to index surfaces embedded in our ambient space, the *shift tensor* or *pullback matrix* Z^i_α is a sort of rank-deficient Jacobian that projects from ambient space onto the surface, and we define the surface-restricted basis vectors to be $\boldsymbol{s}_\alpha = Z^i_\alpha \boldsymbol{e}_i$. Unlike in the flat ambient space, the surface basis is not metric compatible. Instead we find

$$\nabla_\alpha \boldsymbol{s}_\beta = \boldsymbol{n} B_{\alpha\beta}, \tag{4.8}$$

where $\boldsymbol{n}$ is the unit normal. This expression defines $B_{\alpha\beta}$, called the *extrinsic curvature tensor*. See Grinfeld (2013) chapter 11 for a detailed definition of this tensor—essentially it encodes information about the curvature of an embedded surface. For example, its eigenvalues are the principle curvatures, its trace is twice the mean curvature, and its determinant is the Gaussian curvature (Grinfeld, 2013, section 12.4). In moving from the flat ambient space to a potentially curved surface, we have lost metric compatibility of the basis, and if we try a proof analogous to (4.2), it will fail on the second line because

$$\int\int_{\mathcal{A}} \left(\nabla_\alpha u_\beta\right) \boldsymbol{s}^\alpha \otimes \boldsymbol{s}^\beta dA \neq \int\int_{\mathcal{A}} \nabla_\alpha \left(u_\beta \boldsymbol{s}^\alpha \otimes \boldsymbol{s}^\beta\right) dA. \tag{4.9}$$

The only way to salvage the proof for embedded surfaces is to demand that they be flat. That is, *if and only if* $B_{\alpha\beta} = 0$, we have

$$
\begin{aligned}
\int\int_{\mathcal{A}} \boldsymbol{\nabla} \otimes \boldsymbol{u} dA &= \int\int_{\mathcal{A}} \left(\nabla_\alpha u_\beta\right) \boldsymbol{s}^\alpha \otimes \boldsymbol{s}^\beta dA \\
&= \int\int_{\mathcal{A}} \nabla_\alpha \left(u_\beta \boldsymbol{s}^\alpha \otimes \boldsymbol{s}^\beta\right) dA \\
&= \int_{\mathcal{L}} n_\alpha u_\beta \boldsymbol{s}^\alpha \otimes \boldsymbol{s}^\beta dL \\
&= \int_{\mathcal{L}} \boldsymbol{n} \otimes \boldsymbol{u} dL
\end{aligned}
\tag{4.10}
$$

This is exactly the same as (4.2), for there was nothing in that equation that demanded we work in three dimensions. The only difference is that we have named everything to indicate that we are talking about a surface. The generalized Stokes theorem (4.7), on the other hand, has no such restrictions because it is defined on any arbitrary manifold Ω which may or may not be curved.

This restricts the utility of the gradient tensor theorem (4.1) in observational oceanography. The generalized Stokes theorem (4.7) is valid on *any* surface Ω bounded by $\partial\Omega$, and so a ship tracing out $\partial\Omega$ can use measurements of the vorticity or divergence to make inferences about any enclosed surface, be it the free surface of the ocean or an isopycnal surface that outcrops along $\partial\Omega$. They can not, however, similarly use measurements of strain rate. If the traversed boundary is small enough that the measurements are nearly coplanar, then such measurements could still give useful insights about the state of the ocean's surface but not about any other sort of surface that curves significantly into the ocean's interior.

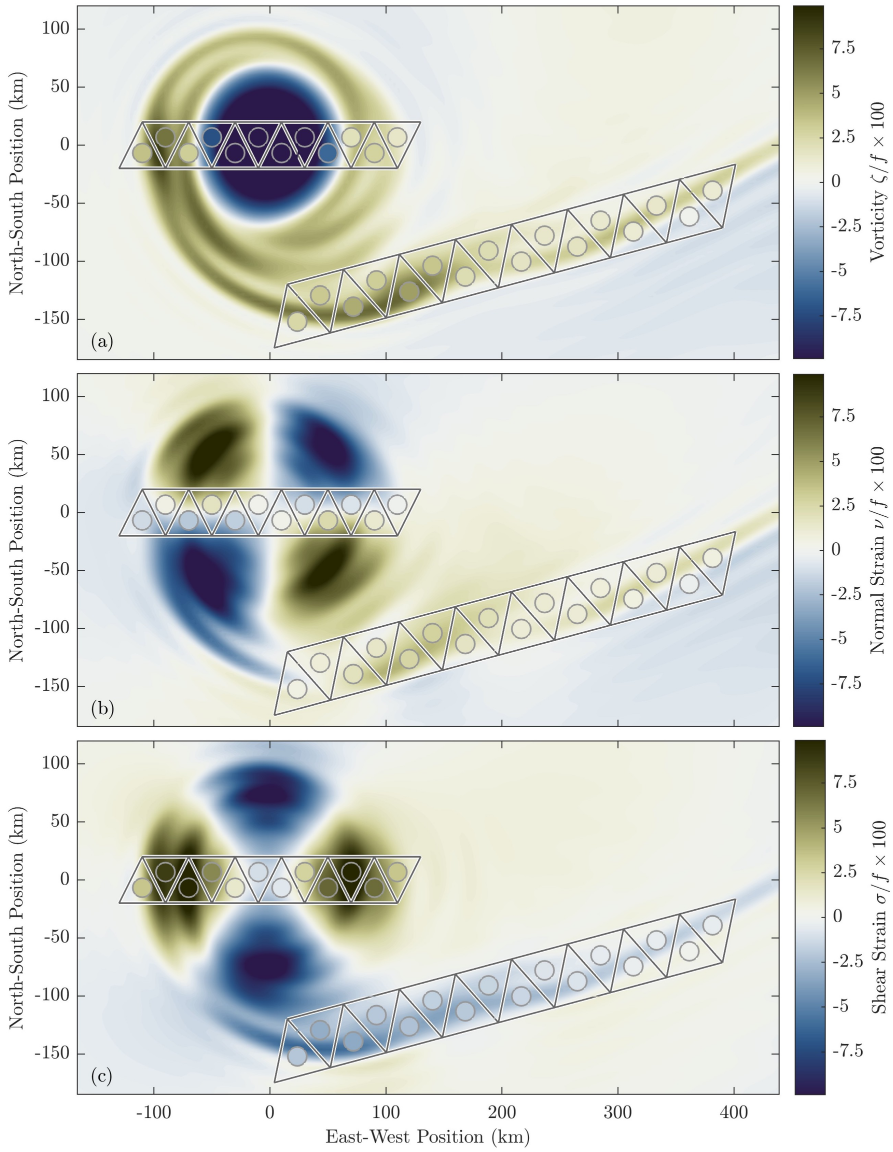

Figure 4.1: This figure was created by Jonathan Lilly, and appears as figure 1 of Lilly et al. (2024). That caption is quoted here: An illustration of the use of the gradient tensor theorem in observational oceanography. The (a) vorticity ζ, (b) normal strain ν, and (c) shear strain σ in a snapshot of a numerical simulation of a quasigeostrophic eddy termed BetaEddyOne (Early and Lilly, 2023) are shown, each normalized by the Coriolis frequency $f \equiv 2\Omega \sin\phi$ where Ω is the angular rotation rate of the Earth and ϕ is the model's central latitude. The eddy is sampled along the triangular tracks, as described in the text, and the colours of the circular disks show the average values of the three quantities within each triangular cell as inferred from the information along its boundary using the 2D gradient tensor theorem. Note that the divergence vanishes for this quasigeostrophic model.

References

Early, J. J. and Lilly, J. M. (2023). BetaEddyOne: A long-lived 1.5 layer quasigeostrophic eddy on a beta plane, with Lagrangian particles. Zenodo.

Gibbs, J. W. (1884). *Elements of vector analysis*. Tuttle, Morehouse & Taylor. Privately printed.

Grinfeld, P. (2013). *Introduction to tensor analysis and the calculus of moving surfaces*. Springer.

Lilly, J. M., Feske, J., Fox-Kemper, B., and Early, J. J. (2024). Integral theorems for the-gradient of a vector field, with a fluid dynamical application. *P. Roy. Soc. Lond. A Mat.*, 480(2293):20230550:1–30.

CHAPTER 5

Conclusion

The ocean is vast and complex, and the diversity of numerical ocean models reflects this. A fundamental choice for any model is how to represent space, and ocean modelers make different choices depending on the region to be modeled and the physical and temporal scales the model will cover. Each choice brings with it its own set of simplifications, approximations, and parameterizations, and the complexity only continues to grow as newer models introduce hybrid coordinates and generalized vertical coordinates.

The goal of this project has been, using off-the-shelf methods from tensor analysis, to unify the many complex coordinate systems that appear in ocean models. As expected, this proved harder than expected. Much of the difficulty in tailoring these methods to geophysical fluid dynamics came from one peculiarity of the field: we often use coordinates that move, but do not move *with the fluid*. That is, GFD lives between the Eulerian and Lagrangian representations of standard fluid mechanics. This is true even in the simplest geophysical situations: we, as observers, always rotate with the planet, but the ocean is never in solid-body rotation.

Though we inherit standard methods of spacial differentiation in curvilinear coordinates directly from differential geometry, the semi-Lagrangian peculiarity of GFD complicates time differentiation. The solution, covered in Chapter 2, is to introduce the setting velocity $\mathcal{V}$: the component of observed velocity due only to motion of the coordinates through the fluid—a passive transformation. The setting velocity along with the metric components calculated in Chapter 3 tell us exactly how to transform into any time-dependent, curvilinear coordinates we'd like using standard definitions of coordinate systems that appear in the GFD literature.

The setting velocity, specifically its derivatives, tells us everything we need to know about the apparent forces we introduce when we transform into each setting. As with any second order tensor, we can decompose the gradient $\boldsymbol{\nabla} \otimes \boldsymbol{\mathcal{V}}$ into its antisymmetric and symmetric parts, respectively describing the apparent forces that arise from rigid and non-rigid transformations—a clean separation of geometrical concerns. The former include the familiar, "fictitious" forces—Coriolis, centrifugal—arising from rigid rotation. The latter are a separate class we dub "fantastical," and differ greatly for different classes of tensor fields.

Though these newly described forces are likely small in many cases, they must appear in our exact equations. Such a general derivation of these terms provides the opportunity to approximate carefully, determining rigorously the impact of our approximations. And indeed, rigor is its own reward. In practice, however, we must know how the fantastical terms scale, and we began a scaling analysis in Chapter 3. A full treatment remains unfinished; it will be instructive to choose some particular cases where we expect larger contributions, for example terrain-following coordinates over steeply sloping topography.

Approximations and parameterizations are necessary at the scale of the world ocean and with limited computational resources. Chapter 3 lays out many standard choices, and unites them conceptually: the traditional and hydrostatic approximations and the generalized Redi diffusion parameterization all appear as applications of projection operators, and they can be freely applied on geometries as simple as the sphere or as complex as the geoid.

This manifests a central theme of tensor analysis and particularly of index notation: on the one hand, our equations speak directly about tensor components—the actual numerical values stored in computer memory—allowing straight-forward translation of equations into computer code; on the other hand, the algebra of components is designed so as always to correspond to geometrically legible operations on tensors themselves—differentiation, advection, projection—as the physical situation demands. We can combine the geometric insight of symbolic vectors with the explicit clarity of Cartesian tensors in a framework more powerful than either. Furthermore, we are free to choose a less abstract, extrinsic interpretation of the equations drawing on our physical intuitions of space, or to eschew this in favor of a more abstract, intrinsic interpretation better suited to integration and discretization (Crane et al., 2013; Crane, 2018).

We begin the treatment of integration in Chapter 4, explicating a peculiar result arising from the reliance on a flat, extrinsic space. More general work on integration will require restriction to antisymmetric tensors only, and will hopefully allow the expansion of this coordinate-agnostic framework to averaging, filtering, and coarse-graining (Aluie et al., 2018). Averaging particularly will admit the parameterization of sub-grid advection (Dukowicz and Smith, 1997), and, combined with the diffusive part mentioned above, provide a coordinate-agnostic form of the full Gent and McWilliams-Redi eddy transfer tensor (Redi, 1982; Gent and McWilliams, 1990; Gent et al., 1995; Griffies et al., 1998; Griffies, 1998).

Another useful extension of this work would be to show that the concept of the setting velocity $\mathcal{V}$ and the intrinsic time derivative for moving settings are a special case of the Arnowitt–Deser–Misner (ADM) formulation of general relativity (Arnowitt and Deser, 1959) taken to the Newtonian limit. The ADM formalism is a method of foliating 4-D Lorentzian spacetime into space-like hypersurfaces, providing a clean separation of the metric into parts describing the physics and parts describing the coordinate artifacts (Arnowitt et al., 2008)—spiritually similar to our second chapter. This approach would have several benefits. First, it could provide a clean, Hamiltonian and Poisson bracket formulation of GFD, simplifying energy budget calculations and tying us more tightly to the geometric mechanics literature (Holm, 2025). Second, it has been a long-term goal of ours to create a computer algebra tool for GFD that would handle fiddly index calculations automatically. Linking this work more closely to general relativity would mean we could more easily use existing tools such as Mathematica's xAct package (Martín-García, 2008). Third, ADM finds extensive applications in numerical relativity (Baumgarte and Shapiro, 2010), and so might inform numerical GFD as well. Finally, it would allow straightforward relativistic corrections to this framework to be added where necessary—perhaps for exoplanets orbiting very close to their star.

Throughout this work we have employed some parsimonious abstraction where powerful, but were careful to remain almost entirely grounded in flat, Euclidean space familiar to the observational oceanographer and the mathematician alike. We believe that the framework developed here is practical enough to be used by oceanographers and abstract enough to interact with the work of mathematicians and physicists considering these problems through the lens of the exterior calculus and geometric mechanics. We hope that others in the field find this work useful and usable, and that they might pick up some of the threads laid down here.

References

Aluie, H., Hecht, M., and Vallis, G. K. (2018). Mapping the energy cascade in the north atlantic ocean: The coarse-graining approach. *Journal of Physical Oceanography*, 48(2):225 – 244.

Arnowitt, R. and Deser, S. (1959). Quantum theory of gravitation: General formulation and linearized theory. *Phys. Rev.*, 113:745–750.

Arnowitt, R., Deser, S., and Misner, C. W. (2008). Republication of: The dynamics of general relativity. *General Relativity and Gravitation*, 40(9):1997–2027.

Baumgarte, T. W. and Shapiro, S. L. (2010). *Numerical relativity: solving Einstein's equations on the computer*. Cambridge University Press.

Crane, K. (2018). Discrete differential geometry: An applied introduction. *Notices of the AMS, Communication*, 1153.

Crane, K., de Goes, F., Desbrun, M., and Schröder, P. (2013). Digital geometry processing with discrete exterior calculus. In *ACM SIGGRAPH 2013 Courses*, SIGGRAPH '13, New York, NY, USA. Association for Computing Machinery.

Dukowicz, J. K. and Smith, R. D. (1997). Stochastic theory of compressible turbulent fluid transport. *Physics of Fluids*, 9(11):3523–3529.

Gent, P. R. and McWilliams, J. C. (1990). Isopycnal mixing in ocean circulation models. *Journal of Physical Oceanography*, 20(1):150–155.

Gent, P. R., Willebrand, J., McDougall, T. J., and McWilliams, J. C. (1995). Parameterizing eddy-induced tracer transports in ocean circulation models. *Journal of Physical Oceanography*, 25(4):463–474.

Griffies, S. M. (1998). The gent–mcwilliams skew flux. *Journal of Physical Oceanography*, 28(5):831–841.

Griffies, S. M., Gnanadesikan, A., Pacanowski, R. C., Larichev, V. D., Dukowicz, J. K., and

Smith, R. D. (1998). Isoneutral diffusion in a z-coordinate ocean model. *Journal of Physical Oceanography*, 28(5):805–830.

Holm, D. D. (2025). *Geometric Mechanics-Part III: Broken Symmetry And Composition Of Maps*. World Scientific.

Martín-García, J. M. (2008). xtensor: a free fast abstract tensor manipulator. In *The Eleventh Marcel Grossmann Meeting: on Recent Developments in Theoretical and Experimental General Relativity, Gravitation and Relativistic Field Theories (in 3 volumes)*, pages 1552–1554. World Scientific.

Redi, M. H. (1982). Oceanic isopycnal mixing by coordinate rotation. *Journal of Physical Oceanography*, 12(10):1154–1158.